8-1-2011

Geometric control of cardiomyogenic induction in human pluripotent stem cells

Celine L. Bauwens
University of Toronto

Hannah Song
University of Toronto, Institute of Biomedical Engineering

Nimalan Thavandiran
University of Toronto

Mark Ungrin
University of Toronto, Institute of Biomedical Engineering

Stéphane Massé
Toronto General Hospital

See next page for additional authors

Geometric Control of Cardiomyogenic Induction from Human Pluripotent Stem Cells

by

Céline Liu Bauwens

A thesis submitted in conformity with the requirements
for the degree of Doctor of Philosophy

Department of Chemical Engineering and Applied Chemistry
University of Toronto

Geometric Control of Cardiomyogenic Induction from Human Pluripotent Stem Cells

Céline Liu Bauwens

Doctor of Philospophy

Department of Chemical Engineering and Applied Chemistry
University of Toronto

2010

Abstract

Pluripotent stem cells provide the opportunity to study human cardiogenesis in vitro, and are a renewable source of tissue for drug testing and disease models, including replacement cardiomyocytes that may be a useful treatment for heart failure. Typically, differentiation is initiated by forming spherical cell aggregates wherein an extraembryonic endoderm (ExE) layer develops on the surface. Given that interactions between endoderm and mesoderm influence embryonic cardiogenesis, we examined the impact of human embryonic stem cell (hESC) aggregate size on endoderm and cardiac development. We first demonstrated aggregate size control by micropatterning hESC colonies at defined diameters and transferring the colonies to suspension. The ratio of endoderm (GATA-6) to neural (PAX6) gene and protein expression increased with decreasing colony size. Subsequently, maximum mesoderm and cardiac induction occurred in larger aggregates when initiated with endoderm-biased hESCs (high GATA-6:PAX6), and in smaller aggregates when initiated with neural-biased hESCs (low GATA-6:PAX6). Additionally, incorporating micropatterned aggregates in a stirred suspension bioreactor increased cell yields and contracting aggregate frequency. We next interrogated the relationship between aggregate size and endoderm and cardiac differentiation efficiency in size-controlled aggregates, generated using forced aggregation, in defined cardiogenic medium. An

inverse relationship between endoderm cell frequency (FoxA2^{+} and GATA6^{+}) and aggregate size was observed, and cardiogenesis was maximized in mid-size aggregates (1000 cells) based on frequency of cardiac progenitors (~50% KDR^{low}/C-KIT^{neg}) on day 5 and cardiomyocytes (~24% cTnT^{+}) on day 16. To elucidate a relationship between endoderm frequency and cardiac differentiation efficiency, aggregates were initiated with varying frequencies of ExE progenitors (SOX7-overexpressing hESCs). Maximum cardiomyocyte frequencies (~27%) occurred in aggregates formed with 10 to 25% ExE progenitors. These findings suggest a geometric relationship between aggregate size and ExE differentiation efficiency subsequently impacts cardiomyocyte yield, elucidating a mechanism for endogenous control of cell fate through cell-cell interactions in the aggregate.

Acknowledgments

There are so many people who have contributed to this project whether it was through their guidance, mentorship or emotional support. First of all, I would like to thank my supervisor, Peter W. Zandstra, for providing me with the opportunity to work in his lab as a 4th year undergraduate student, and extending that opportunity to work in a field that is both interesting and relevant as a graduate student. I want to thank my supervisory committee: Kim Woodhouse, Bill Stanford, and Mansoor Husain. I also wish to acknowledge my many co-authors for their contributions to this work including Raheem Peerani, Sylvia Niebruegge, Mark Ungrin, Cheryle Seguin, Nimalan Thavandiran, Stephane Masse, Elias Sevaptisidis, Kumar Nanthakumar and Eugenia Kumacheva. A number of the protocols and techniques used in this project were adapted from other labs, and so I would like to thank specifically Karolina Kolodziejska from the Husain Lab and Mark Gagliardi from the Keller Lab for taking the time to train me and answer my endless questions. I have been very fortunate to work in a lab that operates like a team and family, where people will devote the time to help you with your experiments, feed your cells on the weekend, and provide intellectual and emotional support and most importantly friendship. In particular I am grateful to Ting Yin, who acts as our mom and watches over us trying to make sure all our needs are met. I am thankful for the support from cherished friends I have made in the lab over the years, especially Kelly Purpura, Karen Chang, Elaine Waese, Genevieve Gavigan and Kento Onishi. And finally I want to thank my family for their encouragement and particularly my husband Steven for his love, support and endless patience during my entire graduate school career. Thank you.

Table of Contents

List of Tables

List of Figures

Chapter 5

List of Appendices

List of Abbreviations

7-AAD	7-aminoactinomycin D
AFP	alpha fetoprotein
ANP	atrial natiuretic factor
AP	action potential
BMP	bone morphogenetic factor
Bt2cAMP	dibutyryl cyclic AMP
cDNA	complementary deoxynucleic acid
CM	conditioned medium
cTnT	cardiac troponin T
Cx-43	Connexin-43
CXCR4	CXC chemokine receptor 4
DE	definitive endoderm
DKK1	dickkopf homolog 1
DLX	distal-less homeobox
Dox	doxycycline
dsRNA	double stranded RNA
EA-53	α-Actinin
EB	embryoid body
ECM	extracellular matrix
ELISA	enzyme linked immunosorbent assay
EPOR	Erythropoietin receptor
ESC	embryonic stem cells
ExE	extraembryonic endoderm
FBS	fetal bovine serum
FGF	fibroblast growth factor
FH	fetal heart tissue
FITC	fluorescein isothiocyanate
FLK1	fetal liver kinase-1
FoxA2	Forkhead box A2
G418	Geneticin
GATA6	GATA binding protein 6
GDF-3	growth differentiation factor-3
GFR-MG	growth factor reduced Matrigel™
GSC	Homeobox protein goosecoid
HAND1	heart and neural crest derivatives expressed protein-1
hESC	human embryonic stem cells
HNF	hepatocyte nuclear factor
hPSC	human pluripotent stem cell
HSPG	heparin sulfate proteoglycan
ICM	inner cell mass
iPS	induced pluripotent stem
Isl-1	Islet-1
KDR	kinase insert domain protein receptor
ko-DMEM	knockout Dulbecco's Modified Eagle's Medium
ko-SR	knockout Serum Replacement

LAMB1	laminin subunit beta-1
MEF	mouse embryonic fibroblasts
Mef2c	myocyte enhancer factor 2C
mESC	mouse embryonic stem cells
MHC	myosin heavy chain
MLC2A	myosin light chain 2A
MP	micropatterned
mRNA	messenger RNA
NE	norepinephrine
NEAA	non essential amino acids
O/E	overexpressing
Oct4	Octamer-4
PAX6	paired box 6
Pdms	poly(dimethylsiloxane)
PE	primitive endoderm
PS	primitive streak
Puro	puromycin
QRT-PCR	quantitative real time – polymerase chain reaction
RA	retinoic acid
RISC	RNA induced silencing complex
RNA	Ribonucleic Acid
Rock inhibitor	p160-Rho associated coiled-coil kinase inhibitor Y-27632
SF	serum-free
siRNA	short interfering RNA
Smad-1	Sma mothers against decapentaplegic
SOX	Sry-related HMG box
SPARC	secreted protein acidic and rich in cystein
T	Brachyury
Tbx	T-box
TGF-β	transforming growth factor beta
VEGF	vascular endothelial growth factor
Wnt	wingless int
XV medium	X-VIVO10™ medium
α-SR-1	α-sarcomeric actin

Chapter 1
Introduction

THE MOTIVATION FOR STUDYING CARDIAC INDUCTION OF HUMAN PLURIPOTENT STEM CELLS

The excitement surrounding research on human pluripotent stem cells (hPSCs) is largely based on the expectation that these cells may one day provide a renewable source of human tissue for cell-based therapies and for testing disease models. Equally as important, however, is the opportunity these cells present for studying human embryonic development in vitro, which for ethical reasons would not otherwise be possible in the human system. Insight into stem cell differentiation to cells belonging to the cardiovascular system is of particular interest because currently the only effective treatment for heart failure is organ transplantation. The regenerative capacity of the heart is limited, and heart failure is associated with massive irreversible loss of cardiomyocytes. Consequently, cell transplantation is emerging as a potential alternative to organ transplantation (Dimmeler, Zeiher et al. 2005; Laflamme and Murry 2005; Rubart and Field 2006; Zhu, Hauch et al. 2009). A number of cell types have been under investigation for their potential to integrate into the heart and improve function following a myocardial infarction including stem cell-derived cardiomyocytes (Caspi, Huber et al. 2007; Laflamme, Chen et al. 2007; Leor, Gerecht et al. 2007; van Laake, Passier et al. 2007), skeletal myoblasts (Menasche 2003; Menasche 2004), and bone marrow-derived cells (Orlic, Kajstura et al. 2001). The ideal donor cell type must have the capacity to replace the lost tissue function of the damaged heart either by integrating and contracting synchronously with host cardiomyocytes or by promoting the healing of the injured host tissue by paracrine factors (Laflamme, Zbinden et al. 2007). Given that skeletal myoblasts and bone marrow–derived cells are relatively easy to obtain, especially autologously, they have been the most extensively investigated in humans but the results of these clinical trials have been inconclusive (Meyer, Wollert et al. 2006; Abdel-Latif, Bolli et al. 2007; Menasche 2008) and initial assertions about the cardiomyogenic potential of these cell types have recently been challenged (Reinecke, Poppa et al. 2002; Balsam, Wagers et al. 2004; Murry, Soonpaa et al. 2004; Nygren, Jovinge et al. 2004). HPSCs are a promising candidate cell source because differentiation to cardiomyocytes has been widely demonstrated as well as differentiation to other non-cardiac cell-types present in the heart (Kehat, Kenyagin-Karsenti et al. 2001; Xu, Police et al. 2002; Mummery, Ward-van Oostwaard et al. 2003). Additionally, undifferentiated hPSCs expand indefinitely and hPSC-derived cardiomyoyctes have a high proliferative capacity (Xu, Police et al. 2002; McDevitt, Laflamme et al. 2005).

Finally, a number of reports have demonstrated stable integration of hPSC-derived cardiomyocytes following transplantation into infarcted rodent hearts, resulting in preserved contractile function (Caspi, Huber et al. 2007; Laflamme, Chen et al. 2007; van Laake, Passier et al. 2007).

Despite the potential of hPSCs, a number of challenges must still be addressed before cell transplantation is a viable approach to treating heart failure. While human embryonic stem cell (hESCs) differentiation has been demonstrated in scalable culture systems (Gerecht-Nir, Cohen et al. 2004; Cameron, Hu et al. 2006), no reports have been made showing significant cardiac yields and robust protocols for large scale production of relatively pure hPSC-derived cardiomyocytes are still in development. A second challenge that remains is poor cell survival and integration following cell transplantation into the non-vascularized, pro-inflammatory environment of the infarcted region (Caspi, Huber et al. 2007; Laflamme, Chen et al. 2007; van Laake, Passier et al. 2007). To resolve this issue a number of approaches are being explored including the incorporation of pro-survival factors during cell injection (Laflamme, Chen et al. 2007), and tissue engineering strategies such as transplanting biodegradable scaffolds seeded with cardiomyocytes (McDevitt, Woodhouse et al. 2003), using biocompatible hydrogels as vehicles for cell delivery (Christman, Vardanian et al. 2004; Martens, Godier et al. 2009), or producing functional cardiac grafts (Iyer, Radisic et al. 2007; Khademhosseini, Eng et al. 2007; Radisic, Park et al. 2007).

Efficient hPSC differentiation towards cardiomyocytes at the purity and scale required for therapeutic applications remains elusive. In attempting to realize the potential for stem cell based therapy to treat heart failure, research to date has focused on improving cardiac induction efficiency during hPSC differentiation largely by exploiting what is known about cardiac development during embryogenesis in other animal systems. However, progress made over the last 5 years in the development of robust systems for hESC maintenance and cardiac differentiation has established a framework from which it becomes possible to assay a wide range of concepts specific to human cardiogenesis.

PLURIPOTENT STEM CELLS

HESC maintenance

Traditionally, the term pluripotent stem cell referred to embryonic stem cells (ESCs), but in 2006 it was demonstrated that adult cells could also be genetically manipulated to take on a pluripotent state (Takahashi and Yamanaka 2006). By definition, pluripotent stem cells are able to self-renew while maintaining the capacity to develop into cells of the three primary germ layers - ectoderm, mesoderm, and endoderm – from which all somatic tissues develop. Consequently, pluripotent stem cells are both a promising donor source for cell therapy, potentially providing sufficient cell numbers for transplantation into a variety of organs, as well as a useful tool to study developmental biology.

Human (h)ESCs are derived by isolating cells from the inner cell mass (ICM) of an embryo at the pre-implantation blastocyst stage and plating the isolated cells onto a feeder layer of cells that support pluripotency, typically mouse embryonic fibroblast (MEF) feeder cells (Thomson, Itskovitz-Eldor et al. 1998; Reubinoff, Pera et al. 2000). Human ESCs express the transcription factor Oct4 and form colonies that are relatively flat and circular with a distinct border (Reubinoff, Pera et al. 2000). Continuous growth of hESCs requires the presence of a feeder layer, or coating the dishes with Matrigel^{TM}, an extracellular matrix (ECM) preparation, and growing the cells in medium that is either feeder-conditioned (Xu, Inokuma et al. 2001), or supplemented with cytokines including fibroblast growth factor (FGF)-2 and transforming growth factor (TGF)-β (Amit, Shariki et al. 2004; Wang, Zhang et al. 2005; Wang, Li et al. 2005; Xu, Peck et al. 2005).

Human ESC colonies typically have to be passaged every 4 to 7 days to maintain pluripotency. One characteristic of hESCs is that they require cell-cell contact and paracrine and autocrine signaling for survival (Pyle, Lock et al. 2006), and as a result exhibit poor viability upon dissociation to single cells. Consequently, hESC passaging has routinely been performed by partial dissociation of hESC colonies using a combination of mechanical and enzymatic dissociation (Thomson, Itskovitz-Eldor et al. 1998; Amit, Carpenter et al. 2000; Reubinoff, Pera et al. 2000). This passaging method produces hESC maintenance cultures containing colonies in a wide range of sizes, and is also a source of variability between passages, as it affects the local

cellular microenvironment. It has been demonstrated that hESC pluripotency is influenced by endogenous signaling which takes place within colonies and can be modulated by varying colony size (Peerani, Rao et al. 2007). In the absence of exogenous cytokines used to maintain pluripotency, hESCs in regions of high localized cell density (defined as the number of cells per 300 μm radius) retain Oct4 expression. It was shown that maintenance of pluripotency in hESC colonies is dictated by the interplay of signals secreted by undifferentiated hESCs and their differentiated progeny, which express markers characteristic of extra-embryonic endoderm (ExE). Enzyme linked immunosorbent assay (ELISA) analysis of ExE- and hESC-conditioned medium (CM) revealed that ExE cells secrete bone morphogenetic protein (BMP)-2 at levels six times higher than hESCs, and that growth differentiation factor-3 (GDF-3), a BMP antagonist, is secreted by hESCs but was not detected in ExE-CM. ExE secretion of BMP-2 inhibits hESC self-renewal via Sma mothers against decapentaplegic (Smad1) signaling. In larger colonies, there is a higher local cell density of hESCs which translates to increased BMP antagonist (GDF-3) activity, thereby promoting pluripotency.

Developments have been made to minimize or eliminate this source of variability. In one approach micro-contact printing is used to pattern ECM onto tissue culture substrates, thereby specifying hESC colony size and geometry (Peerani, Rao et al. 2007; Lee, Peerani et al. 2009). In this method, hESCs are enzymatically dissociated to single cells and plated on the ECM-micropatterned surface at extremely high cell densities so that cells reaggregate and adhere to the ECM islands at a high density. Another method employing microscale technology involves patterning surfaces with microwells in which hESCs can be maintained as 3-dimensional (3-D) aggregates (Khademhosseini, Ferreira et al. 2006). The aggregates grow to a maximum size, defined by the dimensions of the microwells. However, these systems have been strictly used to demonstrate the capability to control colony size and to examine the effects of controlling colony size, and for technical reasons have not been used for long term maintenance of hESC cultures. Some of the more recently derived cell lines, such as the CA1, CA2, and HES2 cell lines, have been adapted for single cell enzymatic dissociation and therefore, in these lines, passage to passage variability arising from partial colony dissociation has been reduced.

Differentiation of hESCs

In vitro ESC differentiation is routinely carried out by forming embryoid bodies (EBs) which are three dimensional aggregates of hESCs in suspension. Aspects of embryonic development are recapitulated within the EB, wherein cells of the three embryonic germ layers - endoderm, ectoderm and mesoderm - develop (Doetschman, Eistetter et al. 1985; Itskovitz-Eldor, Schuldiner et al. 2000; Xu, Inokuma et al. 2001) and subsequently differentiate into committed cell types including neurons, glia, skeletal and cardiac muscle cells, hematopoietic cells, hepatic cells and insulin-secreting (pancreatic) cells (Itskovitz-Eldor, Schuldiner et al. 2000; Xu, Inokuma et al. 2001).

Controlling aggregate size has been one of the major challenges in EB-mediated hESC differentiation. As previously discussed single cell dissociation of hESCs is avoided and therefore human EBs have typically been initiated by partial enzymatic digestion of hESC colonies, similar to the technique used to passage hESC colonies (Kehat, Kenyagin-Karsenti et al. 2001; Xu, Police et al. 2002). This method of EB formation leads to variability in EB size within cultures as well as average EB size between cultures (Itskovitz-Eldor, Schuldiner et al. 2000; Weitzer 2006) and consequently makes it difficult to achieve reproducible, consistent, and efficient hESC differentiation. Attempts to control human EB size have involved either forced aggregation of defined cell numbers (Ng, Davis et al. 2005; Burridge, Anderson et al. 2007; Ungrin, Joshi et al. 2008) or the use of microwells to form 3-D hESC aggregates of specified dimensions which can then be transferred to suspension to form mono-disperse EBs (Khademhosseini, Ferreira et al. 2006; Mohr, de Pablo et al. 2006; Mohr, Zhang et al. 2009).

In the first published report on EBs formed by forced aggregation of defined numbers of hESCs, it was observed that EB size influenced hematopoietic differentiation, with a minimum of 500 cells required for efficient blood formation and 1000 cells for optimum erythropoiesis (Ng, Davis et al. 2005). Building on this EB formation strategy, subsequent studies examined the effect of input hESC status and medium components on the efficiency of forced cell aggregation EB formation (Ungrin, Joshi et al. 2008). It was observed that aggregate formation efficiency was inefficient when initiated with hESC input populations highly expressing Oct4 protein, a marker of pluripotency. Incorporating a “pre-differentiation” step, in which maintenance medium is removed from hESC colonies and replaced with serum-containing medium 72 hours prior to EB

formation, led to a significant improvement in aggregation efficiency approaching 100%. This observation highlighted a separate issue that affects all differentiations studies. Variable input populations, with respect to expression levels of pluripotency markers as well as differentiation-associated markers, are a result of variability of hESC colony size, which is in large part a result of passaging hESC colonies as cell clumps (Peerani, Rao et al. 2007). It was observed that the "pre-differentiation" step could be eliminated and efficient aggregation of hESCs could still be achieved in the presence of p160-Rho associated coiled-coil kinase (ROCK) inhibitor Y-27632. EBs formed via forced aggregation are not only size-specified but also display consistent shape, allowing for the reproducible observation of tissue specific spatial organization within the EB. EBs formed by forced aggregation develop two distinct regions, an inner core that expresses Oct4, and a disordered outer layer that expresses a number of markers associated with primitive endoderm (Ungrin, Joshi et al. 2008).

An alternate means to control EB size uses microwell patterned surfaces. This method involves passaging hESC colonies as small clumps into size-specified microwells that have been either coated with Matrigel (Mohr, de Pablo et al. 2006; Mohr, Zhang et al. 2009) or MEFs (Khademhosseini, Ferreira et al. 2006) and maintaining undifferentiated hESCs as 3-D colonies. The colonies reach a maximum size defined by the volume of the microwell used, and can then be transferred to suspension in differentiation medium to develop as size-specified EBs. EBs cultured in this system have been proven to contain cells expressing proteins associated with each of the embryonic germ layers (Mohr, de Pablo et al. 2006), and have also been used to examine the effect of EB size on cardiac lineage induction from hESCs (Mohr, Zhang et al. 2009).

EARLY EVENTS IN EB DEVELOPMENT PARALLEL GASTRULATION DURING EMBRYOGENESIS

In the eight-cell morula-stage embryo, a process called compaction - in which inner blastomeres form a tight ball - produces the ICM (Figure 1.1A). Meanwhile blastomeres located on the exterior of the morula flatten and form the trophoblast. Following compaction, a fluid-filled cavity called the blastocoele develops inside the embryo (blastocyst stage), and ICM in contact with the blastocoele differentiates to primitive endoderm (PE) which then either differentiates to visceral endoderm where it is in contact with the ICM or parietal endoderm where it is in contact

with the trophoblast. At this stage, the remaining cells within the ICM begin to differentiate into an epithelial layer that is referred to as the epiblast or primitive ectoderm (Johnson and Ziomek 1981; O'Shea 2004). Development of the three primary germ layers occurs in the epiblast by a process called gastrulation (Figure 1.1B). Gastrulation is initiated in the posterior epiblast by movement of cells through the primitive streak (PS) where cells undergo an epithelial to mesenchymal transition, exiting the PS as mesoderm in the proximal-anterior region of the epiblast and as definitive endoderm in the distal-anterior region (Gadue, Huber et al. 2005; Rust, Sadasivam et al. 2006; Murry and Keller 2008).

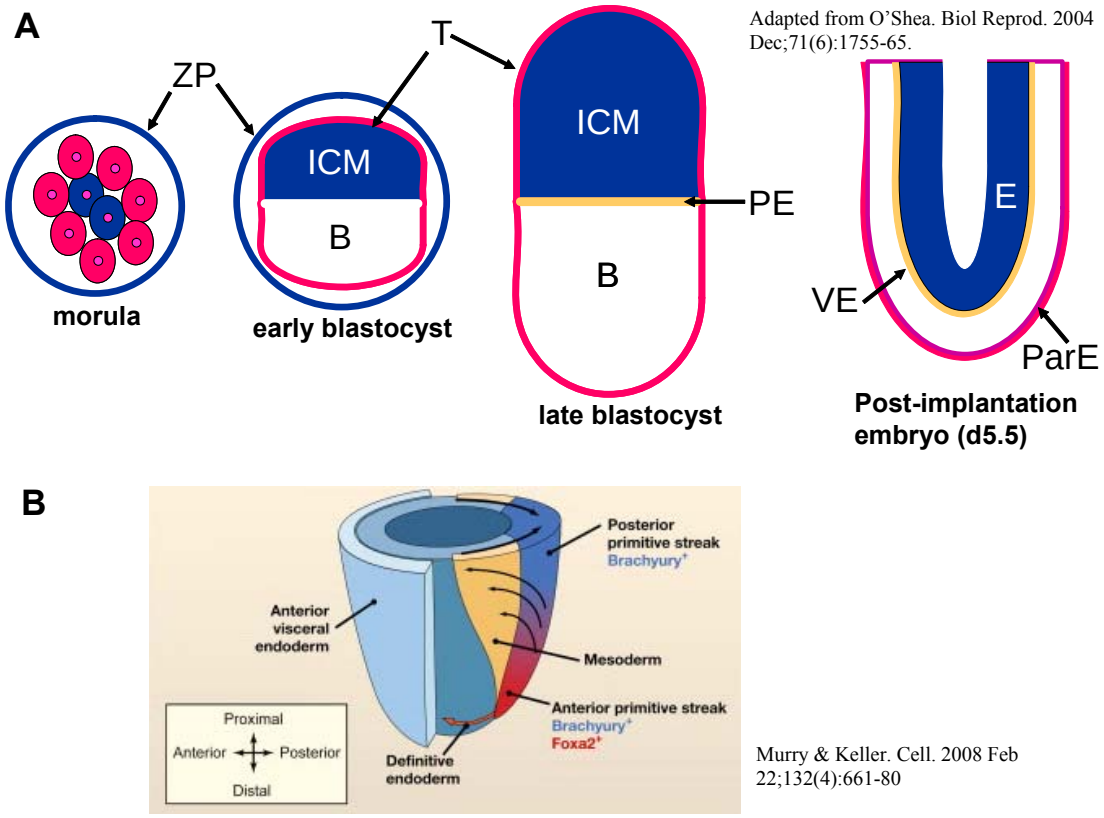

Figure 1.1: Development of the early mouse embryo. (A) In the morula, the inner (blue) cells will form ICM and the outer (pink) cells will form trophoblast. In the early blastocyst, a cavity (the blastocoele, B) forms between the inner cell mass and the trophoblast; the embryo is still enclosed in the zona pellucida (ZP). By the late blastocyst stage, the ICM cells in contact with the blastocoele differentiate into the primitive endoderm (PE), which later forms visceral endoderm on the epiblast side and parietal endoderm on the trophoblast side. At implantation the proamniotic cavity begins to form within the ICM. Cells of the ICM differentiate into an epithelial layer, the epiblast, (E). **(B)** Gastrulation in the mouse embryo. Shown are the posterior region of the primitive streak that expresses the marker Brachyury (blue), and the anterior region of the primitive streak that coexpresses both Brachyury and Foxa2 (red). At the top of the embryo, epiblast cells are shown entering the primitive streak (thick black arrows). The yellow/orange region depicts newly formed mesoderm, and migration of these cells from the primitive streak is indicated by thin black arrows. Also depicted is the movement of the earliest definitive endoderm cells (red arrow at bottom).

EBs are thought to mimic the environment of the peri-implantation embryo where interactions between various cell types facilitate inductive events. Similar to the embryo where an epithelial layer of PE forms and contacts the epiblast, one of the earliest events during EB development is the organization of the cells into an epithelial layer of PE surrounding an inner core of epiblast-like pluripotent cells (Coucouvanis and Martin 1995; Abe, Niwa et al. 1996; Coucouvanis and Martin 1999), followed by the expression of gene and protein markers that are associated with the PS such as Brachyury (Kispert and Herrmann 1994) and Mixl1 (Hart, Hartley et al. 2002). Many proteins involved in commitment to the endoderm and mesoderm lineage in the PS, such as TGF-β, Nodal and Wingless Int (Wnt) (Conlon, Lyons et al. 1994; Hogan 1996; Yamaguchi 2001), are the same and it is different levels of activation and inhibition of pathways associated with these proteins that regulate germ layer induction (Gadue, Huber et al. 2005). In terms of timing, the expression of genes associated with the PS and germ layer commitment in the EB recapitulates gastrulation in the embryo (St-Jacques and McMahon 1996; Dvash and Benvenisty 2004; Keller 2005; Murry and Keller 2008). However, while gastrulation occurs in a precise, spatially organized manner during embryogenesis, differentiation of PS-like cells in the EB is spatially chaotic. It is believed that in the embryo distinct signaling environments exist that are defined by location in relation to extraembryonic and embryonic tissues which secrete signals that direct lineage commitment (Rust, Sadasivam et al. 2006; Murry and Keller 2008). However, in contrast to the epiblast, EBs lack polarity and as a result spatially disorganized germ layer induction may be due to the lack of position-specific cues.

PARALLELS BETWEEN CARDIOGENESIS IN THE EMBRYO AND IN THE EB

During embryogenesis, the heart is the first organ to fully form after gastrulation (Menard, Grey et al. 2004), when oxygen delivery by diffusion is no longer sufficient in the growing embryo. Forming the anatomical structure of the heart involves the precise spatiotemporal coordination of signals from neighboring tissues that promote or inhibit cardiac specification, proliferation and migration of uncommitted precardiac mesoderm. Inductive cues originate from the anterior primitive endoderm (Sugi and Lough 1994; Schultheiss, Xydas et al. 1995; Schultheiss, Burch et al. 1997; Schultheiss and Lassar 1997) and lateral regions of the embryo (Schultheiss, Xydas et al. 1995; Schultheiss, Burch et al. 1997; Schultheiss and Lassar 1997), while cardiogenesis is suppressed in the adjacent mesoderm by factors secreted by the neuronal tube (Climent, Sarasa et al. 1995; Schultheiss, Burch et al. 1997; Raffin, Leong et al. 2000). Members of the TGF-β

superfamily (TGF-β, nodal, activin and BMP) and the FGF family are known cardiogenic morphogens that activate cardiac transcription factors (Menard, Grey et al. 2004). Wnt-related signals and members of the Wnt family are also important for cardiac induction (Sachinidis, Fleischmann et al. 2003), by playing both a repressive role, via the canonical Wnt/β-catenin pathway, and an inductive role via the non-canonical Wnt/Ca^{2+} and c-Jun N-terminal kinase pathways (Povelones and Nusse 2002).

Inductive signals from the anteriolateral(embryogenesis)/primitive(EB) endoderm

During embryonic development, precardiac mesoderm is in close contact with endoderm. A number of studies across various species have demonstrated that interactions between endoderm and overlying mesoderm are involved in cardiac differentiation (Orts Llorca 1963; Jacobson and Duncan 1968; Sugi and Lough 1994; Nascone and Mercola 1995; Schultheiss, Xydas et al. 1995) and, more specifically, play an inductive role as evidenced by the generation of beating cardiac tissue in cocultures of non-cardiogenic embryonic tissue explants and endodermal tissue (Schultheiss, Xydas et al. 1995). The inductive characteristic of the endoderm can be attributed to TGF-β superfamily and FGF family growth factors, expressed by anterior lateral endoderm, that have been reported to be involved in cardiac differentiation.

The TGF-β superfamily, involved in a wide range of developmental processes, includes TGF-βs, activins, nodals and BMPs. Binding of TGF-β family proteins to their receptors leads to activation of intracellular mediators of the Smad family. Smad2 and Smad3 transduce signals for TGF-β-like ligands, such as TGF-β, activin and nodal while Smad1, 5 and 8 transduce signals for BMP-like ligands (Lagna, Hata et al. 1996; Candia, Watabe et al. 1997; Shi, Hata et al. 1997). Upon phosphorylation, these receptor-regulated (R)-Smads form complexes with Smad4, which are subsequently translocated to the nucleus to regulate activation of transcription factors, such as cardiac transcription factors Nkx-2.5, GATA-4, and Tbx factors (Massague and Chen 2000; Schlange, Andree et al. 2000; Moustakas, Souchelnytskyi et al. 2001; Attisano and Wrana 2002; Harvey 2002; Wakefield and Roberts 2002; Attisano and Labbe 2004; Menard, Grey et al. 2004). FGF family proteins (FGF-2 and FGF-4) have been shown to support cardiomyocyte induction during embryonic development mainly by stimulating proliferation of mesodermal cells in vitro (Mima, Ueno et al. 1995; Lough, Barron et al. 1996; Schultheiss and Lassar 1997; Ladd, Yatskievych et al. 1998; Barron, Gao et al. 2000; Kawai, Takahashi et al.

2004). During embryogenesis, these growth factors, originating from the anterior and lateral endoderm, synergize in a precise spatial and temporal program to support and induce cardiogenesis in neighboring precardiac mesoderm (Figure 1.2).

Studies performed using avian embryo explants demonstrated the coordinated timing of signals from the endoderm that direct heart formation during embryogenesis (Ladd, Yatskievych et al. 1998). TGF-β1 and activin appear to have a similar effect in inducing cardiomyocyte differentiation in posterior epiblast tissue (including regions not fated to form heart) (Yatskievych, Ladd et al. 1997; Ladd, Yatskievych et al. 1998), but not in non-cardiogenic mesoderm (Schultheiss, Burch et al. 1997; Ladd, Yatskievych et al. 1998). Conversely, BMP-2 and -4, in combination with FGF-4, induce cardiac differentiation of non-cardiogenic mesoderm (Lough, Barron et al. 1996; Schultheiss and Lassar 1997; Ladd, Yatskievych et al. 1998; Barron, Gao et al. 2000), but fail to support cardiogenesis in posterior epiblast. FGF-2 is expressed in both endoderm as well as myocardial cells of the developing embryo (Parlow, Bolender et al. 1991; Sugi, Sasse et al. 1993). Studies indicate that FGF is necessary for proliferation of precardiac mesoderm given that hybridization of FGF-2 mRNA to a complementary oligodeoxynucleotide, on day 4 of explant cultures, results in a dramatic reduction of proliferating myocardial cells, but not when exogenous FGF-2 was added with the oligodeoxynucleotide (Mima, Ueno et al. 1995). From these findings, it appears that directing pre-gastrula epiblast to terminally differentiated cardiomyocytes consists of TGF-β or activin signaling during early embryonic development to specify the mesendoderm lineage, followed by BMP signaling to induce terminal cardiomyocyte differentiation in precardiac mesoderm, which is supported by FGF's role in precardiac mesoderm proliferation.

Observations on the cardiogenic effects of these growth factors in the embryo have been reinforced in the ESC differentiation system. EB cultures initiated with ESCs that have been primed with BMP-2 or TGF-β for 24 hours express higher levels of mRNA for brachyury (mesodermal marker) and cardiac transcription factors Nkx-2.5 and myocyte enhancer factor 2C (Mef2c), and exhibit larger beating areas and increased α-actinin staining (Behfar, Zingman et al. 2002). It has also been shown that a combination of FGF-2 and BMP-2 can efficiently enhance cardiac induction of ESC differentiation cultures (Kawai, Takahashi et al. 2004).

Similar to cardiogenesis in the developing embryo, it is expected that the order and timing of signals is critical during ESC differentiation to cardiomyocytes.

Nodal, a TGF-β protein that signals by binding activin receptors via membrane-bound Cripto protein (Reissmann, Jornvall et al. 2001; Yeo and Whitman 2001), appears to play a role in cardiac specification during early differentiation. Timing of Nodal signaling is important, as endogenous expression of its cofactor Cripto is detected at the earliest stages of ESC differentiation and is no longer present at stages where EB contractions are observed (Parisi, D'Andrea et al. 2003). In kinetic studies using Cripto-/- ESCs it was demonstrated that addition of recombinant Cripto during the first 2 days of culture restored the differentiation ability of Cripto-/- ESCs, whereas addition at later time-points led to dramatically reduced cardiomyocyte differentiation (Xu, Liguori et al. 1998; Parisi, D'Andrea et al. 2003). Impaired cardiac induction and differentiation of ESCs upon addition of Nodal antagonist demonstrates that Cripto signaling is Nodal-dependent. It should be noted that specification of the cardiac fate seems to occur at the expense of the neural fate, given that addition of Cripto protein to Cripto-/- ESCs during the first 2 days restores cardiomyocyte differentiation and results in a dramatic inhibition of neural differentiation, while Cripto addition from day 3 and on results in progressive impairment of cardiac differentiation and increases differentiation to a neural phenotype (Parisi, D'Andrea et al. 2003).

BMP signaling impacts cardiac differentiation in EBs in a temporal manner. In a time course study investigating different time windows of noggin (a BMP inhibitor) exposure on incidence of EB beating, it was observed that depending on the developmental stage of the differentiation culture BMP signaling can have both a positive and negative effect on the efficiency of cardiac induction (Yuasa, Itabashi et al. 2005). Inhibiting BMP from 3 days prior to EB formation until day 3 of differentiation yielded a 95% incidence of beating EBs, whereas initiating BMP inhibition upon EB formation or later reduced beating incidence to less than 40%. This observation is consistent with what has been determined in posterior epiblast and precardiac mesoderm explants, where it has been established that BMP signaling is required for terminal cardiomyocyte differentiation but appears to inhibit mesoderm specification during early differentiation.

An assessment of the data indicates that precardiac cells interpret BMP signals in a cell-type specific manner. As has been outlined previously, TGF-β/activin/Nodal proteins signal via different Smad mediators than BMP proteins. BMP inhibition of TGF-β/activin/Nodal activity during early cardiac differentiation may be due to competition for Smad4 by Smad2/3 (BMP downstream transducers) and Smad1/5/8 (TGF-β, activin and Nodal downstream transducers). Smad4 has been shown to be essential during cardiogenesis. In mouse embryos, disruption of Smad4 specifically in the myocardium leads to reduced proliferation and increased apoptosis of cardiomyocytes, heart defects and eventually embryonic lethality (Qi, Yang et al. 2007; Song, Yan et al. 2007). Therefore cells at different stages of differentiation may be exhibiting different responses to BMP signaling as a result of Smad4 sequestering by the TGF-β/activin/Nodal pathways.

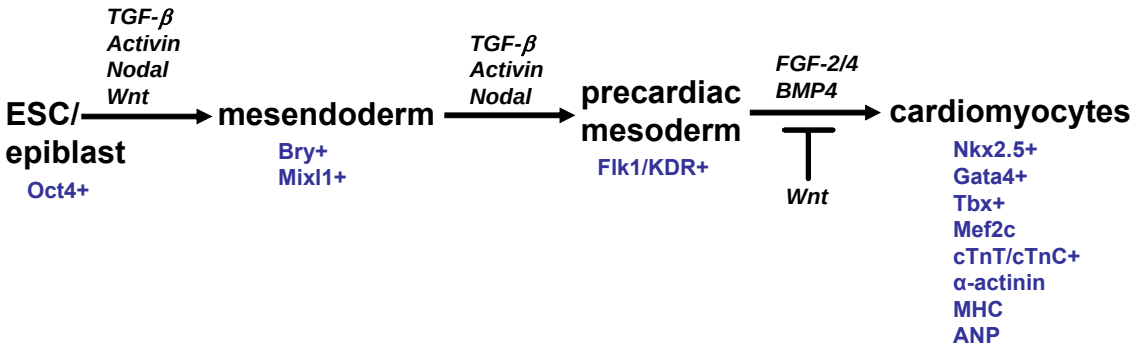

Figure 1.2: Signals known to be involved in directing cardiogenesis and the markers expressed at each stage of development.

Inductive/Inhibitory signals from the neuronal tube

Wnt signaling proteins play both a repressive and supportive role in heart morphogenesis. Canonical Wnt signaling suppresses cardiac differentiation by degradation of β-catenin. Wnts' repressive activity is inhibited by antagonists Crescent and dickkopf homolog 1 (DKK1) (expressed in anterior endoderm during gastrulation), which subsequently results in the induction of beating muscle. Inhibition of Wnt signaling promotes heart formation in the anterior lateral mesoderm, whereas active Wnt signaling in the posterior lateral mesoderm promotes blood development (Marvin, Di Rocco et al. 2001). In the non-canonical pathway Wnt11 prevents signaling of other Wnts, amplifying the cardiogenic signal (Menard, Grey et al. 2004). This

pathway promotes heart induction by upregulating Nkx-2.5 and GATA-4 in xenopus embryos and the P19 pluripotent cell line (Pandur, Lasche et al. 2002). It has been shown, through loss- and gain-of-function experiments that Wnt11 is required for heart formation in xenopus embryos and is sufficient to induce a contractile phenotype in embryonic explants. Treating P19 cells with murine Wnt-11 conditioned medium triggers cardiogenesis, which indicates that the function of Wnt-11 in heart development has been conserved in higher vertebrates (Pandur, Lasche et al. 2002). In mESCs, a positive correlation has been observed between Wnt and Nkx-2.5 expression. Furthermore, in the same mouse (m)ESC study, treatment of EBs with medium containing Wnt11 increased expression of Nkx2.5 in a dose-dependent manner.

Transcription factors: GATA proteins, Nkx-2.5, Smads, T-box proteins

Activation of cardiac gene promoters cannot be carried out by one transcription factor alone, but results from the coordinated activity of multiple transcription factors. Cardiac transcription factors include, among others, Nkx-2.5, GATA-4, 5, 6, Tbx5 and Tbx20, and several Smad proteins (Menard, Grey et al. 2004).

The activity of GATA proteins is modulated by their interactions with other transcriptional coactivators and repressors. GATA-4 promotes cardiac muscle development and regulates expression of several cardiac specific genes including myosin heavy chain (MHC), cardiac troponin T and cardiac troponin C (cTnT/C), and Atrial Natriuretic Protein (ANP) (Svensson, Tufts et al. 1999). Nkx-2.5 is an important coactivator of GATA-4 in initiating transcription of cardiac specific genes. T-box gene family transcription factors appear to contribute to several aspects of cardiac development including cardiac lineage determination, chamber specification and specialization of the conduction system. T-box genes act in conjunction with other families of transcription factors (Nkx and GATA) to regulate cardiac gene expression (Bruneau, Nemer et al. 2001; Hiroi, Kudoh et al. 2001; Takeuchi and Bruneau 2009).

Smad proteins mediate BMP signaling. BMPs phosphorylate cytoplasmic R-Smads1, 5, or 8 which interact with Smad4. This Smad complex is then translocated to the nucleus where it associates with other transcription factors to activate BMP-responsive genes (Attisano and Wrana 2000). Precardiac cells interpret the BMP signals in a cell-type specific manner. A possible molecular basis linking cardiac gene regulation and the BMP signaling pathway has been proposed from experiments that link Smad4 activation of Nkx-2.5 transcription with

GATA-4 acting as a cofactor. Mesodermal cells recognize and interpret the BMP-cardiac-promoting signal because the activating region of the mouse Nkx-2.5 gene contains binding sites for Smad adjacent to two essential GATA sites (Lien, McAnally et al. 2002).

HUMAN EMBRYONIC STEM CELL DIFFERENTIATION TO CARDIOMYOCYTES.

Cardiac induction in serum-containing medium

The first published study demonstrating cardiomyocyte differentiation from hESCs employed EB-based induction (Kehat, Kenyagin-Karsenti et al. 2001). EBs were formed by dissociating hESC colonies into clumps containing 3 to 20 cells and culturing these clumps in suspension in serum-containing medium. After 7 to 10 days in suspension, EBs were plated onto culture dishes and spontaneously contracting areas were observed in 8.1% of the EBs after 20 days. Electron microscopy and electrophysiologic recordings displayed characteristic cardiomyocyte morphology and action potentials, respectively. Cells dissected from these contracting areas stained positive for several cardiac specific antibodies including α-myosin heavy chain (MHC), α-actinin, desmin, troponin I and ANP. In a subsequent report on EB-based hESC differentiation to cardiomyocytes, beating was observed in 70% of EBs (Xu, Police et al. 2002). It was suggested that the increased efficiency could have been due to differences in culture conditions during hESC maintenance, in methods of EB formation, and in the quality of serum used for differentiation. In the same study, using Percoll density centrifugation the population was enriched to a concentration of approximately 70% cardiomyocytes (Xu, Police et al. 2002). A third study reported 10 to 25% of EBs were spontaneously contracting after EB-based hESC differentiation (He, Ma et al. 2003). A number of potential sources of variability may account for the different cardiac induction efficiencies achieved between different researchers. Using the number of contracting EBs as a measure of cardiac induction efficiency is one possible source of variability given that detection of beating may vary between individuals and that frequency of beating EBs does not accurately reflect the efficiency of cardiomyocytes generated per input hESC. Another source of variability is that in each of these studies the method of EB formation from hESCs was carried out by enzymatic dissociation of hESC colonies into cell clumps. It is likely that the average EB size, as well as variability of EB sizes fluctuated significantly between labs. Additionally these EBs were cultured in the presence of fetal bovine serum (FBS), a mixture of undefined components known to exhibit lot-to-lot variability.

Cardiac induction in endoderm co-cultures

An alternate approach to EB based differentiation has been to induce cardiac induction of hESC colonies by coculturing them with endoderm cells, perhaps mimicking the observation in the embryo where endodermal tissues appear to promote and/or support mesoderm and cardiac induction during embryogenesis. Cardiogenesis was observed in hESC aggregates cultured on a visceral endoderm feeder layer (END-2 cell line), as evidenced by the appearance of beating areas in 35% of aggregates, and the emergence of cells expressing α-actinin, tropomyosin, and ryadonine receptors (Mummery, Ward-van Oostwaard et al. 2003; Passier, Oostwaard et al. 2005). In EBs cultured in END-2-conditioned, serum-free medium (Xu, Graichen et al. 2008), beating was observed in 60 to 70% of EBs after 12 days of differentiation. The positive effect that END-2-conditioned medium (END2-CM) exerted on cardiac induction of hESCs was associated with an absence of insulin in the serum free medium. An ELISA analysis on END2-CM revealed a significant drop in insulin concentration to negligible levels after 3 to 4 days of exposure to END-2 cells, and beating activity and the expression of cardiac genes decreased with increasing concentrations of exogenously added insulin to END2-CM. A subsequent report examining the mechanism by which insulin leads to reduced cardiogenesis during hESC differentiation found that the presence of insulin did not prevent differentiation of any specific lineage but favored neurectoderm differentiation at the expense of the mesendodermal lineages (Freund, Ward-van Oostwaard et al. 2008).

Cardiac induction in serum-free, defined conditions

Recently it has been demonstrated that it is possible to efficiently generate hESC-derived cardiomyocytes in the absence of serum or mouse cell conditioned medium and without co-culturing hESCs with animal-derived inductive cell types (Yang, Soonpaa et al. 2008). The protocol, based on signaling that occurs during embryonic heart formation, consists of adding combinations of growth factors to the EBs in stages temporally associated with the appropriate period of development. The first stage (EB days 1 to 4) is associated with the induction of a PS-like cell population. Activin A and BMP4, growth factors which have been shown to upregulate PS markers brachyury and Wnt3A (Kispert and Herrmann 1994; Liu, Wakamiya et al. 1999), are added to the EBs. In the next stage (EB days 4 to 8), the cardiac mesoderm commitment stage, DKK1 and vascular endothelial growth factor (VEGF) are added. VEGF promotes expansion

and maturation of mesoderm cells (population expressing kinase insert domain protein receptor, KDR, known as fetal liver kinase-1, FLK1, in the mouse system), while DKK1 inhibits Wnt activity. Although Wnt signaling is required at the onset of differentiation for PS induction (Lindsley, Gill et al. 2006; Naito, Shiojima et al. 2006; Ueno, Weidinger et al. 2007) at this stage endogenous Wnt signaling promotes induction of the definitive endoderm at the expense of cardiac mesoderm (Gadue, Huber et al. 2006). In the final stage (starting on EB day 12), the cardiac cell expansion stage, DKK1 and VEGF continue to be present in the medium and FGF-2 is added to support expansion of the cardiac population. Human ESCs differentiated under these conditions yielded a population of cardiac progenitors on EB day 6, identified by expression of KDR at low levels and absence of CKIT expression, and ultimately yielded a population with 30% of cells expressing cTnT by EB day 14. Plating EBs on day 4 routinely resulted in contracting sheets of cardiomyocytes after 7 to 10 days.

A 2-D system for directed cardiac differentiation of hESCs has also been developed (Laflamme, Chen et al. 2007). In this technique, first hESC colonies are seeded onto Matrigel^{TM}-coated plates and cultured in the presence of MEF-CM for 6 days to reach confluence. Cardiac induction is initiated by replacing MEF-CM with serum-free medium containing Activin A for 24 hours, followed by 4 days of treatment with BMP4. Following day 5, the cells are cultured in the complete absence of cytokines. Twelve days following Activin A treatment, widespread spontaneous contractions are observed, and typically 30% of cells express the cardiac contractile protein marker α-actinin. It was demonstrated that by employing Percoll gradient centrifugation cardiomyocytes could be enriched in these cultures to a frequency of 82.6 ± 6.6%.

SCALABLE PRODUCTION OF HPSC-DERIVED CARDIOMYOCYTES

While hPSCs provide a unique opportunity to study human embryonic development that would not otherwise be possible *in vivo*, these cells are also an exciting source of renewable tissue for novel clinical applications and cell transplantation strategies to treat disease. The ability to generate large numbers of HPS cell-derived differentiated cells is critical to developing these strategies. Stirred suspension cultures are a popular approach to scale-up static dish-based cell cultures because they improve culture homogeneity, permit online monitoring and control of pH and dissolved oxygen concentration, and continuous medium perfusion can be easily enabled (Collins, Miller et al. 1998; Madlambayan, Rogers et al. 2001; Cabrita, Ferreira et al. 2003;

Kwon, Kim et al. 2003; Zandstra, Bauwens et al. 2003; Dang, Gerecht-Nir et al. 2004; Bauwens, Yin et al. 2005).

Scalable stirred suspension bioprocesses for the generation of mESC-derived cardiomyocytes have been well developed (Zandstra, Bauwens et al. 2003; Bauwens, Yin et al. 2005; Schroeder, Niebruegge et al. 2005). The first major challenge to implementing stirred suspension bioreactors for EB-based differentiation was that EBs tend to agglomerate during the first 4 days of differentiation due to the expression of surface markers on ESCs that promote cell-cell aggregation (Dang, Kyba et al. 2002). Initial attempts to prevent EB agglomeration focused on hydrogel encapsulation (Magyar, Nemir et al. 2001; Dang, Gerecht-Nir et al. 2004; Bauwens, Yin et al. 2005; Dang and Zandstra 2005) of ESC aggregates to provide a barrier between EBs. It was subsequently demonstrated that aggregate formation could be controlled by optimizing stirring conditions, specifically examining impeller type and stirring speed (Schroeder, Niebruegge et al. 2005; Niebruegge, Nehring et al. 2008). To purify the heterogeneous differentiating cultures for cardiomyocytes and to deplete undifferentiated cells, a genetic selection technique was used (Klug, Soonpaa et al. 1996; Li, Pevny et al. 1998; Marchetti, Gimond et al. 2002; Zandstra, Bauwens et al. 2003), whereby ESCs were genetically engineered to be neomycin resistant upon expression of myosin heavy chain (MHC). This technique has been demonstrated to efficiently enrich mESC-derived cardiomyoyctes to greater than 70% in the stirred suspension system (Zandstra, Bauwens et al. 2003). Improved culture homogeneity has not only been achieved via stirring, but also by incorporating a settling tube to separate EBs from the culture medium which permitted continuous medium perfusion thereby preventing wide variations in medium component concentrations including glucose and lactate (Bauwens, Yin et al. 2005; Niebruegge, Nehring et al. 2008). Additionally, by implementing direct control of dissolved oxygen concentration in a bioreactor system, improved cardiomyocyte yields per input ESC have been observed under hypoxic conditions (Bauwens, Yin et al. 2005).

The central challenge in generating large numbers of hESC-derived differentiated cell types has been the poor proliferation that has been observed during hESC differentiation. In contrast to what has been observed during mESC differentiation, during EB-based hESC differentiation in static culture cell expansion is typically not observed (Gerecht-Nir, Cohen et al. 2004; Cameron, Hu et al. 2006). Stirred suspension culture of human EBs has generally consisted of an initial 24 hour static EB formation step to prevent hESC aggregates from breaking apart under dynamic

conditions (Cameron, Hu et al. 2006). Interestingly, when human EBs are cultured in dynamic systems, such as stirred suspension bioreactors, proliferation does occur, however cell-fold expansion is still far lower (less than 20-fold) (Gerecht-Nir, Cohen et al. 2004; Cameron, Hu et al. 2006) than what has been observed during mESC differentiation (greater than 60-fold) (Zandstra, Bauwens et al. 2003; Dang, Gerecht-Nir et al. 2004; Bauwens, Yin et al. 2005). While the improved cell expansions may be attributed to the obvious benefits of stirred suspension such as medium homogeneity and reduced variations in metabolic byproducts, the observation that under dynamic conditions human EB concentrations are maintained, while under static conditions EB concentrations sharply decrease in the first 4 days of culture indicate that cell expansion is largely due to the prevention of EB agglomeration in stirred suspension (Cameron, Hu et al. 2006). Further confirmation of reduced EB agglomeration under dynamic conditions is the visual observation that EBs grown in spinner flasks are more homogenous in size and shape than those cultured statically (Cameron, Hu et al. 2006). Importantly, it was demonstrated that representative tissues from the three germ layers are produced in human EBs cultured in stirred suspension (Cameron, Hu et al. 2006) and that differentiation efficiency to the hematopoietic (Cameron, Hu et al. 2006) and cardiac lineages (Niebruegge, Bauwens et al. 2009) are at least comparable to what is achieved under static conditions.

Other dynamic cell culture systems have also been explored for hESC differentiation (Gerecht-Nir, Cohen et al. 2004). Massive cell death and EB agglomeration was observed in human EBs cultured in high aspect rotating vessels. EB agglomeration was prevented in slow turning lateral vessels, and differentiation to cells representing the three germ layers was observed. These observations suggest that while mixing is crucial for cell expansion during human EB differentiation, it is also essential to ensure that stirring is mild enough to prevent EB agglomeration and cell death.

Oxygen concentration has been shown to influence mouse pluripotent stem cell differentiation towards the hematopoietic and cardiac lineages (Gassmann, Fandrey et al. 1996; Sauer, Rahimi et al. 2000; Dang, Gerecht-Nir et al. 2004; Bauwens, Yin et al. 2005). Under hypoxic conditions cardiac induction is enhanced, paralleling embryogenesis, wherein the development of the cardiovascular system takes place as diffusion of oxygen becomes limited by the growth of the embryo (Ramirez-Bergeron and Simon 2001). It is believed that the mechanism for the effect that hypoxia exerts on cardiomyocyte differentiation involves the activation of hypoxia inducible

factor 1 (HIF-1) which activates a number of growth factors that are associated with cardiogenesis including VEGF and FGF-2 (Gassmann, Fandrey et al. 1996; Ramirez-Bergeron and Simon 2001; Dang, Gerecht-Nir et al. 2004).

Improving the yield of specific differentiated cell populations can be achieved by applying the developments that have been made to define cytokine and growth factor conditions that promote commitment of specific cell lineages from hESCs, optimizing hESC aggregate size, improving feeding strategies, controlling oxygen concentration, and incorporating specific cell line enrichment strategies such as antibiotic selection in a scalable dynamic culture system.

THE CELL AGGREGATE AS A SYSTEM TO EXAMINE THE EFFECT OF ENDOGENOUS SIGNALING ON CARDIAC INDUCTION

Differentiation can be skewed in hPSC aggregates to favor cardiac induction

As a differentiation system, the EB has often been viewed as a simple technique to demonstrate the capacity of pluripotent stem cells to differentiate to a number of different cell types, but a poor technique as far as controlling differentiation of stem cells to one specific cell fate. A defining characteristic of the EB is that it gives rise to a heterogeneous population representing all the somatic tissue types. However, given that during embryogenesis spatial and temporal cues from neighboring tissues guide development, it is likely that the heterogeneity within the EB produces an environment with the necessary complexity of signals, regulated by the timing and proportion of emerging inductive tissue-associated cells, to produce all the cell types in the developing embryo. For this reason, the aggregate-based differentiation system is a valuable tool for studying the effect of endogenous signaling on induction efficiency of specific cell fates during pluripotent stem cell differentiation.

The term embryoid body, or EB, is widely used to refer to uncontrolled differentiation induced by culturing aggregates of pluripotent stem cells in suspension, and should be clearly distinguished from aggregate-based differentiation cultures wherein culture parameters are strictly controlled to promote differentiation of a specific cell type. Although the EB cannot give rise to a pure population of any specific cell fate, it is known that the proportions of cells belonging to the mesoderm lineage can be modulated in hPSC aggregates by manipulating the culture system in a variety of ways including addition of exogenous factors (Yang, Soonpaa et al.

2008) and controlling oxygen concentration (Bauwens, Yin et al. 2005) as previously discussed, as well as by genetically modifying input stem cells (Holtzinger, Rosenfeld et al. 2010), and optimizing aggregate size (Burridge, Anderson et al. 2007; Mohr, Zhang et al. 2009).

Aggregate size influences cardiac induction efficiency

As has been previously discussed, a variety of methods have been developed to control hESC aggregate size and this parameter has been shown to influence cardiac induction efficiency (Burridge, Anderson et al. 2007; Mohr, Zhang et al. 2009). In one study using forced aggregation to form hESC aggregates starting with 1000, 3000 and 10000 cells per aggregate, the frequency of spontaneously contracting aggregates was analyzed with respect to input cell number (Burridge, Anderson et al. 2007). It was observed that the frequency of beating outgrowths arising from size-controlled aggregates of all sizes (approximately 10-25%) was always higher than the frequency of beating outgrowths arising from non-size controlled EBs formed in mass culture (approximately 2%). The highest frequency of beating aggregates and highest levels of cardiac gene expression occurred in cultures initiated with the highest aggregate size (10000 cells/aggregate). Another report demonstrated differentiating hESC aggregate size control by maintaining undifferentiated hESC colonies in microwells (ranging in diameter from 100 to 500 μm) and subsequently transferring these 3-D colonies to suspension in serum to induce differentiation . While the maximum frequencies of contracting aggregates (approximately 20%) were observed in cultures initiated from 300 μm microwells, the maximum frequency of cardiac marker myosin light chain (MLC)2A-expressing cells (approximately 3.25%) were detected in cultures initiated from 100 μm microwells. The apparently contradictory findings in these two studies can probably be attributed to differences in methods of aggregate formation (forced aggregation versus microwell) as well as criteria for evaluating aggregate size (cell number versus diameter) and cardiac differentiation (contracting aggregates, gene expression versus protein expression of cardiac markers). Furthermore, these studies were performed using serum-based induction of differentiation which typically results in very poor cardiomyocyte yields (< 5%) making it difficult to interpret the small differences in differentiation efficiency between conditions. However, while significant progress still remains to be made in developing robust methods for directing cardiac differentiation in size-controlled

hESC aggregates, these studies do demonstrate that aggregate size influences cardiac induction of pluripotent stem cells.

The mechanism behind the influence of aggregate size on cardiac induction is still unclear. In size-controlled mESC aggregates generated from microwells ranging from 150 to 450 μm in diameter, it has been observed that the effect of aggregate size on cardiac induction corresponds to differential gene expression levels of Wnt5A and Wnt11 (Hwang, Chung et al. 2009). Specifically, higher levels of beating and cardiac gene expression in larger aggregates (450 μm diameter) corresponded with Wnt11 gene expression and reduced Wnt5A gene expression, whereas smaller aggregates (150 μm diameter) expressed high levels of Wnt5A and Wnt11 expression was undetectable. The mode by which aggregate size influences the expression level of these molecules is unclear, although the authors suggest it may be due to higher levels of endoderm cells present in the largest aggregate size condition (450 μm diameter). It has been recently demonstrated that varying the ratio of endoderm cells in the aggregate influences cardiac differentiation of mESCs (Holtzinger, Rosenfeld et al. 2010). In this study, aggregates were formed by mixing different ratios of mESCs that were transfected with a vector for Doxycycline (Dox)-inducible overexpression of GATA-4 and the parental untransfected cell line. In the case where GATA-4 was induced in 2-day old aggregates, enhanced cardiac differentiation was observed with 50% GATA-4 inducible mESCs (0%, 50% and 100% GATA-4-containing aggregates were examined). The cells that developed into cardiac cells were the non-GATA-4-induced cells. GATA-4-overexpressing cells went on to express Sry-related HMG box (SOX)17 and terminally differentiated to liver. It was concluded that the presence of these $SOX17^{+}$ cells promoted cardiac induction of the non-GATA-4 induced cells.

A number of parameters are affected by varying aggregate size. Diffusion of oxygen and medium components becomes more limited as aggregate size increases. Observations made in studies examining the effect of hESC colony size on pluripotency, in which larger colonies maintained high levels of Oct4 expression while differentiation to the extra-embryonic lineage was promoted in smaller colonies (Peerani, Rao et al. 2007), are likely relevant in a 3-D system. The expectation being that larger aggregates would differentiate more slowly and ExE induction would occur at a higher frequency in smaller aggregates. Geometric relationships also vary with aggregate size, given that the ratio of the surface area to volume of a sphere decreases with

increasing sphere size. It has been widely published in reports examining spatial organization during EB development that one of the first events involves the organization of an outer layer of ExE cells surrounding a pluripotent epiblast-like core (Coucouvanis and Martin 1995; Abe, Niwa et al. 1996; Coucouvanis and Martin 1999; Rula, Cai et al. 2007; Ungrin, Joshi et al. 2008; Moore, Cai et al. 2009). Given that as aggregate size increases, there are fewer cells on the surface relative to interior cells, and that the outer layer of cells consists of ExE cells, it may be that the frequency of ExE cells that develop in an aggregate decreases with increasing aggregate size. As has been previously discussed, it has been observed during both embryogenesis and ESC differentiation that ExE associated tissues and cell lines promote cardiac induction. Therefore, the influence that varying aggregate size exerts on cardiac induction efficiency may be due to directly modulating the frequency of ExE cells present.

An approach to elucidate a mechanism for the effect of hESC aggregate size on cardiac induction efficiency

A number of studies are needed to establish whether the effect of aggregate size on cardiac differentiation efficiency is determined by the ExE differentiation capacity of the aggregate being related to the geometric relationship between the volume of cells on the surface of the aggregate and the total volume of the aggregate. First, an inverse relationship between aggregate size and endoderm frequency has to be observed during the early stages of differentiation prior to cardiac induction. Concurrently, cardiac induction and differentiation must also be tracked with respect to aggregate size and related to an optimal endoderm frequency during early aggregate differentiation. The observation of a trend between aggregate size, endoderm cell frequency and cardiac induction efficiency that is consistent with our hypothesis is, however, insufficient to prove the hypothesis. To confirm that cardiac induction efficiency can be modulated by controlling aggregate size via a mechanism in which aggregate size directly influences ExE cell frequency requires an experiment in which aggregate size and ExE cell frequency is specified independently. This may be accomplished by generating hESC aggregates with varying ratios of ExE cells to hESCs as well as varying ratios of hESCs with impaired ability to differentiate towards ExE to unmanipulated hESCs. To date studies exploring aggregate size control on cardiac differentiation of hESCs have been performed in serum-containing conditions leading to poor cardiac yields wherein small differences in differentiation efficiency between conditions are difficult to meaningfully interpret (Burridge, Anderson et al. 2007; Mohr, Zhang et al. 2009).

Ideally, these studies would be carried out under defined conditions that direct cardiac differentiation (Yang, Soonpaa et al. 2008).

Inhibiting ExE differentiation of hESCs can be accomplished by knocking down genes that are required for ExE development. In F9 embryonal carcinoma cells induced to differentiate with retinoic acid (RA) and dibutyryl cyclic AMP (Bt2cAMP), silencing of transcription factors GATA-4 and GATA-6 combined or SOX7 alone led to reduced expression of ExE-associated markers SOX17 and FoxA2 and impaired development of the morphology that is characteristic of ExE differentiation (Futaki, Hayashi et al. 2004). It appears that SOX7 activity is required upstream of GATA-4 and GATA-6, given that SOX7 silencing led to reduced mRNA and protein expression levels of GATA-4 and GATA-6, while GATA-4/6 silencing had little effect on SOX7 mRNA and protein expression levels. Furthermore, exogenous expression of either GATA-4 and GATA-6 or SOX7 in F9 clones in which SOX7 was stably silenced rescued parietal endoderm differentiation. These observations indicated that SOX7 induces GATA-4/6 expression which is necessary for primitive endoderm development. Based on these data, one method to impair ExE development in hESCs is to inhibit SOX7 expression. Ribonucleic Acid (RNA) interference, used in the F9 embryonal carcinoma studies, can efficiently block expression of the SOX7 transcription factor. The mechanism of RNA interference involves introducing into the cell short double-stranded fragments called short interfering RNAs (siRNAs) which are processed by an enzyme called Dicer resulting in double stranded (ds)RNA with two to three nucleotide long overhangs on the 3' ends. These siRNAs are then separated into single strands and the antisense strand along with Dicer gets incorporated into the RNA induced silencing complex (RISC). After integration into the RISC, the guide strand now guides the entire RISC to target complementary messenger (m)RNA and induce cleavage of the mRNA, thereby preventing it from being used as a translation template (Ahlquist 2002; Shrey, Suchit et al. 2009).

In the studies that will be presented herein, ExE-inducible cells were obtained using SOX7-overexpressing (O/E) hESCs (Seguin, Draper et al. 2008). It has recently been demonstrated that constitutive expression of SOX7 in hESCs produces ExE progenitors (Seguin, Draper et al. 2008). SOX7 complementary (c) deoxynucleic acid (DNA) was introduced to CA1 hESCs via a Cre-inducible expression vector. The vector consists of a CAG promoter driving expression of a floxed bGeo-polyA followed by SOX7-puromycin (puro). Therefore, stably transfected clones

are neomycin resistant and can be selected via treatment with geneticin (G418). Cre-transfection of stably selected clones leads to the excision of the floxed bGeo-polyA, resulting in CAG-driven expression of SOX7 cDNA. SOX7-expressing cells can then be selected with puromycin treatment. Within one passage of SOX7 overexpression (O/E), hESCs exhibit a flattened, epithilial morphology and express endoderm-associated proteins GATA-4, SOX17 and alpha fetoprotein (AFP) as well as pluripotency markers Oct4 and Nanog. Microarray-based expression profiling revealed that, respective to No Cre controls, SOX7 O/E hESCs upregulated ExE markers laminin subunit beta-1 **(**LAMB1), heparin sulfate proteoglycan (HSPG)2, and secreted protein acidic and rich in cystein (SPARC) (Hogan, Cooper et al. 1980; Semoff, Hogan et al. 1982; Mason, Taylor et al. 1986). Additionally, SOX7 O/E hESCs exhibited a characteristic ExE gene expression profile which included GATA-4, GATA-6, HNF4A, FoxA2, AFP, LAMB1, vHNF1 and SOX7, and lacked expression of definitive endoderm (DE)-associated markers (CXC chemokine receptor) CXCR4, (Homeobox protein goosecoid) GSC, and distal-less homeobox (DLX)5 and FoxQ1. Gene expression analysis suggested these cells represent progenitors with predisposition to the ExE lineage. In an ExE differentiation assay, using BMP4-mediated induction, relative gene expression of AFP, LAMB1, vHNF1 and SOX7 was significantly higher in SOX7 O/E hESCs compared to No Cre control hESCs. Additionally, after 5 days of exposure to BMP4, immunoblot assays showed that SOX7 protein levels were detected in control hESCs and were further upregulated in SOX7 O/E hESC. Flow cytometry revealed that 87.73% of the BMP4-treated control hESC population expresses AFP. Meanwhile in SOX7 O/E hESCs 89.13% of the cells express AFP and BMP4-treatment raises expression frequency to 92.62%. Interestingly, while maintenance cultures of SOX7 O/E hESCs retain expression of Oct4 and Nanog, the expression of these pluripotency markers decreases following BMP-mediated differentiation. It has been suggested that expression of these pluripotency markers in SOX7 O/E hESCs is involved in maintaining the precursor phenotype of these cells by preventing terminal differentiation.

To examine the effects of controlling ExE frequency independently of aggregate size on cardiac induction during hESC differentiation, forced aggregation of single cell suspensions in Aggrewells^{TM} is a system that can be easily enabled to generate aggregates with varying ratios of SOX7 siRNA-transfected hESCs or SOX7 O/E hESCs.

HYPOTHESIS

There is an optimal aggregate size for cardiac induction during hESC differentiation that corresponds to the optimal frequency of extraembryonic endoderm (ExE) cells (located on the aggregate surface) in early stage differentiating hESC aggregates.

PROJECT OBJECTIVES AND SPECIFIC AIMS

Overall goal

To develop a method to generate uniform hESC aggregates of controlled size, and further to use this system to study the viable range of aggregate sizes for cardiac induction as well as to elucidate a mechanism for the effect of aggregate size on cardiac induction.

Specific aim 1: Establish a technique for robust generation of uniform hESC aggregates of controlled size.

a) Develop a technique employing micropatterning to generate uniform hESC aggregates and control aggregate size
b) Demonstrate cardiac differentiation in micropatterned hESC aggregates
c) Examine differentiation trajectory in size-controlled hESC aggregates with respect to MP-hESC colony and aggregate size

Specific aim 2: Enable large-scale differentiation of cardiomyocytes from MP-hESC aggregates

a) Evaluate cardiac induction in MP-hESC aggregates in a stirred suspension, oxygen-controlled bioreactor.

Specific aim 3: Reveal the effect of aggregate size on endoderm composition in early-stage hESC aggregates and subsequently demonstrate that cardiac induction is modulated by the endoderm composition during early hESC differentiation

a) Establish a serum-free forced aggregation based system for cardiac induction in size controlled hESC aggregates
b) Quantitatively track ExE composition in early-stage differentiating hESC aggregates
c) Examine the effect of inhibiting ExE differentiation on the efficiency of cardiac induction independently of hESC aggregate size.

SUMMARY

Studies have demonstrated that aggregate size influences cardiac differentiation efficiency during hESC differentiation. Furthermore, it has been widely observed that an ExE layer develops on the surface of the aggregate shortly after aggregate formation. Given the inverse relationship between aggregate size and the frequency of surface cells on the aggregate, we examined the relationship between endoderm cell frequency and cardiac induction efficiency as a possible mechanism behind the influence of aggregate size on cardiogenesis during hESC differentiation.

Methods were developed to control hESC aggregate size in order to investigate the hypothesis that hESC aggregate size influenced cardiac induction by modulating the ratio of endoderm cells during early differentiation. First, differentiation was examined in aggregates generated by micropatterning hESC colonies at defined diameters and transferring intact colonies to suspension in differentiation medium (Chapter 2). In this system, it was revealed that hESC colony size affects the ratio of endoderm- to neural- associated cells in the starting population and this ratio subsequently influences cardiac induction efficiency upon differentiation as aggregates. Normalizing differentiation efficiency results to the ratio of endoderm to neural gene expression in the input hESC population revealed that aggregate size does influence cardiac induction, whereby cardiac induction is optimized in smaller aggregates when the input population expresses higher levels of endoderm-associated genes and in larger aggregates when the input population expresses lower endoderm gene expression levels. Furthermore, when micropatterned aggregates (generated from 400 μm and 800 μm diameter hESC colonies) were cultured in stirred suspension, enhanced cell yields and cardiac differentiation were achieved compared to stirred suspension differentiation of non-size controlled EBs (Chapter 3).

Given that hESC colony size affected the input population status which influenced cardiac induction in subsequently generated hESC aggregates, forced aggregation was implemented to generate aggregates at different sizes from one consistent hESC population (Chapter 4). In these studies, a clear trend emerged in which endoderm differentiation decreased with increasing aggregate size, and cardiac induction and differentiation could be optimized by varying aggregate size. A direct relationship between ExE frequency and cardiac differentiation was established by generating aggregates from varying ratios of ExE progenitor cells and hESCs.

From these studies, it was established that the influence of aggregate size on cardiac induction is related to the frequency of endoderm cells that develop on the surface of the aggregate. Aggregate size appears to dictate endoderm differentiation frequency in an inverse relationship whereby the endoderm composition decreases with increasing aggregate size. We theorized that this relationship is related to the ratio of the surface area to volume of a sphere, given that an ExE cell layer develops on the EB surface during differentiation. Specifically, the frequency of endoderm cells that will develop during early aggregate-based differentiation will be lower in larger-sized aggregates. The findings in this work are significant not only towards gaining a deeper understanding of the mechanism that guide cardiac development but also towards improving cardiac induction efficiency during hESC differentiation and the methods developed herein can contribute towards large scale culture of relatively enriched hESC-derived cardiomyocytes.

Chapter 2
Control of Human Embryonic Stem Cell Colony and Aggregate Size Heterogeneity Influences Differentiation Trajectories

This chapter has been published in *Stem Cells*. (Bauwens et al., 2008; 26(9): 2300-10). Co-authors include Raheem Peerani, Sylvia Niebruegge, Kimberly A. Woodhouse, Eugenia Kumacheva, Mansoor Husain, and Peter W. Zandstra. Permission to reproduce this work has been obtained from AlphaMed Press and all co-authors.

ABSTRACT

To better understand endogenous parameters that influence pluripotent cell differentiation we used human embryonic stem cells (hESC) as a model system. We demonstrate that differentiation trajectories in aggregate [embryoid body (EB)]-induced differentiation, a common approach to mimic some of the spatial and temporal aspects of in vivo development, are affected by three factors; input hESC composition, input hESC colony size, and EB size. Using a micro-contact printing approach, size-specified hESC colonies were formed by plating single cell suspensions onto micropatterned (MP) extracellular matrix islands. Subsequently, size-controlled EBs were formed by transferring entire colonies into suspension culture enabling the independent investigation of colony and aggregate size effects on differentiation induction. Gene and protein expression analysis of MP-hESC populations revealed that the ratio of GATA-6 (endoderm-associated marker) to paired box (PAX)6 (neural-associated marker) expression increased with decreasing colony size. Moreover, upon forming EBs from these MP-hESCs, we observed that differentiation trajectories were affected by both colony and EB size influenced parameters. In MP-EBs generated from endoderm-biased (high GATA-6:PAX6) input hESC, higher mesoderm and cardiac induction was observed at larger EB sizes. Conversely, neural-biased (low GATA-6:PAX6) input hESC generated MP-EBs exhibited higher cardiac induction in smaller EBs. Our analysis demonstrates that heterogeneity in hESC colony and aggregate size, typical in most differentiation strategies, produces subsets of appropriate conditions for differentiation into specific cell types. Moreover, our findings suggest that the local microenvironment modulates endogenous parameters that can be used to influence pluripotent cell differentiation trajectories.

INTRODUCTION

The promise of human pluripotent cells as a renewable source of specialized cells has been limited by progress in the development of robust differentiation protocols. Since the first reports of successful human embryonic stem cell (hESC) derivation and maintenance (Thomson, Itskovitz-Eldor et al. 1998; Reubinoff, Pera et al. 2000), significant efforts have been made to develop methods to control their differentiation into functional cells and tissues. The generation of induced pluripotent stem (iPS) cells from human cells (Takahashi and Yamanaka 2006; Takahashi, Tanabe et al. 2007; Yu, Vodyanik et al. 2007) further motivates our need to design

controlled and reproducible mature cell production strategies. Initiating hESC differentiation either in attached colonies or by forming embryoid bodies (EBs) has demonstrated in vitro lineage potential in each of the three germ layers (endoderm, ectoderm, and mesoderm), including pancreatic β-cells, neural cells, cardiomyocytes and blood cells (Thomson, Itskovitz-Eldor et al. 1998; Itskovitz-Eldor, Schuldiner et al. 2000; Schuldiner, Eiges et al. 2001; Xu, Inokuma et al. 2001). Differentiation in EBs recapitulates many aspects of embryonic development (Keller 1995). However, although it has been recognized that the developmentally relevant emergence of specialized tissues and their subsequent differentiation to mature functional cell types can be influenced by local inductive cues, few studies have used microenvironmental control to prospectively regulate endogenous parameters that influence pluripotent cell differentiation trajectories.

In the embryo it is recognized that cardiogenesis is directed via the coordination of inductive cues from the anterior primitive endoderm (Sugi and Lough 1994; Schultheiss, Xydas et al. 1995; Sugi and Lough 1995; Schultheiss, Burch et al. 1997; Schultheiss and Lassar 1997) and inhibitory cues originating from neurogenic tissue (Climent, Sarasa et al. 1995; Schultheiss, Burch et al. 1997; Raffin, Leong et al. 2000). Accordingly, methods to drive mesoderm and cardiac induction during hESC differentiation have included co-culturing hESCs with the visceral endoderm-like cell line END-2 (Mummery, Ward-van Oostwaard et al. 2003) or the addition of Transforming Growth Factor Beta (TGF-β) family proteins (most commonly activin A and Bone Morphogenetic Protein (BMP)-2 or BMP-4) that are known to be secreted by primitive endoderm (Burridge, Anderson et al. 2007; Laflamme, Chen et al. 2007). These studies aim to exploit observations made in the embryo to direct cardiogenesis through exogenous factor-mediated control. We hypothesize that, in addition to these exogenous factors, endogenous parameters such as local cellularity and organization can impact *in vitro* hESC differentiation. These endogenous parameters may play a role in tissue development during embryogenesis. In this report we explore some of these parameters and document their effect on hESC differentiation trajectories.

Many parameters can influence hESC differentiation outcome, including the handling and status of the input hESC population, media composition, and the method of inducing differentiation (Kitsberg 2007). Human ESC propagation typically requires paracrine and autocrine signals as well as physical cell-cell contact (Schatten, Smith et al. 2005; Pyle, Lock et al. 2006). As a

result, single cell dissociation is usually avoided during hESC passaging (Thomson, Itskovitz-Eldor et al. 1998; Amit, Carpenter et al. 2000) and hEB formation (Kehat, Kenyagin-Karsenti et al. 2001; Xu, Police et al. 2002). Partial dissociation of hESC colonies results in a wide range of colony and aggregate (EB) sizes. This yields a potential source of variability in subsequent differentiation experiments (Peerani, Rao et al. 2007). Recently, control of human EB size has been reported by a number of groups using either forced aggregation of defined cell numbers (Ng, Davis et al. 2005; Burridge, Anderson et al. 2007; Ungrin, Joshi et al. 2008) or microwells to form 3-D hESC aggregates of specified dimensions which can then be transferred to suspension to form mono-disperse EBs (Khademhosseini, Ferreira et al. 2006; Mohr, de Pablo et al. 2006). EB size may not only be an important parameter to improve reproducibility of hESC differentiation experiments but also a potentially important parameter to regulate endogenously influenced cell type-specific differentiation, as has been recently reported (Burridge, Anderson et al. 2007). However, the interaction between controlling EB size and endogenously-driven cell type-specific differentiation bias, has not been explored.

Here we detail the development of a multi-stage EB-based differentiation method to control colony and EB size that takes advantage of the microcontact printing technique we have previously described (Peerani, Rao et al. 2007). Using this system we demonstrate that the ratio of endoderm- to neural-associated gene and protein expression can be manipulated as a function of colony size, and that this ratio varies between passages in conventionally propagated hESC cultures. Furthermore, by generating homogeneously-sized colonies and EBs we revealed that optimizing this ratio is important for maximizing endogenous mesoderm and cardiac induction during hESC differentiation. These data suggest that improved reproducibility and efficiency of cell type-specific differentiation will not only require controlling colony and EB size, but also new technologies to control and characterize the status of the hESC population prior to initiating differentiation.

MATERIALS AND METHODS

hESC maintenance

The H9 and H2B cell lines used in these experiments were obtained from the Israel Institute of Technology; the use of the cells in this project has been approved by the Canadian Stem Cell Oversight Committee. Human ESC (passages 40 to 50) colonies were maintained on irradiated MEFs in knockout Dulbecco's Modified Eagle's Medium (ko-DMEM, Invitrogen) supplemented with 20% knockout Serum Replacement (ko-SR, Invitrogen) and 4 ng/mL Fibroblast Growth Factor (FGF)-2 (PeproTech). Passaging was performed every 4 days by dissociating the cells into small clumps using Collagenase type IV (2 mg/mL, Invitrogen) and replating on a mouse embryonic fibroblast (MEF) feeder layer at a subculture ratio of 1:6.

Matrigel™ Patterning

Micro-contact printing was employed to pattern Matrigel™ (BD Biosciences) onto tissue culture surfaces. The protocol used (Figure 2.1A) to print the patterns has been adapted from a published technique(Tan, Liu et al. 2004). Briefly, a variety of stamps, made out of poly(dimethylsiloxane) (PDMS) using soft lithography(Younan 1998), were used for printing different specified pattern geometries. The PDMS stamps were sterilized in 70% ethanol overnight, inked with an aqueous solution of pH 5 1:30 growth factor reduced Matrigel™ (GFR-MG) for 1 hour, rinsed with sterile ddH_2O and dried with sterile N_2. After rinsing and drying, a monolayer of protein remains on the surface. This layer is transferred to the substrate by placing the stamp in conformal contact with the substrate for more than 10 seconds. The substrates used were tissue culture treated 60 mm dishes (Falcon). This substrate is optimal for both protein adsorption and passivation by 5%w/v Pluronic F-127 (MW=12600Da) (Sigma) which is used to prevent protein adsorption and cell attachment to unpatterned regions of the substrate(Tan, Liu et al. 2004). Using this protocol, cells can be seeded on the substrate with little non-specific binding to the passivated regions and no migration of cells between features.

Seeding hESCs on a GFR-MG™-patterned surface

GFR-MG was micropatterned at three feature diameters: 200, 400, and 800 μm (referred to as 200MP, 400MP, and 800MP respectively). Human ESC colonies were dissociated to single cells using TrypLE™ (Invitrogen). TrypLE™ is a dissociation enzyme reagent that effectively dissociates hESC colonies/aggregates to single cells with high viability (see Figure S1-1). Single cell suspensions of hESC were resuspended in completely defined X-VIVO10™ medium (Cambrex)(XV medium) with 2 mM L-Glutamine (Invitrogen), 1x nonessential amino acids (NEAA) (Invitrogen), 0.1 M β-mercaptoethanol (Sigma) and supplemented with 40 ng/ml FGF-2 and 0.1 ng/ml TGFβ-1 (R&D Systems), and subsequently plated on the patterns at a concentration of 1.5×10^6 cells/mL. Twelve hours post-seeding, the patterned cells were washed three times with XV medium to prevent cell attachment on unpatterned areas (Figure 2.1A).

Formation and differentiation of EB aggregates from hESC colonies

To form EBs, 2 or 3 day old confluent micropatterned (MP)-hESC colonies were scraped off the dishes gently (to preserve intact colonies), and resuspended in hESC differentiation medium containing ko-DMEM, 20% FBS (Gibco), 1x NEAA, 2 mM L-Glutamine (Invitrogen), 0.1 M β-mercaptoethanol (Sigma), and 50U/mL penicillin/streptomycin (Gibco). Cell number in hESC colonies and suspension aggregates were measured by staining cells with a fluorescent DNA binding dye (Cyquant, Invitrogen) and measuring average fluorescence intensity with a fluorescence microplate reader (Spectramax Gemini). Aggregates were transferred to suspension on ultra-low attachment non-tissue culture treated plates (Corning) for 4 days and then plated onto 0.5% gelatin coated tissue culture treated dishes to induce cardiac differentiation in EB outgrowths. Cultures were carried out for 16 days following EB formation. EBs formed using published EB formation protocols served as controls (Xu, Police et al. 2002).

Quantitative analysis of EB size distribution

The number of aggregates formed was determined by manual counting on a microscope 1 day after transferring colonies to suspension culture. To measure aggregate size distribution under the different aggregate formation conditions, image analysis was performed with Image-Pro1 Plus software (Media Cybernetic). The number of cells per EB was determined by dissociating a known number of EBs to single cells and counting cells.

Flow cytometry

Pluripotency of the starting (input) hESC population was evaluated by flow cytometric analysis of Oct4 protein expression. Human ESC colonies were enzymatically dissociated to single cells and fixed and permeabilized with the IntraPrep fixation and permeabilization kit (Immunotech). Fixed and permeabilized cells were incubated at a 1:100 dilution of Oct-4 antibody (Santa Cruz Biotechnology) for 20 min at room temperature, followed by an incubation with secondary fluorescein isothiocyanate (FITC)-conjugated IgG antibody (Molecular Probes) at a 1:100 dilution for 20 min at room temperature. Viability was assessed using 7-aminoactinomycin D (7-AAD) (Invitrogen). Cells were analyzed with a flow cytometer (XL; Beckman-Coulter), using EXpoADCXL4 software (Beckman-Coulter). Positive staining was defined as the emission of a level of fluorescence that exceeded levels obtained by 99.5% of cells from the control population stained with only the secondary antibody.

Quantitative RT-PCR analysis

Cells were digested in Trizol Reagent (Invitrogen), followed by chloroform extraction and precipitation with iso-propyl alcohol. The RNA was then purified using RNAEasy columns (Qiagen) with an on-column DNaseI digestion step. cDNA was generated from purified RNA by using Superscript-III reverse transcriptase (Invitrogen) as per the manufacturer's instructions. 10 ng of cDNA was used per PCR reaction using iQ-SYBR-green master mix (BioRad) in triplicate. Relative expression was determined by delta-delta Ct method with the expression of beta-actin as internal housekeeping reference (expression of GAPDH was used as a second internal housekeeping reference). Total RNA from human fetal heart, human fetal liver, and human fetal brain were used as positive controls (Stratagene). Primer sequences, derived from the MGH Primerbank (Wang and Seed 2003), were as follows: Oct4 (5' primer), CTTGAATCCCGAATGGAAAGGG, and (3' primer), CCTTCCCAAATAGAACCCCCA, GATA-6 (5' primer), AGGGCTCGGTGAGTCCAAT, and (3' primer), CGCTGCTGGTGAATAAAAAGGA, PAX6 (5' primer), AAGAGCAACGTCACCAGTTTC, and (3' primer), GGAGCCCGGTTGATACCAG, Brachyury (5' primer), TGCTTCCCTGAGACCCAGTT, and (3' primer), GATCACTTCTTTCCTTTGCATCAAG, Mixl1 (5' primer), CCGAGTCCAGGATCCAGGTA, and (3' primer), CTCTGACGCCGAGACTTGG, α-Actinin (5' primer), GGGTCCGTTTGCCAGTCAG, and (3'

primer), GGCTTTCCTTAGGTGGGAGTT, Nanog (5' primer), CAAAGGCAAACAACCCACTT, and (3' primer), TCTGCTGGAGGCTGAGGTAT, CXCR4 (5' primer), CACCGCATCTGGAGAACCA, and (3' primer), GCCCATTTCCTCGGTGTAGTT, Sox3 (5' primer), GCCGACTGGAAACTGCTGA, and (3' primer), CGTAGCGGTGCATCTGAGG, TroponinT (5' primer), GGACGAAGACGAGCAGGAG, and (3' primer), CTTCCGGTGGATGTCATCAAA, β-actin (5' primer), CATGTACGTTGCTATCCAGGC, and (3' primer), CTCCTTAATGTCACGCACGAT, GAPDH (5' primer), CTCCACGACGTACTCAGCG, and (3' primer), TGTTGCCATCAATGACCCCTT. Specificity of amplification was assured with analysis of dissociation curves of all reactions. For all samples a control was performed without reverse transcriptase and no amplification was detected in these controls.

Immunostaining analysis

Fluorescent images of α-Actinin (EA-53, 1:800, Sigma), Connexin-43 (1:25, Molecular Probes), GATA-6 (1:20, R&D Systems) and Oct4 (1:200, Santa Cruz Biotechnology) protein expression were obtained and quantitatively analyzed using the Compartmental Analysis or Target Activation assay algorithms available with the Cellomics Arrayscan V^{TI} platform (Cellomics).

Statistics

To evaluate differences in gene expression level between conditions, statistics were manually computed using the Wilcoxon signed rank test for a paired difference experiment at a significance level of $P < 0.05$. To evaluate differences in EB size between conditions, statistics were computed in Origin 7.5 using the paired t-test at a significance level of $P < 0.05$. Error bars on plots represent the standard deviation of the mean of three or more replicates ($n>3$).

RESULTS

An approach for generating size-controlled hESC colonies and EBs

Typically, EB-based hESC differentiation involves partial enzymatic dissociation of hESC colonies resulting in a suspension of cell clumps of varying sizes (Figure 2.1B). We have developed a process, illustrated in Figure 2.1A, for generating uniform EBs of controlled size based on micropatterning hESC colonies at defined diameters. Briefly, hESC colonies are

dissociated to single cells and replated at high density onto micropatterned Matrigel™ islands. Upon confluence, MP-hESC colonies are transferred to suspension culture by detaching them intact with a cell scraper and resuspending the colonies in hESC differentiation medium. Figure 2.1C depicts the overall approach, outlining three aspects of this system which could affect endogenous control of differentiation trajectory: 1) Status of the input hESC population; 2) Micropatterned (MP)-hESC colony size; and 3) MP-EB size.

Even under maintenance conditions, hESC cultures do not consist of a homogeneous pluripotent population but contain hESC-derived differentiated cells (Henderson, Draper et al. 2002; Furusawa, Ohkoshi et al. 2004). Therefore the composition of the input hESC population varies between passages and could impact cell fate trajectory during differentiation. Colony size is also an important parameter in determining self-renewal and differentiation fate, as hESC maintenance relies on paracrine signaling from neighboring undifferentiated cells to antagonize pro-differentiation signals (Peerani, Rao et al. 2007). Finally, EB size could affect differentiation as control of this parameter may modulate spatial signaling within the aggregate.

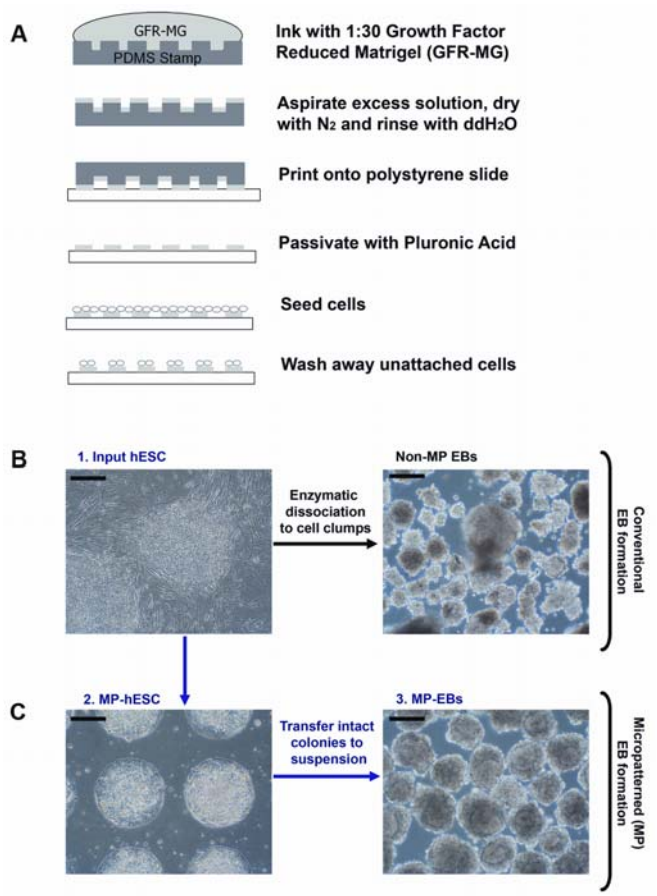

Figure 2.1: Overview of conventional and micropatterned (MP) hESC colony and EB formation. (A) Outline of the process for micropatterning Matrigel^{TM} (MG) on a cell culture substrate, and subsequently seeding cells onto MG-patterned substrate. **(B)** In conventional EB formation, hESC colonies (input hESC) are enzymatically dissociated to cell clumps and transferred to ultra-low attachment tissue culture plates in hESC differentiation medium. **(C)** To generate size-controlled colonies, hESCs are dissociated to single cells and plated at high density (1×10^6 cells/mL) onto patterned Matrigel^{TM} islands and cultured to confluence (2-3 days) in serum-free maintenance medium. To form MP-EBs, intact colonies are detached using a cell scraper and transferred to suspension in differentiation medium. Scale bar = 250 μm

The influence of colony size on differentiation trajectory in MP-hESC colonies

To evaluate the effect of colony size on differentiation trajectory, hESC colonies were patterned at three diameters (Figure 2.2A): 200, 400 and 800 μm (200MP, 400MP, and 800MP respectively). Additionally, non-patterned (non-MP) conventional hESC colonies were cultured in parallel for comparison. A flow cytometry analysis of six separate input hESC populations demonstrates that in each run the majority of cells express the pluripotency protein Oct4 with expression frequencies ranging from 57% to 78.4% in six independent input populations (Figure 2.2B). To determine the effect of colony size on differentiation trajectory, quantitative

(q)RTPCR was performed to compare gene expression levels between input hESC populations and their corresponding day 2 or 3 colony size-controlled, micropatterned (MP)-hESC derivatives. Oct4, GATA-6, and PAX6 gene expression levels were tested as a surrogate measure for undifferentiated cells, endodermal and neural differentiation/commitment respectively. Importantly, these trends were reproduced with a second gene set [Nanog for undifferentiated cells, CXCR4 for endoderm, and Sox3 for neural (Figure S1-2)]. As demonstrated in the three representative runs shown in Figure 2.2C, variability in lineage-specific gene expression in the input-hESC population led to variability in gene expression in the MP-hESC populations. Despite variations between runs, similar trends were observed in each run in terms of the effect of colony size on gene expression level (see Table 2-I for statistical validation of these trends). Non-MP hESCs expressed similar levels of expression for all three genes as the input hESC populations, thus demonstrating that the process of passaging onto Matrigel^{TM} in serum-free medium itself does not skew the population. Non-MP and 200MP colonies maintained the Oct4 gene expression level of their input hESC, whereas a significant increase in Oct4 gene expression levels was observed in the larger colonies (400MP and 800MP). It should be noted that our gene expression analysis detects the Oct4A and Oct4B isoforms. It has recently been reported that expression of the Oct4B isoform is not exclusive to undifferentiated ESCs and is predominantly expressed in the cytoplasm (Lee, Kim et al. 2006). Using immunofluorescence, we have demonstrated that Oct4 protein expression in the input hESC population is localized in the nucleus (Figure S1-3), suggesting that we are measuring Oct4A isoform expression. Compared to input hESCs, the GATA-6 gene expression level was maintained in non-MP hESCs. In MP-hESCs, expression of this endoderm marker rose significantly in small colonies (200MP), with gene expression level decreasing as colony size increased. Conversely, PAX6 gene expression levels suggest that markers of neural differentiation rise significantly in larger colonies (400MP and 800MP) than in smaller colonies (200MP) (Table 2-I). We followed the gene expression analysis with an examination of protein expression of these markers in our MP-hESC colonies. The frequency of Oct4 protein-expressing cells was similar at each colony size (Figure 2.2E), ranging between 80 to 85%, despite increasing Oct4 gene expression with increasing colony size. Conversely, GATA-6 protein expression frequency, consistent with the GATA-6 gene expression data, was significantly higher in the small 200MP colony condition (55 to 60%). PAX6 protein expression was not detectable at this stage of differentiation. Interestingly, while GATA-6 and Oct4 co-

expression was observed in the small 200MP colonies (Figure 2.2D-i), in the larger 400MP and 800MP hESC colonies co-expression was generally not observed (Figure 2.2D-ii and 2.2D-iii). These data suggest that controlling colony size can impact changes in gene expression in cells that still express pluripotency markers to skew the probability of the cells taking one differentiation trajectory over another.

Next, we employed an analysis of the ratio of endoderm-to-neural gene expression levels (GATA-6:PAX6) in the input hESC and output MP-hESC populations to investigate relationships between colony size and differentiation trajectory with respect to the input hESC composition (Figure 2.3A). In runs initiated with *intermediate* input GATA-6:PAX6 ratios between 0.35 and 0.55 (i.e. a "balanced" population), it was observed that the output MP-hESC ratio of endoderm (GATA-6) to neural (PAX6) gene expression was always higher than the input hESC ratio, and that GATA-6:PAX6 decreased with increasing colony size. Input hESC populations with GATA-6:PAX6 ratios that were at *high* (> 0.55) and *low* (< 0.35) extremes resulted in almost no change in GATA-6:PAX6 ratio in the non-MP, 400MP and 800MP conditions, possibly indicating that these ratios represent cell populations that are not easily manipulated. The smallest colony condition (200MP) displayed an increase in the GATA-6:PAX6 ratio post-MP regardless of the input hESC ratio. The increase in endoderm gene expression post-MP in the 200MP condition may be attributed to the rapid differentiation of hESCs occurring at low localized cell densities (localized cell density refers to the number of cells per unit radius; in this case the number of cells per 500 μm radius). Not surprisingly, non-MP colonies showed no changes in ratios after a conventional passage was performed in parallel with the patterned conditions. As illustrated in Figure 2.3B, these results reveal two important parameters that affect differentiation trajectory in this system, input hESC composition and MP-hESC colony size. Schematically, input hESCs typically display a range of GATA-6 and PAX6 expressions levels (Figure 2.3B-i), which subsequently shift upon micropatterning according to colony size. In these studies it was observed that larger colonies support enrichment of neural-fated cells while smaller colonies support the enrichment of endoderm-fated cells (Figure 2.3B-ii).

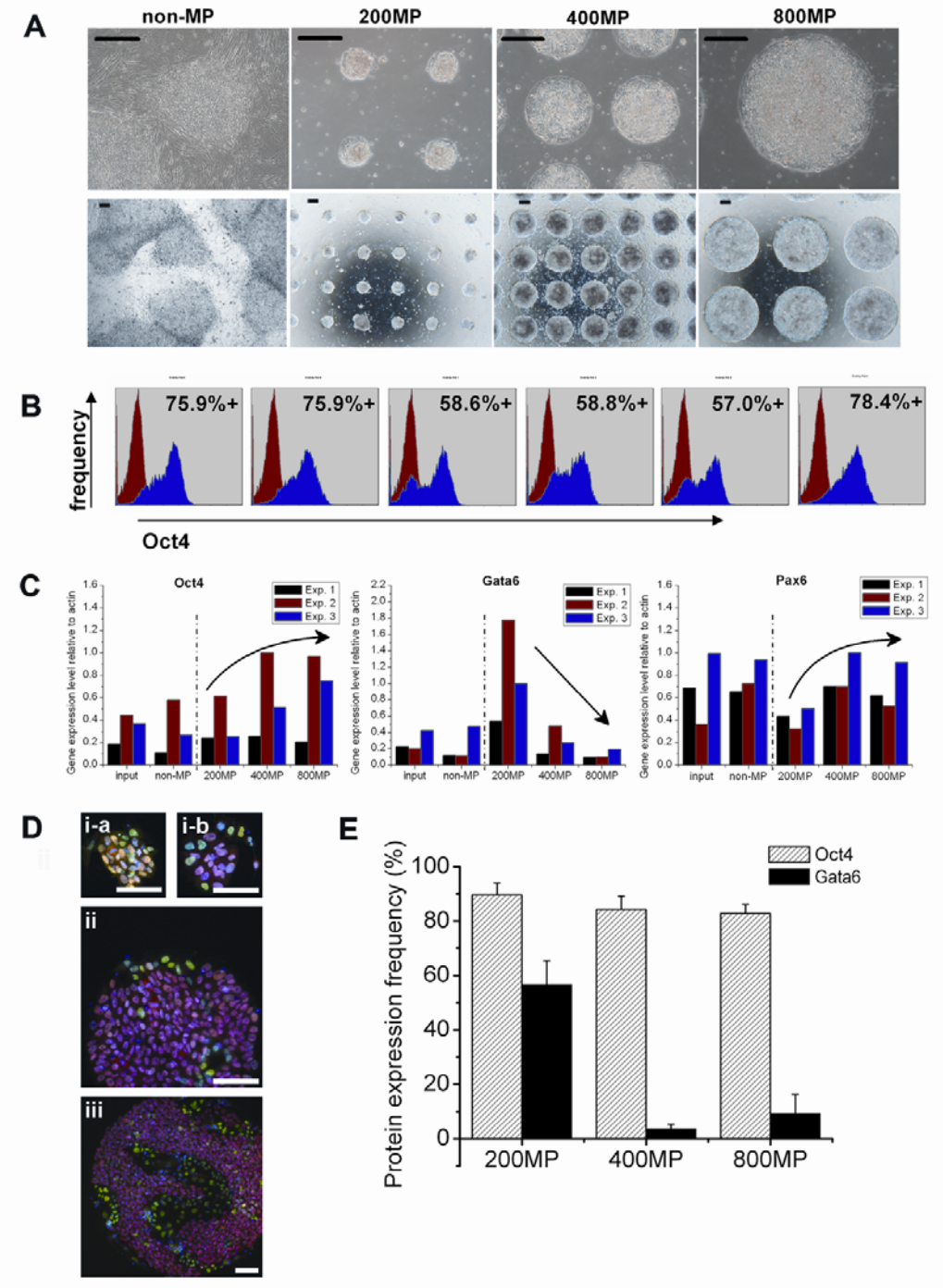

Figure 2.2: Analysis of size controlled MP-hESC colonies reveals the influence of colony size on differentiation trajectory. (A) Bright field images, at high (top panel) and low (bottom panel) magnification, of non-patterned (non-MP) hESC colonies and colonies patterned at 200, 400 and 800 μm diameters (200MP, 400MP, and 800MP respectively). Scale bars = 250 μm. **(B)** Representative flow cytometry results of input hESC Oct4 protein expression from six independent runs. Blue: Oct4-stained population. Percentages indicate frequency of positive-staining cells compared to secondary antibody control (red). **(C)** Representative qRTPCR analysis for 3 out of 7 trials for expression of Oct4, Gata6, and Pax6 (Collective results of all trials found in Table 2-I). **(D)** Immunofluorescence images displaying Oct4 (red) and Gata6 (green) protein expression in 200MP (i), 400MP (ii) and 800MP (iii) colonies. Hoechst was used as a nuclear stain. Scale bars represent 175 μm. **(E)** Gata6 and Oct4 protein expression frequencies in 200MP, 400MP, and 800MP hESC colonies.

TABLE 2-I. Gene expression level ranges of pre-patterned (Input hESC) and post-patterned (Non-MP and MP-hESC) hESC cultures (n=7)

	Mean (Range) Gene Expression Level[a]		
	Oct4	***Gata6***	***Pax6***
Input hESC	0.33 (0.16-0.71)	0.27 (0.20-0.43)	0.77 (0.36-0.98)
Non-MP	0.32 (0.11-0.58)	0.24 (0.11-0.48)	0.77 (0.66-0.94)
200MP	0.37 (0.25-0.61)	1.11 (0.54-1.78)[b, c]	0.42 (0.32-0.51)[b, c]
400MP	0.65 (0.26-1)[b, c, d]	0.42 (0.03-1.00)[d]	0.68 (0.44-0.99)[d]
800MP	0.66 (0.21-0.97) [b, c, d]	0.19 (0.0045-0.48)[d, e]	0.66 (0.36-0.92)[d]

[a]When significant differences exist they are displayed for each condition with conditions in previous row
[b]differs significantly from input hESC
[c]differs significantly from non-MP
[d]differs significantly from 200MP
[e]differs significantly from 400MP

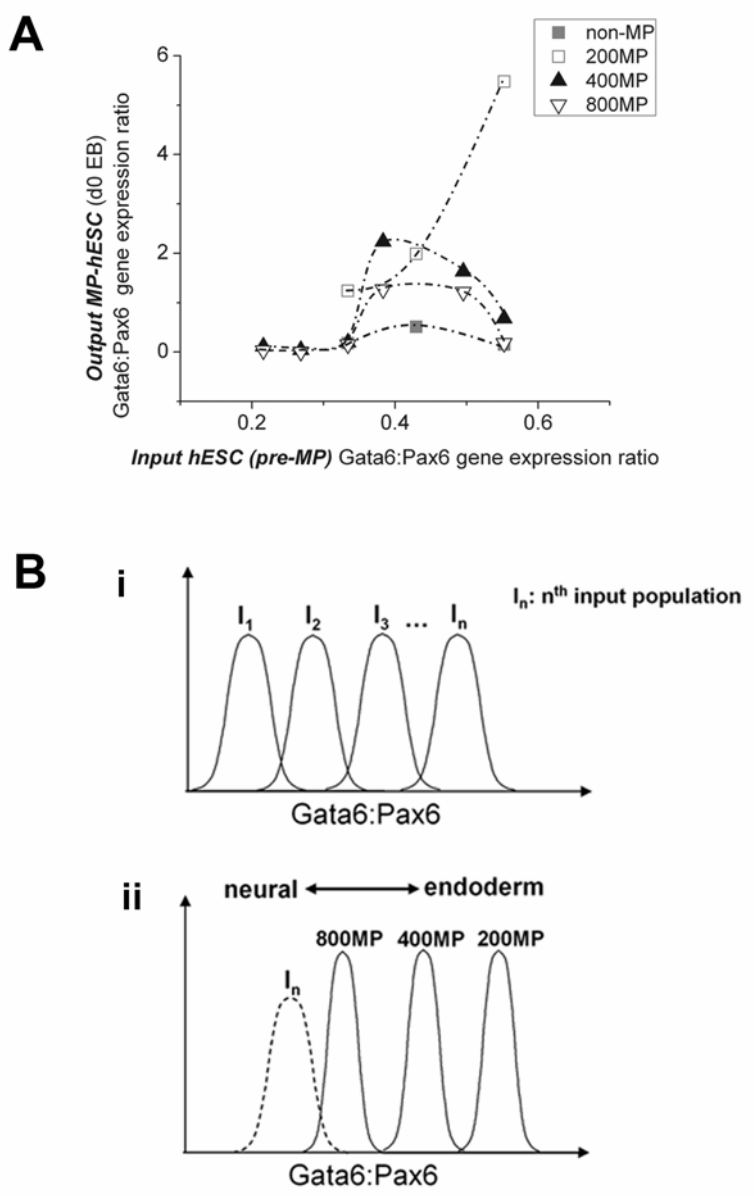

Figure 2.3: Gata6 to Pax6 gene expression ratios in MP-hESC cultures are influenced by input hESC composition and colony size. (A) The effect of (output) MP-hESC colony size on the gene expression ratio Gata6:Pax6 with respect to the corresponding input hESC Gata6:Pax6. **(B)** Schematics illustrating (i) variations in distribution of Gata6:Pax6 gene expression ratios between each input hESC populations (I), and (ii) the relationship between the Gata6:Pax6 gene expression ratio of any given Input hESC population (I, dotted line) and its corresponding MP-hESC Gata6:Pax6 ratios at each colony size (200MP, 400MP, and 800MP, solid lines).

The influence of colony size on differentiation trajectories in hESC-derived EBs

To evaluate our ability to control EB size using our patterning method, image analysis was performed on light microscopy images of day 1 EBs (Figure 2.4A) to calculate size distributions based on EB diameter. Narrower size distributions were observed in MP-EB cultures compared

to non-MP EB cultures. Furthermore, significantly different EB size distributions were observed between EB cultures generated from each hESC colony size examined (200MP, 400MP, and 800MP) (Figure 2.4B-i). In addition to EB diameter, colony and aggregate size control was also evaluated using a fluorescent DNA method (Cyquant, Invitrogen) to measure cell number (Figure 2.4B-ii). This analysis demonstrated that the number of cells in each colony is comparable to the number of cells in each aggregate upon EB formation. Furthermore, based on cell number, significant differences in EB size were observed between 200MP and 800MP, and 400MP and 800MP (Figure 2.4B-ii).

Within the EB, differentiation is guided by spatial cues and interactions between various cell types. Accordingly, it is probable that the specific composition (or gene expression status) of the hESC population used to initiate EBs is an influential factor in determining cell fate during EB development. Given that mesoderm commitment and cardiogenesis in the embryo is thought to be regulated through coordinated inductive and inhibitory signals from neighboring endoderm (Schultheiss, Xydas et al. 1995; Sugi and Lough 1995; Zhu, Sasse et al. 1999) and neural tissue respectively (Marvin, Di Rocco et al. 2001; Tzahor and Lassar 2001), and that the ratio of neural- and endoderm-associated gene expression in hESC cultures can be manipulated by varying colony size, we next examined if this ratio influenced mesoderm and cardiac induction in size-controlled EBs. Using qRTPCR, mesoderm- (Brachyury (Bry) and Mixl1) and cardiac- (α-Actinin) associated gene expression levels were measured in EB outgrowths eight days (day 8) after EB formation. Brachyury is transiently expressed in early mesoderm (Hakuno, Takahashi et al. 2005), and has been shown to be expressed at elevated levels between day 4 and day 10 of EB differentiation (Bettiol, Sartiani et al. 2007; Kolodziejska, Ashraf et al. 2008). Mixl1 is expressed in the primitive streak (Pearce and Evans 1999; Robb, Hartley et al. 2000), and in hESC-derived EBs from day 3 to day 10 (Pick, Azzola et al. 2007). α-Actinin is a cardiac contractile protein gene that has also been detected in differentiating hESC-derived EBs by day 12 (Passier, Oostwaard et al. 2005; Beqqali, Kloots et al. 2006). Plotting gene expression levels of day 8 EB outgrowths with respect to the neural and endoderm composition of their starting MP-hESC populations (Figure 2.5A) revealed similar expression profiles for both mesoderm and cardiac markers. It was observed that gene expression levels of all mesoderm and cardiac markers examined were maximized in 400MP and 800MP EBs generated from MP-hESC populations with GATA-6:PAX6 expression level ratios above 0.1 (Figure 2.5A), whereas gene

expression was virtually undetectable in EBs generated from neural-enriched MP-hESCs (GATA-6:PAX6 < 0.01, mostly 800MP) and endoderm-enriched MP-hESCs (GATA-6:PAX6 > 1, 200MP colonies). Non-MP cultures gave rise to starting population compositions across the range observed for cardiac gene induction in MP-hESC cultures (0.1 to 1); however resulted in notably lower gene expression levels for all mesoderm and cardiac differentiation markers, likely due to heterogeneity in responsiveness. Given that non-MP EBs were generated from non size-controlled hESC colonies (Figure 2.2A) the measured GATA-6 and PAX6 gene expression levels for non-MP hESCs represent an average of different colony (Figure 2.4B) sizes with varying ratios of endoderm-fated and neural-fated cells. While the average GATA-6:PAX6 ratio for the non-MP condition falls within the optimum range for cardiac induction, it includes high ratios for small GATA-6-expressing colonies and low ratios for large PAX6-expressing colonies which were observed to result in poor cardiac induction (Figure 2.5B).

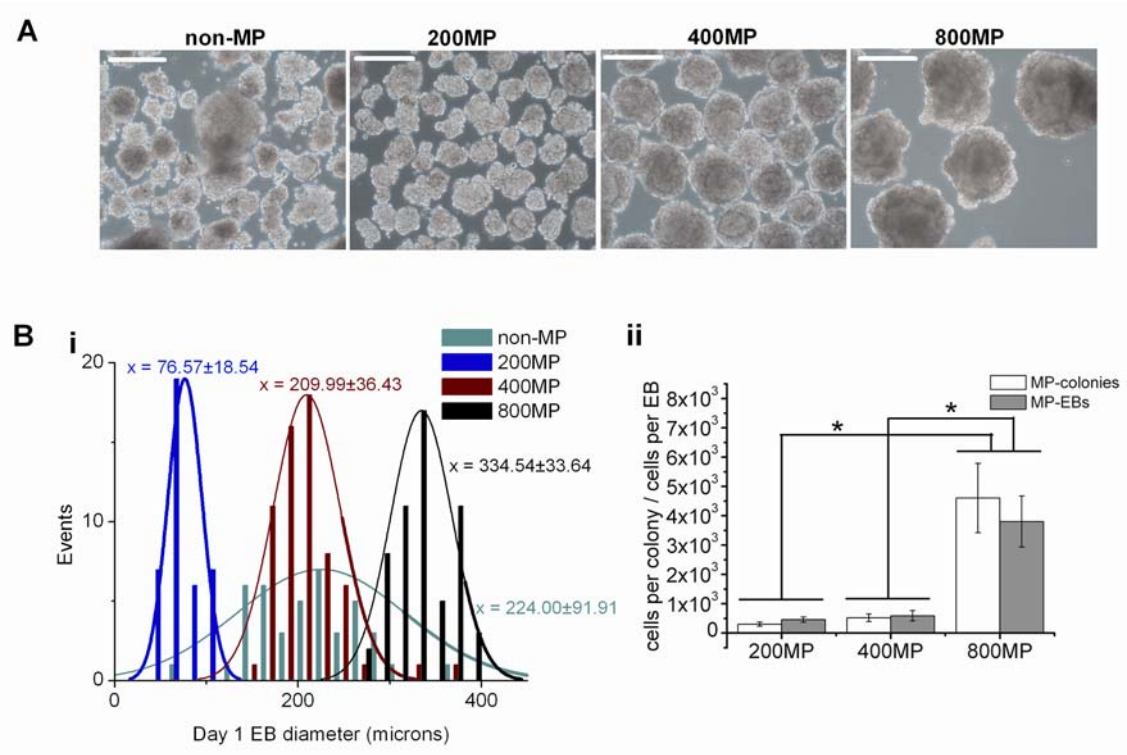

Figure 2.4: Formation of size-controlled MP-EBs. (A) Bright filed images of EBs generated under the 4 conditions tested: non-patterned colonies (non-MP) and colonies patterned at 200, 400 and 800 μm diameters (200MP, 400MP, and 800MP respectively). Scale bars = 250 μm. **(B)** Quantitative demonstration of EB size control in EBs generated from size-controlled hESC colonies by (i) EB diameter, and (ii) by comparing cell number in colonies to cell number in subsequently generated aggregates using fluorescent DNA staining.

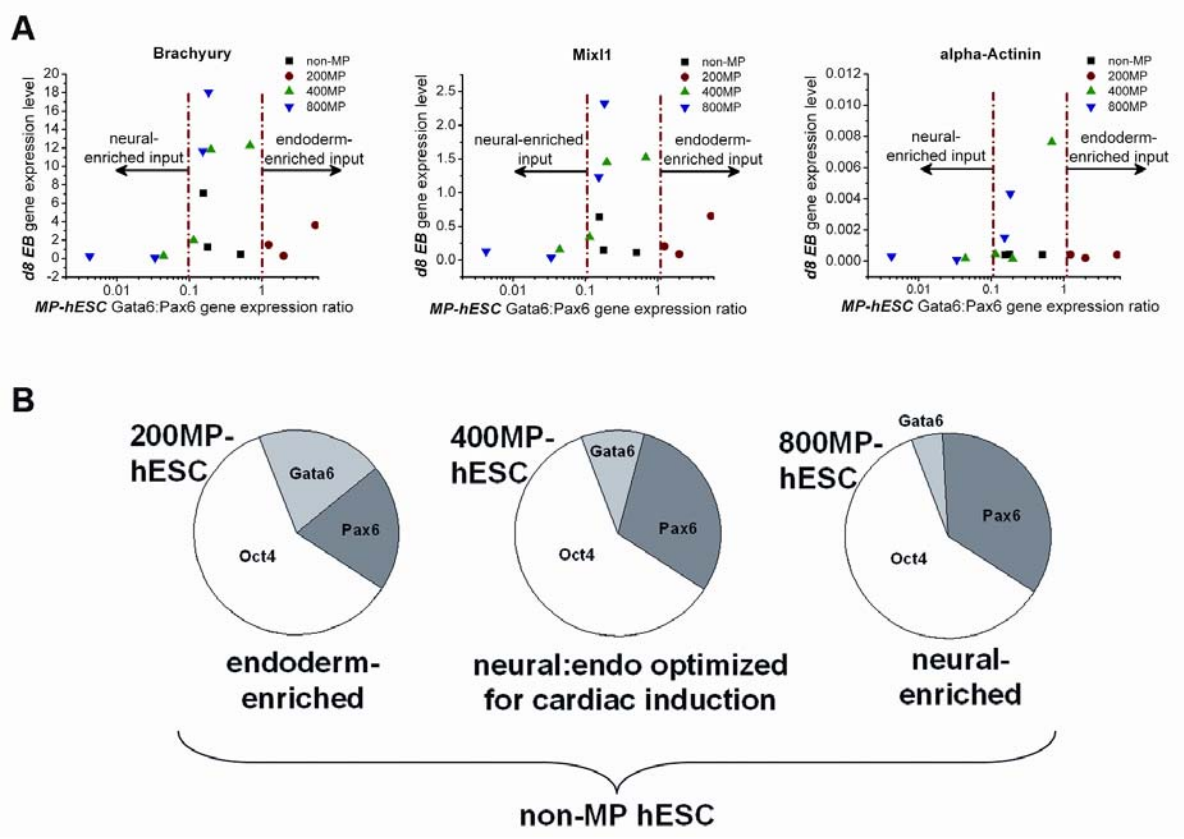

Figure 2.5: The interactive effect of MP-hESC colony size and cell composition on mesoderm and cardiac induction in MP-EBs. (A) Gene expression levels measured for mesoderm markers Brachyury (Bry) and Mixl1, and cardiac marker α-Actinin in day 8 (d8) EBs plotted with respect to the Gata6:Pax6 gene expression ratio in the corresponding MP-hESC starting population, and as a function of MP-hESC colony size. Neural-enriched and endoderm-enriched starting MP-hESCs generate MP-EBs that display poor mesoderm and cardiac induction, as indicated by the marked regions on the plots. **(B)** A schematic summarizing the observed effect of controlling colony size on MP-hESC composition, and the consequence of MP-hESC composition on cardiac induction.

Mature cell differentiation in MP-EBs and the effect of input hESC composition and colony/EB size on cardiac induction

Starting at day 8 of EB culture, contracting areas appeared in MP-EB outgrowths suggesting that these cells exhibit spontaneous electrical activity. Optical mapping with di-4-ANEPPS demonstrated that changes in membrane potential corresponded visually with contractions (data not shown). Immunostaining revealed positive expression of contractile protein markers α-sarcomeric actin (α-SR-1) and α-Actinin (EA-53), as well as the gap junction protein Connexin-43 (Cx-43) (Figure 2.6A). Staining day 20 EB outgrowths with α-SR-1 demonstrated a cluster of cardiac cells, whereas EA-53 expression in day 20 replated single cells exhibited the clear cardiac morphology of striated, highly organized fibers. Immunofluorescence analysis of Cx-43

expression on day 22 from dissociated MP-EBs that had been replated at high density displayed a web-like pattern of staining highly concentrated between cell membranes, indicating functional cell coupling.

To quantitatively evaluate mature differentiation from MP-EB induced differentiation cultures, day 16 MP-EB outgrowths were dissociated to single cells and cultured for 2 days as a monolayer on fibronectin-gelatin coated plates and then immunostained with EA-53 to detect cardiac differentiation. Quantitative immunofluorescence was used to image the cells and detect positive protein expression, revealing the presence of EA-53^{+} cardiomyocytes (Figure 2.6B). The effect of MP-EB size and MP-hESC composition (level of GATA-6 and PAX6 gene expression) on cardiomyocyte frequency was analyzed. In runs initiated from neural-enriched MP-hESC populations (high-PAX6/low-GATA-6 gene expression), higher frequencies of EA-53 expression were observed in smaller MP-EBs (Figure 2.6C-i). Conversely, in runs initiated from endoderm-enriched MP-hESC populations (low-PAX6/high-GATA-6 gene expression), the frequency of EA-53 expression was higher in larger MP-EBs (Figure 2.6C-ii). Additionally, tracking the appearance of beating areas and neural rosettes in the MP-EB cultures (Figure 2.6D), it was observed that within individual runs, neural rosettes were always present in larger EB sizes than those in which beating areas were detected. But between runs, the specific MP-EB size that gave rise to the appearance of neural rosettes or beating areas shifted. A proposed mechanism for our observations is summarized in Figure 2.6E, wherein, mirroring what happens upon manipulating hESC colony size, the endoderm composition is higher in smaller MP-EBs and is lower in larger MP-EBs, however the specific MP-EB size that optimizes cardiac induction shifts based on the cell composition of the input hESC population.

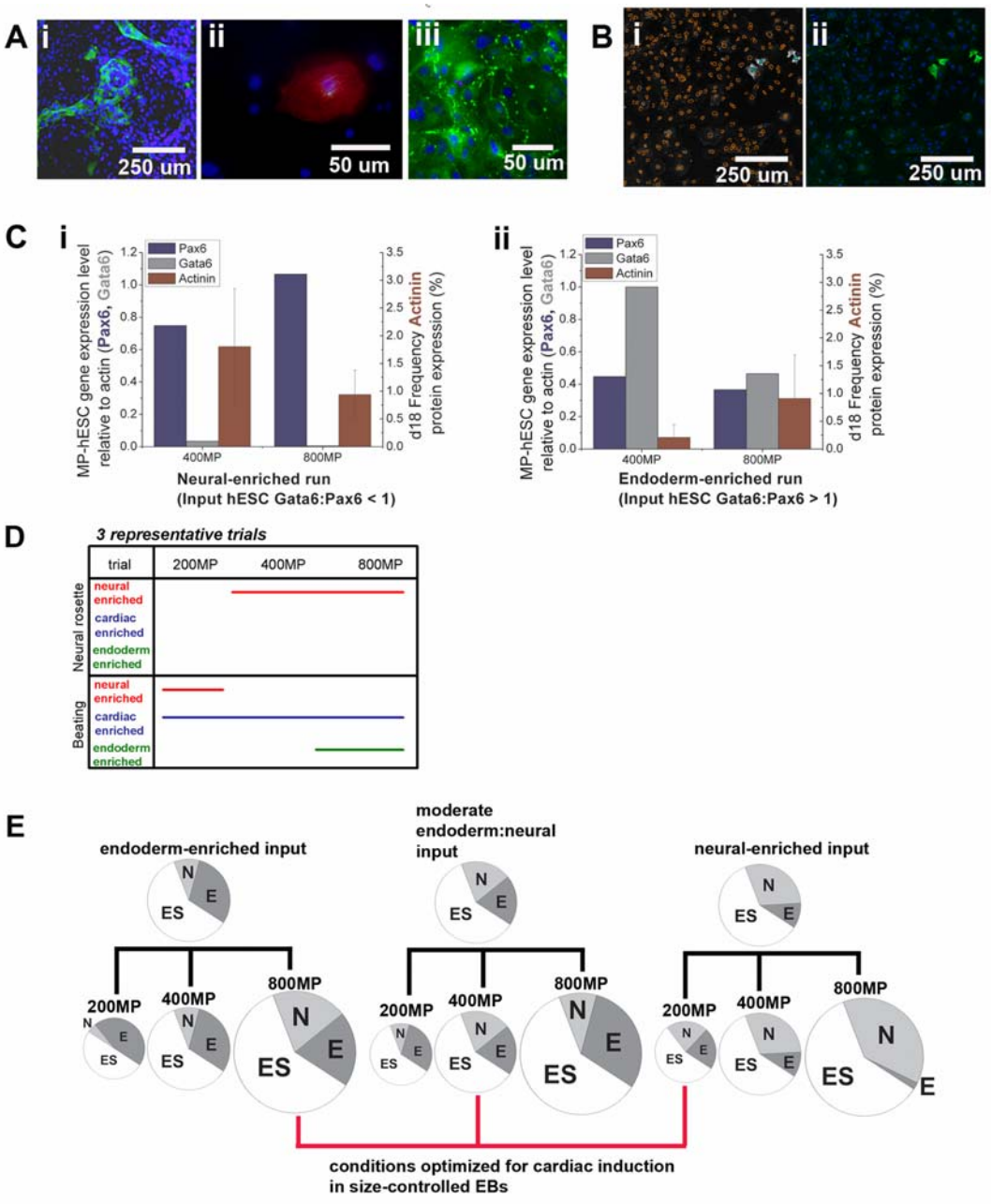

Figure 2.6: MP EBs can be used to form mature cell types and the output is dependent on colony and EB size. (A) Immunostaining on a replated monolayer demonstrated expression of (i) alpha sarcomeric actin (α-SR-1) in day 21 (d21) EB outgrowths, (ii) α-actinin (EA-53) at day 20, and (iii) gap junction protein Cx-43 at day 22. **(B)** Representative α-Actinin immunofluorescence images from Cellomics analysis i) demonstrating the algorithm used to detect positive α-Actinin, and (ii) the corresponding overlay image. **(C)** A comparison of α-Actinin-expression frequency at two EB sizes (400MP and 800MP) from independent runs initiated with either a neural-enriched (Gata6-low/Pax6-high) or an endoderm-enriched (Gata6-high/Pax6-low) MP-hESC population. **(D)** Tracking neural rosettes and spontaneously contracting areas in day 8 EBs (3 representative trials). **(E)** The observed effect of differences in endoderm and neural cell composition in the input hESC population that are further modulated in MP-hESC by controlling colony size, and ultimately impact MP-EB-based cardiac induction.

DISCUSSION

EB-based differentiation is a powerful system because it can mimic in vivo embryonic development and provides a platform to study the effects of cell-cell interactions and spatial organization on cell type-specific commitment. During embryogenesis, factors secreted by anterior lateral endoderm are thought to direct cardiac differentiation of neighboring mesoderm, as well as to promote cell survival and proliferation (Schultheiss, Xydas et al. 1995; Sugi and Lough 1995; Antin, Yatskievych et al. 1996; Zhu, Sasse et al. 1999), while parietal endoderm (Stary, Schneider et al. 2006) and visceral endoderm (Hogan, Taylor et al. 1981; Mummery, Ward-van Oostwaard et al. 2003; Bin, Sheng et al. 2006) have been shown to enhance ESC differentiation to cardiomyocytes. Given that one of the first events in EB development is the formation of an endoderm layer surrounding a pluripotent epiblast core (Keller 1995; Grabel, Becker et al. 1998), we hypothesized that controlling EB size would modulate the ratio of cardiac-inducing visceral endoderm cells to pluripotent hESCs within the EB proportionally to the surface area (endoderm) to volume (hESC) ratio of the EB. In other words, we expected that the endoderm:hESC ratio would decrease with increasing EB size. Accordingly, there would be an ideal EB size corresponding to the ideal ratio of endoderm cells to hESCs to optimize cardiac induction.

A number of groups are targeting EB size control to improve hESC differentiation (Ng, Davis et al. 2005; Khademhosseini, Ferreira et al. 2006; Mohr, de Pablo et al. 2006; Burridge, Anderson et al. 2007). One limitation of our system is that EBs are formed from 2-dimensional colonies prior to transferring them to suspension. Ultimately, it would be advantageous if the cell trajectory control we have in our 2-D system can be translated to direct methods for 3-dimensional cell patterning (Khademhosseini, Ferreira et al. 2006; Mohr, de Pablo et al. 2006). We observed that controlling EB size (Rosenthal, Macdonald et al. 2007) alone was insufficient to achieve reproducible cardiac induction. In fact, comparing cardiac induction in separate EB size-controlled runs with respect to EB size alone yielded more variability than in parallel non size-controlled runs, with no clear pattern between EB size and cardiac induction efficiency. It became apparent that EB size-controlled cultures were more sensitive to differences in the starting population, which is typically comprised of cells expressing pluripotent hESC markers and markers of early hESC derivatives. We thus concluded that analyzing the expression of

pluripotency markers (Oct4, Nanog) was inadequate for assessing the input population, and that the composition of cell types expressing markers associated with lineage commitment are useful indicators for differentiation trajectory biases. Interestingly, using quantitative image analysis, we have observed both the co-expression and unique expression of pluripotency markers and differentiation associated markers at the protein level. This data suggest that both cell-cell interactions and endogenous parameters influence cell differentiation trajectories. In our system the effect of EB size on mesoderm/cardiac induction was dependent on the ratio of endoderm-gene expressing to neural-gene expressing cells. Importantly, this ratio could exist at a wide range of values within an input hESC population expressing robust levels of typical pluripotency-associated markers. While signals from neighboring endoderm promote cardiac induction, we did not observe an increase in cardiac induction in endoderm marker expression enriched starting populations, which demonstrates the necessity to balance the ratio of undifferentiated cells and endoderm/endoderm precursor cells in differentiating EBs. Input populations exhibiting high endoderm-associated marker expression produced differentiation cultures with increased mesoderm/cardiac induction in larger EBs, while neural-marker enriched input populations resulted in increased mesoderm/cardiac induction in smaller EBs. This observation corresponds with our previously stated hypothesis that you can modulate the ratio of outer endoderm cells and inner hESCs by controlling EB size; however this ratio is also a function of the initial ratio of endoderm-associated and neural-associated cells in the hESC population prior to initiating micropatterned colonies.

Controlling the EB size revealed that hESC differentiation studies are hampered by variations in the gene expression profiles of hESC input populations. Our data suggests that colony size can be manipulated to generate the appropriate input cell composition for increased mesoderm/cardiac induction efficiency during EB-mediated hESC differentiation. The ratio of endoderm to neural precursors may be an indicator of an input population's mesoderm/cardiac induction efficiency because, as previously discussed, endoderm is believed to secrete pro-cardiogenic factors while signals (such as Wnts) from the neural tube have been shown to block heart formation in the embryo (Marvin, Di Rocco et al. 2001; Tzahor and Lassar 2001). By micropatterning hESC colonies of defined diameters, we demonstrated that the level of pluripotency gene expression as well as the ratio of endoderm-associated to neural-associated cells is a function of colony size (Figure 2.3). Larger colonies exhibit higher levels of expression

of pluripotency genes (Oct4 and Nanog) and lower ratios of endoderm-associated to neural-associated cells, while smaller colonies exhibit lower expression levels of pluripotency-associated genes and higher ratios of endoderm-associated to neural-associated cells. These observations are consistent with the literature including our previous report that enhanced maintenance of the hESC phenotype in larger colonies was attributable to an antagonistic interaction between secreted factors from pluripotent and extra-embryonic endoderm cells that regulates Small mothers against Decapentaplegic (Smad)1 activation (Peerani, Rao et al. 2007). In a larger colony, the higher local cell density (cell number per unit radius) leads to higher levels of BMP antagonists (such as GDF3), which are secreted by hESCs, thereby supporting self renewal by suppressing Smad1 activation. Meanwhile in smaller colonies, with lower local hESC densities, the secretion of BMP2 by extra-embryonic endoderm activates Smad1 thus suppressing self renewal. Further, it has been demonstrated that strong interference of endogenous BMP-2 signaling in hESC cultures leads to the induction of cells expressing the characteristic neuroectoderm markers Pax-6 and nestin (Pera, Andrade et al. 2004). Therefore, in smaller colonies (low local cell densities) lower levels of BMP-2 antagonist factor promote endoderm differentiation (higher GATA-6:PAX6), while in larger colonies (higher local cell densities) higher levels of BMP-antagonist suppress endoderm differentiation leading to higher levels of Oct4 and PAX6 expression.

In conclusion, our findings here have revealed three critical parameters currently neglected in most hESC differentiation experiments: (1) the status of the input hESC composition, (2) hESC colony size, and (3) EB size. Specifically, reproducible, efficient (endogenous) mesoderm/cardiac induction is dependent on (1) the ratio of endoderm to neural precursors in the input hESC population, which (2) can be modulated by controlling hESC colony size, as well as on (3) EB size possibly through a mechanism in which size modulates the ratio of endoderm cells to hESCs during EB development prior to the mesoderm/cardiac induction phase. In combination with future approaches aimed at selecting input hESC populations with more permissive gene expression profiles for specific differentiation trajectories, we posit that micro-patterning will enable more rigorous optimization of other tissue environment factors that depend on colony- and EB- size.

Chapter 3
Generation of Human Embryonic Stem Cell-Derived Mesoderm and Cardiac Cells Using Size-Specified Aggregates in an Oxygen-Controlled Bioreactor

This chapter has been published in *Biotechnology and Bioengineering*. (Niebruegge et al., 2009; 102(2): 493-507). Contributions by Céline Bauwens include development of methods to control EB size by micropatterning hESCs, bioreactor protocols, and design of hypoxia studies. Co-authors include Sylvia Niebruegge, Raheem Peerani, Nimalan Thavandiran, Stephane Masse, Elias Sevaptisidis, Kumar Nanthakumar, Kimberly A. Woodhouse, Mansoor Husain, Eugenia Kumacheva, and Peter W. Zandstra. Permission to reproduce this work has been obtained from Whiley-Blackwell and all co-authors.

ABSTRACT

The ability to generate human pluripotent stem cell-derived cell types at sufficiently high numbers and in a reproducible manner is fundamental for clinical and biopharmaceutical applications. Current experimental methods for the differentiation of pluripotent cells such as human embryonic stem cells (hESC) rely on the generation of heterogeneous aggregates of cells, also called "embryoid bodies" (EBs), in small scale static culture. These protocols are typically (1) not scalable, (2) result in a wide range of EB sizes and (3) expose cells to fluctuations in physicochemical parameters. With the goal of establishing a robust bioprocess we first screened different scalable suspension systems for their ability to support the growth and differentiation of hESCs. Next homogeneity of initial cell aggregates was improved by employing a micro-printing strategy to generate large numbers of size-specified hESC aggregates. Finally, these technologies were integrated into a fully controlled bioreactor system and the impact of oxygen concentration was investigated. Our results demonstrate the beneficial effects of stirred bioreactor culture, aggregate size-control and hypoxia (4% oxygen tension) on both cell growth and cell differentiation towards cardiomyocytes. QRT-PCR data for markers such as brachyury, LIM domain homeobox gene Isl-1, Troponin T and Myosin Light Chain 2v, as well as immunohistochemistry and functional analysis by response to chronotropic agents, documented the impact of these parameters on cardiac differentiation. This study provides an important foundation towards the robust generation of clinically relevant numbers of hESC derived cells.

INTRODUCTION

Embryonic and pluripotent stem cells are capable of self renewal and multilineage differentiation (Evans and Kaufman 1981; Thomson, Itskovitz-Eldor et al. 1998). The ability of human embryonic stem cells (hESC) to differentiate to specialized cells including neural progenitor cells, cardiomyocytes and insulin producing cells (Carpenter, Inokuma et al. 2001; Gerecht-Nir, Fishman et al. 2004; Segev, Fishman et al. 2004) underpins excitement in the use of these cells for accelerating drug discovery and developing new cellular therapeutics. Cardiomyocytes and cardiac progenitors, generated either through embryoid body (EB) formation (Kehat, Kenyagin-Karsenti et al. 2001; Xu, Police et al. 2002; Huber, Itzhaki et al. 2007; Leor, Gerecht et al. 2007), coculture (Mummery, Ward-van Oostwaard et al. 2003; Passier, Oostwaard et al. 2005; Bin, Sheng et al. 2006) or serum-free cytokine induction (Li, Powell et al. 2005; McDevitt, Laflamme

et al. 2005; Passier, Oostwaard et al. 2005; Kattman, Huber et al. 2006; Ludwig, Bergendahl et al. 2006; Xu, He et al. 2006; Kattman, Adler et al. 2007; Laflamme, Chen et al. 2007; Yang, Soonpaa et al. 2008; Zhang, Li et al. 2008), have been successfully derived from hESC. These cells exhibit many of the properties of native cardiac cells including electrophysiological responsiveness (Kehat, Gepstein et al. 2002; He, Ma et al. 2003; Satin, Kehat et al. 2004; Xue, Cho et al. 2005; Binah, Dolnikov et al. 2007) and in vivo function (Kehat, Khimovich et al. 2004; Xue, Cho et al. 2005; Moon, Park et al. 2006). Recent animal models with ESC-derived cardiomyocytes of mouse and human origin support the potential of this cell source for heart repair (Kehat, Khimovich et al. 2004; Laflamme, Gold et al. 2005; Menard, Hagege et al. 2005; Kolossov, Bostani et al. 2006; Caspi, Huber et al. 2007; Dai, Field et al. 2007; Ebelt, Jungblut et al. 2007; Leor, Gerecht et al. 2007). This promising technology, however, is limited by the number of cells that will be required to manufacture a cardiac cell patch, or to replace damaged tissues. It is estimated that in a typical cardiac infarct as many as one billion cardiac cells die (Murry, Reinecke et al. 2006); their replacement may enable the structural and functional healing of an adult heart.

Although bioprocesses for mouse (m)ESC propagation and differentiation have been well established (Keller 1995; Kurosawa, Imamura et al. 2003; Bauwens, Yin et al. 2005; Fok and Zandstra 2005; Schroeder, Niebruegge et al. 2005), the translation of these technologies to hESCs has been challenging, principally because hESC growth rates have been slower, and heterogeneity in culture and media formulations have limited optimization of differentiation efficiencies and population expansions. Progress has been made in the development of engineered systems to generate hESC-derived cells, including stirred and rotating cultures for hESC differentiation (Gerecht-Nir, Cohen et al. 2004; Cameron, Hu et al. 2006) and hESC growth in microbioreactors or matrices (Figallo, Cannizzaro et al. 2007; Gerecht, Burdick et al. 2007). However these systems typically do not control the microenvironment that the cells are exposed to or regulate heterogeneity in cellular parameters such as aggregate size. In recent studies we have demonstrated that the rate and trajectories of hESC differentiation can be controlled by engineering hESC niche properties using a robust micropatterning-technology (Peerani, Rao et al. 2007; Bauwens, Peerani et al. 2008). This technique provides an important strategy towards micro-environmental regulation and directed differentiation, which we have utilized here for the formation of size-controlled aggregates of hESCs.

Cell fate decisions can also be influenced by cell extrinsic factors such as cell-cell interactions, soluble factors and physicochemical parameters. Low oxygen tension (2-5%) has been shown to enhance mouse and human ESC proliferation (Forsyth, Musio et al. 2006; Gibbons, Hewitt et al. 2006), and we have previously used this parameter to enhance cardiac differentiation from mESCs (Zandstra, Bauwens et al. 2003; Bauwens, Yin et al. 2005). It is further noteworthy that, during embryogenesis and particularly during the development of the cardiovascular system, many cues and processes are influenced by hypoxia (Ramirez-Bergeron and Simon 2001; Ramirez-Bergeron, Runge et al. 2004; Buggisch, Ateghang et al. 2007).

By combining both tools, engineering the cellular microenvironment using micropatterning-based aggregate control and physicochemical (oxygen) control using bioreactors, we here report a novel two-step bioprocess for the generation of human pluripotent cell-derived mesoderm and cardiac cells in a stirred suspension system. Quantitative RT-PCR, immunohistochemistry and functional analysis using optical mapping demonstrated the capacity of this system to generate ESC-derived cells including cardiomyocytes. This approach forms an important foundation for the development of scalable and controllable bioprocesses for pluripotent cell expansion and differentiation.

METHODS

hESC maintenance

Human ESC (H9, passages 37 to 52; HES2, passages 24 to 26) were routinely maintained on irradiated feeder-layers of mouse embryonic fibroblasts (mEFs) in KnockOut (ko)-Dulbecco's Modified Eagle Medium (DMEM, Invitrogen) with 20% ko-Serum Replacement (SR) (Invitrogen) and supplemented with 4 ng/mL FGF-2 (PeproTech). Cells were dissociated into small clumps using 0.1 % collagenase IV (Invitrogen) and passaged every 7 days. For passaging, plates were incubated with Collagenase type IV (2 mg/mL, Invitrogen) for 10 min. After aspirating, the collagenase was replaced with hESC maintenance medium. The colonies were then scraped-off the dish and gently pipetted to generate small cell clumps that were replated on a mEF feeder layer at a subculture ratio of 1:6. Karyotype results for H9 cells are provided in Supplementary Figure 1.

Formation of EBs

Before forming EBs from hESC maintained on mEFs, cells were pre-differentiated by replacing maintenance medium with differentiation medium: 20% fetal bovine serum (Hyclone), 0.1 mM β-mercaptoethanol (Sigma), 0.1 mM non-essential amino acids (NEAA), 2 mM L-glutamine, 50 U/mL penicillin, and 50 μg streptomycin in ko-DMEM (all from Gibco). After 24 h cells were incubated with collagenase type IV (2 mg/mL, Invitrogen) for 10 min and then the collagenase was replaced by differentiation medium. To initiate EB formation cells were scraped-off and small clumps were generated by gently pipetting 8x. These cell clumps were cultured in suspension on ultra-low attachment non-tissue culture treated plates (Corning) for additional 24 h before transferring into the desired culture system (described below).

Micropatterned EBs

To control aggregate size, a micro-contact printing technique was developed whereby hESC colonies are cultured on a micro-patterned ECM surface (Peerani, Rao et al. 2007). The micro-contact printing process employed a published technique by Tan (Tan, Tien et al. 2002; Tan, Liu et al. 2004). Briefly, Poly(dimethylsiloxane) (PDMS) circular stamps with diameter, D (400 μm and 800 μm), and pitch, P (500 μm) were fabricated using standard soft lithography techniques (Younan Xia 1998). Stamps were inked with an aqueous solution of pH 5 Matrigel™ for 1 h. After rinsing away excess Matrigel™ and drying stamps with sterile N_2, a monolayer of protein remained on the surface of the stamp. This layer was transferred to a tissue culture treated substrate (tissue culture dish) after the stamp has been placed in conformal contact with the substrate for more than 10 sec. The pattern was passivated with 5% w/v Pluronic™-127 (Sigma) which is used to prevent protein adsorption and cell attachment to unpatterned regions of the substrate. Matrigel™ patterns were seeded with a single cell suspension of hESCs prepared as follows: Colonies of hESCs cultured on mEFs were incubated with 0.25% Trypsin-EDTA (Gibco) for 3 min. Trypsin-EDTA was inactivated with serum-containing hESC differentiation medium. Vigorous pipetting was used to mechanically dissociate the colonies to single cells. Cells were centrifuged and then resuspended in serum-free (SF) hESC maintenance medium (XV medium) consisting of X-Vivo 10 (XV, Biowhittaker), 2mM glutamax, 0.1mM NEAA, 0.1mM β-mercaptoethanol, 40 ng/mL FGF-2, and 0.1 ng/mL TGF-β. This single cell suspension of hESCs was plated onto patterns at 1.5 x 10^6 cells/mL. At 12 h post-seeding, patterned cells were

washed 3x with XV medium to prevent cell attachment on unpatterned areas. As many as ~9500 size-controlled aggregates could be generated on a single microscopes slide (9500 EBs/ 9.6cm²). Patterned colonies were fed daily with 3mL SF-medium until d2 or d3 when the colonies were transferred to suspension culture to initiate differentiation. To form differentiating aggregates, d3 patterned hESC colonies were gently scraped off the dishes, and resuspended in hESC differentiation medium consisting of ko-DMEM, 20% FBS, 2mM glutamax, 0.1mM NEAA, 0.1mM β-mercaptoethanol, 50 IU/mL penicillin and 50 μg/mL streptomycin. These aggregates were cultured in suspension in the culture systems described below.

Culture systems

Ultra-low attachment plates were used for static culture and small-scale dynamic cultivations on an orbital shaker (Rotomix VWR, 50 rpm). A Barnstead rotisserie system was employed for roller-bottle culture (50 mL, 40 rpm). For stirred suspension cultivations, we employed spinner flasks from a DasGip cellferm-pro bioreactor system provided with a glass bulb impeller (125 mL, 40 rpm) and a plastic paddle equipped Bellco spinner (150 mL, 40 rpm). All bioreactor cultures were performed with the DasGip cellferm-pro system, a parallel cultivation system that is capable of monitoring and controlling oxygen tension and pH in up to eight parallel 500-mL vessels. Cultures were maintained under either normoxic (21% O_2 tension) or hypoxic (4% O_2 tension) conditions in a medium volume of 125 mL. Medium was replaced every 4 d.

Cell and EB counts

EB numbers and number of contracting EBs were quantified by taking samples of 1mL cell suspension on d2, d5, d9, d13 and d16 of differentiation. EBs were counted in a 24-well plate using an inverted-microscope. The same sample was used to determine cell number and viability by dissociating EBs to single cells followed by trypan-blue staining.

Quantitative RT-PCR

Total RNA was extracted from the cells by homogenization in Trizol (Invitrogen). Extraction with chloroform was followed by precipitation with iso-propyl alcohol. RNA was purified using RNAEasy columns (Qiagen) with an on-column DNase-I digestion step. cDNA was generated from purified RNA with Superscript-III reverse transcriptase (Invitrogen) as per manufacturer's

instructions. 10 ng of cDNA was used per PCR reaction with iQ-SYBR-green master mix (BioRad) in triplicate. Relative expression was determined by delta-delta Ct method with the expression of α-actin as housekeeping reference. Table 3-I provides a list of all primer sequences derived from the MGH Primerbank (Wang and Seed 2003). Specificity of amplification was assured with analysis of dissociation curves of all reactions. Human fetal heart (FH; BioChain, Total RNA human fetal heart) was used as reference. For all samples a control was performed without reverse transcriptase and no amplification was detected in these controls.

Table 3-I – Overview of primer sequences used for quantitative RT-PCR

• Gene	5' Primer	3' Primer
beta-Actin	CATGTACGTTGCTATCCAGGC	CTCCTTAATGTCACGCACGAT
Oct4	CTTGAATCCCGAATGGGAAAGGG	CCTTCCCAAATAGAACCCCCA
Brachyury T	TGCTTCCCTGAGACCCAGTT	GATCACTTCTTTCCTTTGCATCAAG
Mesp1	CTCTGTTGGAGACCTGGATG	CCTGCTTGCCTCAAAGTG
Nkx2.5	GGTGGAGCTGGAGAAGACAGA	CGACGCCGAAGTTCACGAAGT
FoxC1	ACGGCATCTACCAGTTCATC	TCCTTCTCCTCCTTGTCCTT
Isl1	TGATGAAGCAACTCCAGCAG	GGACTGGCTACCATGCTGTT
Tbx2	ACCCTGAGATGCCCAAAC	CAGTGACGGCGATGAAGT
Tbx5	TACCACCACACCCATCAAC	ACACCAAGACAGGGACAGAC
Mef2c	CGAGATACCCACAACACACG-	TTCGTTCCGGTGATCCTC
α-Actinin	GGGTCCGTTTGCCAGTCAG	GGCTTTCCTTAGGTGGGAGTT
Troponin T	GGACGAAGACGAGCAGGAG	CTTCCGGTGGATGTCATCAAA
MLC2v	TGGGCGAGTGAACGTGAAAAA	CACTTTGAATGCGTTGAGAATGG

Immunocytochemistry and confocal laser scanning microscopy

Fluorescence pictures were obtained from d16 cell aggregates after cells were incubated with Collagenase type IV (2mg/mL, Invitrogen) for 6 min and cell clumps were vigorously pipetted. Single cells were seeded on fibronectin/gelatin-coated (1 mg fibronectin in 80 mL of 0.02 % gelatin) 4-well chamber slides (LabTek) at a density of 1 x 10^4 cells/well. Cells were cultured for 3 d before staining was performed as previously described (Bauwens, Yin et al. 2005). The following antibodies were used: α-actinin (EA-53, 1:800, Sigma), sarcomeric actin (A2172,

1:500, Sigma) and secondary antibodies (Alexa 546 and Alexa 488, both 1:200, Molecular Probes). Cells were imaged using an Olympus FV1000 confocal laser microscope.

Electrophysiological characterisation

Spontaneous electrical activity of hESC derived cardiomyocytes can be assessed by optical mapping. D13 EBs were harvested and plated on fibronectin/gelatin-coated culture dishes and cultured for additional 2 d before analysis. For action potential (AP) tracking, plated EBs were incubated for 8 min in the dark with 5 μM of di-8-ANNEPS in Tyrode's salt solution (T2397, Sigma) followed by three washes with Tyrode solution. Recordings of EBs exhibiting contracting areas were performed in Tyrode in the dark and at stabilized 37°C. Additionally, norepinephrine (1 mM, diluted in differentiation medium) was applied during AP tracking. Experiments were performed using a CMOS optical mapping system with a microscope capable of magnification and image intensification (Ultima, Brain Vision Inc, Japan). Fluorescence was excited at 531 nm ± 20 nm with a 150 W halogen light source (MHF-G150LR, Moritek Corp, Japan,). Emission signal was long pass filtered at 610 nm and recorded for a period of 15s with temporal resolution as fast as 1 kHz. Changes in dye signal were recorded and analyzed using BV-analyzer software (Brain Vision Inc, Japan).

Statistics

Values are presented as means ±SD, if not otherwise indicated. Statistical significance was assessed with one-tailed Student's t-test at a significance level of 5% and was noted when the p-value for three independent experiments was less than 0.05. Best-fit regression curves were assessed for the means of cell numbers and percentage of contracting EBs with polynomial fit analysis in an order of 2 (fit curve min = 2, fit curve max = 16). All numerical analysis was performed using Origin 7.5 (OriginLab, Northhampton, MA) graphing and data analysis software.

RESULTS

Dynamic culture supports cell expansion and yield of contracting EBs

As a first step in developing a bioprocess capable of supporting the production of differentiated cells from hESCs, we screened a number of dynamic culture systems and compared cell growth

to static plate controls. Almost no cell expansion was documented for hESCs grown in static culture after 16d of differentiation (d16 cell-fold expansion 1.0 ± 0.4; Fig. 1A). Switching to dynamic culture, as reported by others in mESC (Carpenedo, Sargent et al. 2007), resulted in an improved cell growth, shown here for hESCs cultured in ultra-low attachment dishes on an orbital shaker table (2.0 ± 0.7). Next we evaluated different scalable culture systems. We found a cell-fold expansion of 3.8 ± 1.9 in roller bottles, whereas culture in glass-bulb equipped spinner flasks resulted in an expansion of 5.0 ± 2.8. In spinner systems with a plastic paddle impeller, cell expansion was found to be 3.8 ± 0.8. These findings suggest that cell growth of differentiating hESCs is significantly improved by dynamic culture conditions, demonstrated in four suspension systems differing in agitation forces and vessel geometry. Furthermore, in comparison to static culture, a higher percentage of EBs with contracting areas was observed in all dynamic systems tested (Fig. 3.1B). In conclusion a spinner system equipped with a single glass-bulb impeller (DasGip cellferm-pro spinner flask) was found to be the most favorable for cell growth and percentage of contracting EBs.

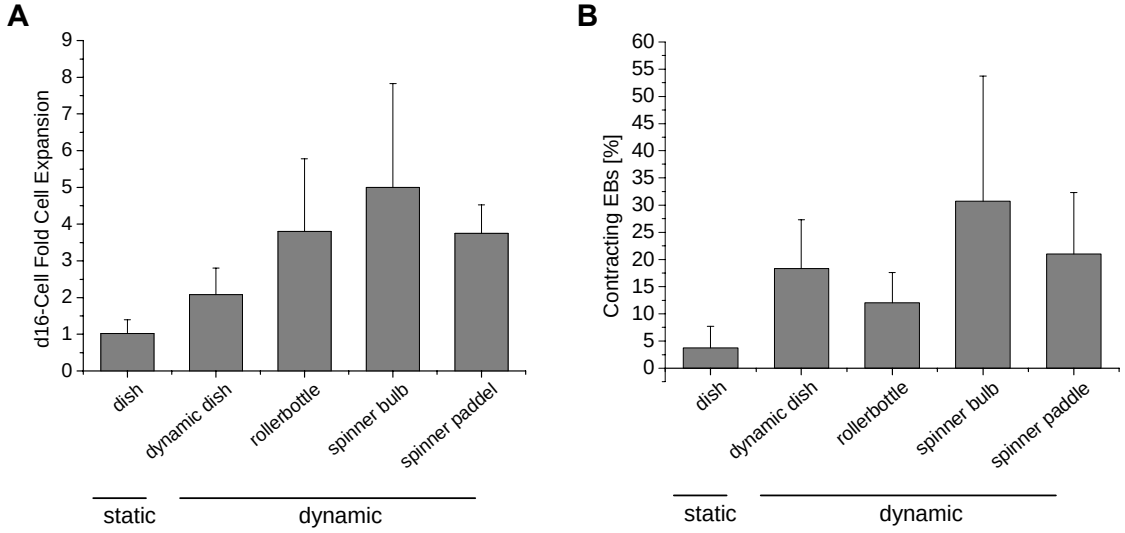

Figure 3.1: Dynamic culture supports cell expansion and increases percentage of contracting EBs. A: Cell-fold expansion of H9 hESCs on d16 of differentiation. By comparing static culture with dynamic culture an improved cell growth was found in all dynamic systems tested. Ultra-low attachment dishes were used for static culture and as well for dynamic cultivations on an orbital shaker. A Barnstead rotisserie system was employed for rollerbottle culture. Stirred suspension cultivations were performed in a DasGip cell-ferm pro spinner system equipped with a glass bulb impeller and in a Bellco spinner equipped with a plastic paddle impeller. **B**: Percentage of EBs with contracting areas. In comparison to static culture on 16d higher percentage of EBs with contracting areas was observed in all dynamic systems tested. Data are reported as mean with standard deviation of two independent experiments.

Robust generation of size-controlled EBs

Creating EBs with conventionally used protocols results in heterogeneous size distributions (Ungrin, Joshi et al. 2008), which may influence cell fate. Typically, both a wide range of EB sizes, and significant variations in mean EB sizes between separate runs, are observed. In order to control input cell population properties, we have developed a robust micropatterning technique, whereby hESCs were cultured on circular-features varying in diameters (Peerani, Rao et al. 2007). This technology was adapted to the generation of size-specific aggregates by adding a colony removal step (Fig. 3.2). Pattern sizes of 400 and 800 μm diameters were chosen based on earlier results suggesting that small patterns (≤ 200 μm result in predominantly primitive endoderm differentiation (Peerani, Rao et al. 2007), while large patterns (≥ 800 μm), and thus large aggregates of cells, may exhibit limited growth and proliferation (Dang, Gerecht-Nir et al. 2004). Two-to-four days after hESCs were printed on Matrigel^{TM}-coated circular patterns, cells were scraped-off. Patterned aggregates were more homogenous in their size distribution and shape than EBs induced by traditional techniques (Fig. 3.2A). Noteworthy, on a single microscope slide as many as ~9500 size-controlled aggregates could be generated, making this technology amenable to the generation of large numbers of size-controlled aggregates to seed bioreactors.

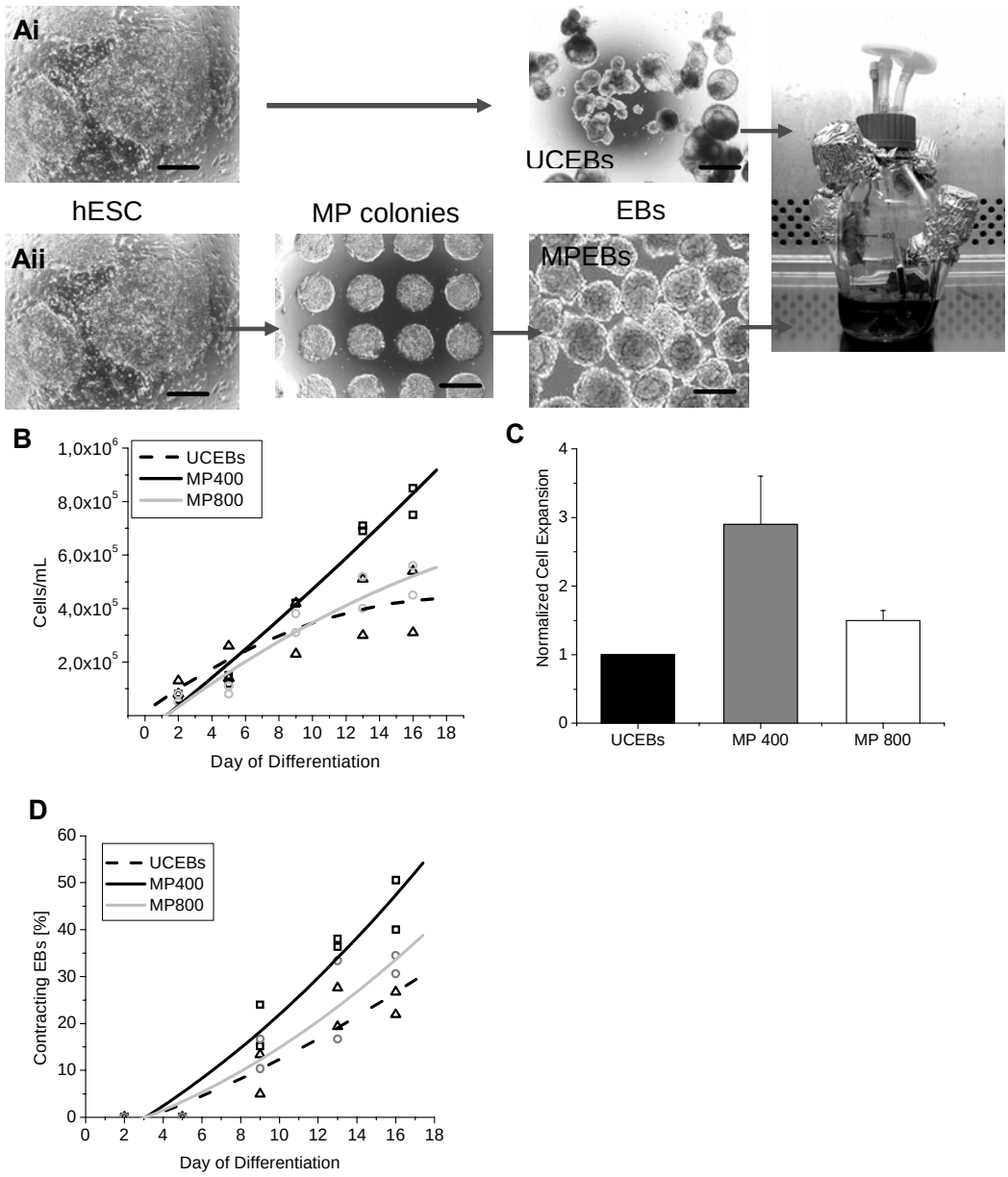

Figure 3.2: Conventional hEB protocols result in heterogeneous aggregates, whereas micropatterned aggregates are more uniform in size and shape. (A) Undifferentiated H9 hESC cells on mEFs were used to induce EB formation using a colony scraping-off technique resulting in uncontrolled formed EBs (UCEBs) (i). For micropatterning (ii), hESCs on mEFs were scraped-off and seeded as single cells on patterned features. To form differentiating aggregates, d3 patterned hESC colonies were scraped-off the dish followed by inoculation into stirred suspension cultures (scale bars: 400 μm). **(B)** Highest cell outputs were achieved with MP400 aggregates. hESC colonies were patterned with an initial feature diameter of 400 μm and 800 μm (MP400, MP800), respectively, followed by growth in stirred suspension. Cell growth was compared to growth of EBs generated by scraping-off (uncontrolled, UCEBs). **(C)** Cell expansion of cells derived from MP400 and MP800, respectively, normalized to expansion of UCEBs. **(D)** EBs with contracting areas were observed in all three conditions. Data are reported from two independent experiments each performed with UCEBs (black, dash line), MP400 EBs (black, straight line) and MP800 EBs (grey, straight line). Polynomial regression analysis was used to model best-fit curves.

Removing heterogeneity and controlling EB size allows for more robust cell growth in suspension culture

The above results indicated that controlling aggregate size leads to more uniform EB populations. As a next step, we investigated if the size-specified aggregates could be grown in scalable suspension systems. Control aggregates, and aggregates formed using micropatterning, were formed and cultured in differentiation medium for 24 h in low-attachment dishes, and then inoculated into spinner flasks equipped with a single glass-bulb impeller (125 mL). Interestingly, although all three aggregate conditions were seeded at the same initial cell density, dramatic differences were observed in the overall cell output (Fig. 3.2B, C). Specifically, we found an improved yield of differentiating cells from micro-patterned hESC colonies (MP) as opposed to uncontrolled EBs (UCEBs); significant differences were also observed as a function of micro-patterned aggregate diameter [400 μm (MP400) vs. 800 μm (MP800)]. Trend-lines generated using polynomial regression with related datapoints for two independent experiments are shown in Figures 3.2B to D and highlight the impact of each culture condition. After 16 days of differentiation the MP400 culture delivered the highest yield of differentiating cells; for example, in one representative experiment (Figure 3.2B) cell outputs were MP400: 7.5 x 10^5 vs. MP800: 4.5 x 10^5 vs. UCEBs: 3.1 x 10^5 cells/mL. In all three culture conditions, cell viability was consistently >93%. Figure 3.2C demonstrates the significant differences in cell expansion observed over 3 experiments, with the outputs from the MP400 and MP800 cultures normalized to the UCEBs cultures. Aggregates derived from MP400 cells were found to expand 2.9x (± 0.7) more, whereas MP800 derived cells expanded 1.5x (± 0.14) more, compared to UCEBs. Cell expansion was significantly increased in MP400 aggregates ($p= 0.01$) as compared to MP800. Notably, even after 16d in culture, MPEBs are more uniform in size and more compact than UCEBs, which typically exhibit a necrotic morphology (Suppl. Figure S2-2). EBs with contracting areas were observed under all three conditions. The highest percentage of contracting EBs were found in MP400 culture (Fig. 3.2D).

Impact of oxygen on cell expansion

As a next step in the development of this bioprocess we explored conditions that may further improve the yield of total cells or differentiated target cells in dynamic suspension systems. Our previous findings with mESCs suggested that oxygen concentration may be used as a parameter

to guide cardiomyogenic induction in differentiating ESCs (Bauwens, Yin et al. 2005). In the studies reported here, we incorporated this parameter into our bioprocess for hESC differentiation. EB formation was initiated by scraping-off hESCs colonies. After an additional 24h in static culture 40 EBs/mL were seeded into the bioreactor vessel (DasGip system, 125 mL volume). In order to compare cell densities achieved in the bioreactor system under hypoxic (4% oxygen tension) and normoxic conditions (21% oxygen tension, Fig. 3.3A) vs. cell densities obtained under uncontrolled conditions (UC, employing an identical culture vessel), trend lines for the two independent experiments were determined using polynomial regression. As shown in Figure 3.3B the highest cell densities and d16 cell-fold expansion were observed under hypoxia. For instance, in a representative experiment the highest cell density, 7.4×10^5 cells/mL, was achieved under hypoxic conditions as compared to 5.6×10^5 cells/mL under normoxic conditions. Cell expansion normalized to cell expansion in uncontrolled conditions (Fig. 3.3C) confirms the significant beneficial effect of hypoxia on cell growth. On d16 of differentiation cell-fold expansion was found to be significantly higher under hypoxic as compared to normoxic conditions ($1.75x \pm 0.16$ vs. $1.4x \pm 0.22$; ($p= 0.04$)). EBs with contracting areas were found in all three cultures (Fig. 3.3D).

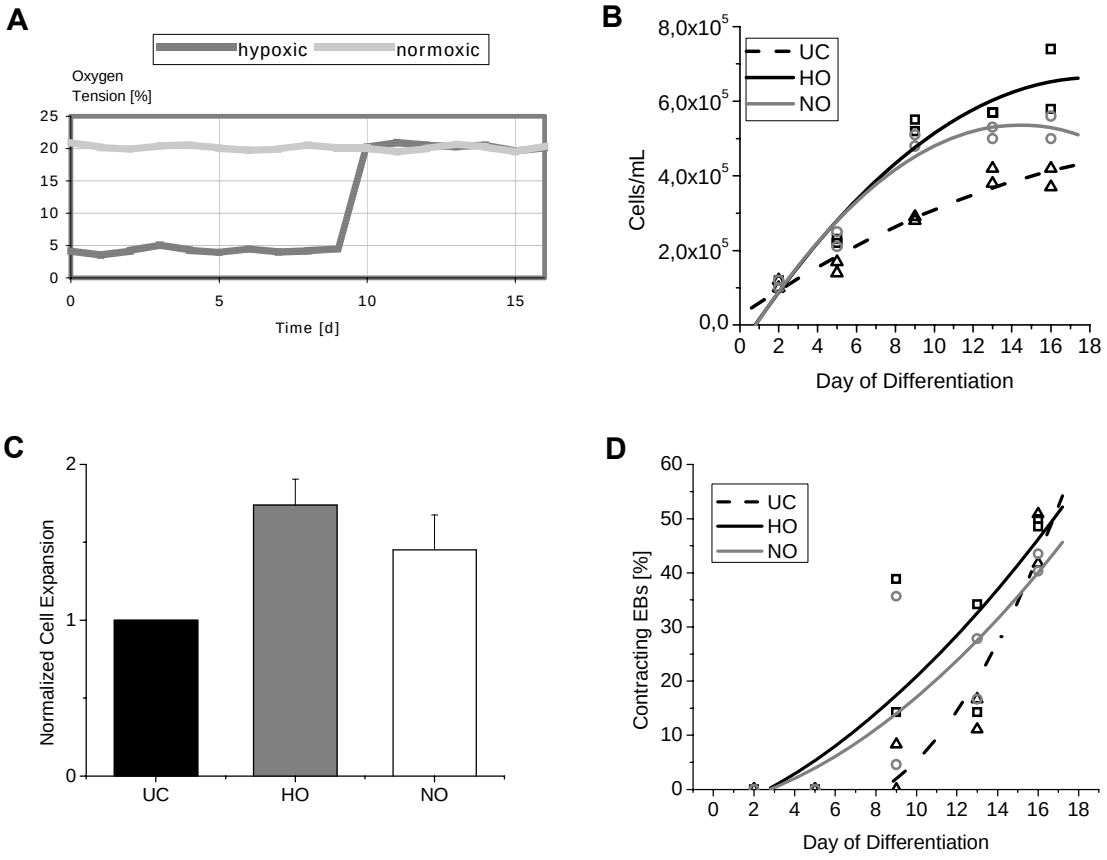

Figure 3.3: Hypoxia culture in a controlled bioreactor supports cell growth. (A) Oxygen tension profiles in controlled normoxic and hypoxic bioreactor culture. **(B)** Growth kinetics of H9 EBs under different oxygen conditions. hEBs generated by colony scraping-off were cultured in a bioreactor system under hypoxic (pO_2 = 4%; HO) and normoxic (pO_2 = 21%; NO) conditions, respectively. Growth was compared to EBs cultured in a comparable culture vessel but under uncontrolled (UC, incubator) oxygen conditions. Highest cell densities were achieved under hypoxic conditions. **(C)** Cell expansion normalized to cell growth under uncontrolled conditions demonstrates beneficial effect of hypoxia on cell growth. **(D)** EBs with contracting areas were observed in all three conditions. Data are reported from two independent experiments each performed under uncontrolled conditions (black, dash line), hypoxic (black, straight line) and normoxic conditions (black, straight line). Polynomial regression analysis was used to model best-fit curves.

Combining micropatterning, dynamic culture and oxygen regulation results in a bioprocess with enhanced cell output.

Our results demonstrate that size-specified EB formation, dynamic systems and oxygen tension all influence cell proliferation and differentiation output. Consequently, as a next step, we combined these tools to establish an integrated bioprocess. Performing all experiments with both H9 and HES2 cells allowed us to validate our process strategy with two cell lines. Human ESC colonies were patterned at an initial diameter of 400 μm followed by culture in either dish or in

stirred suspension culture under normoxic and hypoxic conditions, respectively. EBs conventionally generated with the scraping-off protocol and cultured in uncontrolled conditions (UC, incubator) served as controls. Raw data are displayed in Figure 3.4 along with best-fit curves, which were assessed for each condition in order to highlight trends. In dish culture, cell growth kinetics for both H9 and HES2 cells demonstrate an improved cell growth for micropatterned EBs cultured under hypoxic conditions as opposed to uncontrolled conditions (Fig. 3.4Ai). A similar trend was found in stirred suspension culture (Fig. 3.4Aii). For instance highest cell yields were observed for size-controlled H9 EBs in low oxygen environment resulting in $5.2 \times 10^5 \pm 2.8 \times 10^4$ cells/mL (HO) as opposed to $4.0 \times 10^5 \pm 2.3 \times 10^4$ cells/mL (NO) vs. $2.2 \times 10^5 \pm 8.5 \times 10^4$ cells/mL (UC). Table 3-II provides a summary of final cell numbers with related standard deviations and significance levels generated in all three conditions highlighting the significant improvement in cell expansion achieved with the novel approach. Data for cell expansion normalized to uncontrolled conditions support those findings as shown in Figure 3.4Bi and 3.4Bii. Importantly, although H9-culture resulted in higher overall cell expansion, similar growth kinetic trends were monitored for both H9 and HES2 cell cultures. High viabilities were consistently observed in all conditions, such that in a working volume of 125 mL, outputs of e.g. 6.1×10^7 (H9, hypoxic) vs. 5.2×10^7 (H9, normoxic) cells were enabled. The impact of the new protocol on cell output is summarized in Figure 3.4Ci by comparing state-of-the-art dish cultures to our approach. Notably the novel strategy led to a 5.2 (± 0.26; H9)-fold cell expansion as opposed to 1.5 (± 0.08)-fold in uncontrolled dish culture translating to a 3.5x improved cell yield. Contracting areas were observed under all conditions and reflect cardiac differentiation within the EBs. A significant increase of EBs exhibiting contracting areas was observed in size-controlled EBs in hypoxic culture as opposed to conventional dish culture, resulting in 48.8% ± 2.8 vs. 19.0% ± 2.3 contracting EBs (Fig. 3.4Cii). Table 3-II summarizes data for percentage of contracting EBs in all three conditions. Significance levels highlight the beneficial effect of controlled over uncontrolled conditions.

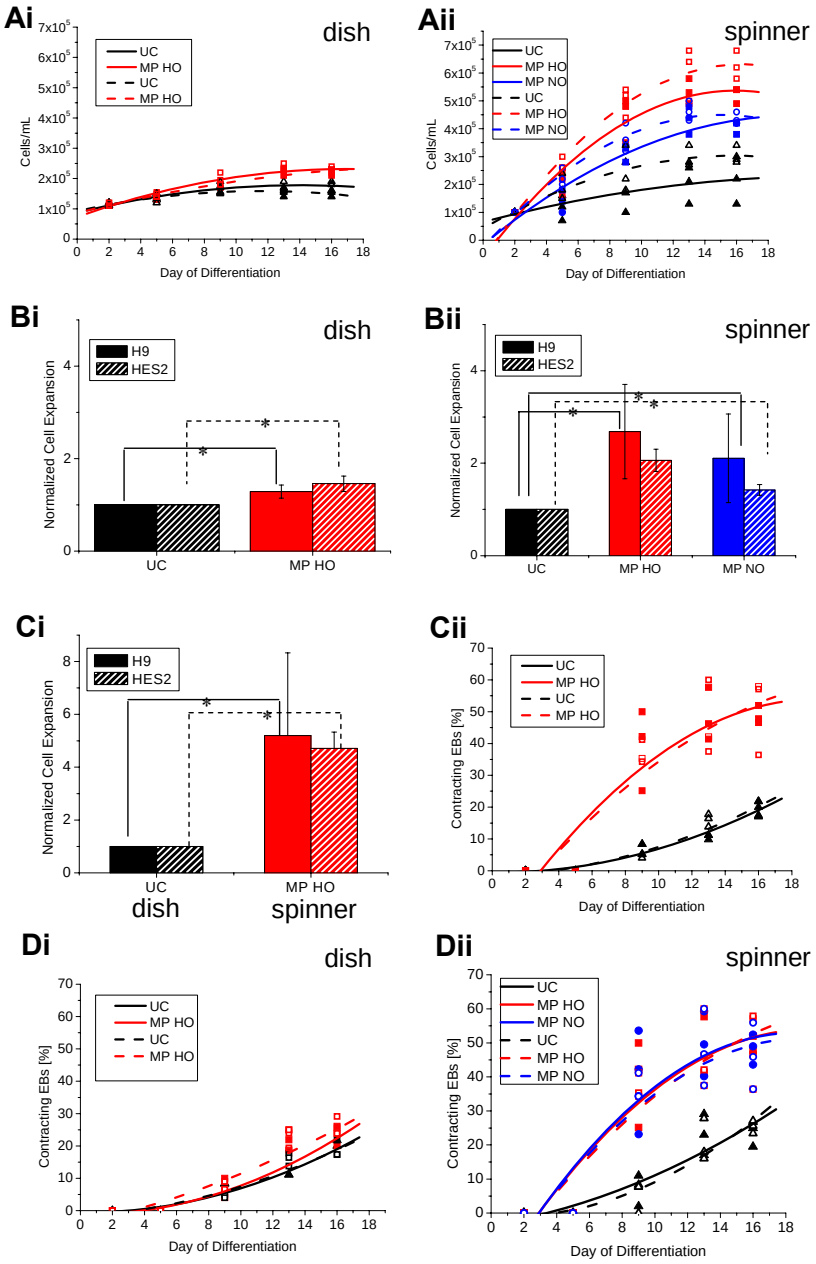

Figure 3.4: Combination of micro-patterning technique and bioreactor regulated environment enhances cell yield. Micropatterned aggregates (MP) of an initial size of 400 µm were grown under oxygen-controlled conditions (normoxic (NO); blue symbols and hypoxic (HO); red symbols). Uncontrolled-formed EBs cultured in uncontrolled oxygen conditions (UC, black symbols) served as internal controls. Each experiment was performed with H9 cells (straight lines) and HES2 cells (dash lines) for 16 days in dish and spinner culture. **(A)** Under hypoxic conditions cell growth was improved in both dish (i) and spinner culture (ii). **(B)** Normalized cell expansion demonstrates beneficial effect of hypoxia on cell growth in dish (i) and spinner culture (ii). Statistical significance at the $p<0.05$ level in comparison to control conditions (UC) is denoted by *. **(C)** Normalized cell expansion (i) for d16 of differentiation highlights advantage of size- and oxygen-control on cell expansion by comparing the optimized approach to state-of-the-art culture. Statistical significance at the $p<0.05$ level in comparison to control conditions (UC) is denoted by *. Percentages of contracting EBs grown in common dish culture vs. new protocol (ii). **(D)** Percentage of aggregates exhibiting contracting areas during dish (i) and spinner culture (ii). All data are reported from three independent experiments each performed under uncontrolled, hypoxic and normoxic conditions. Polynomial regression analysis was used to assess best-fit curves.

Table 3-II	Dish		Spinner		
	UC	HO	UC	NO	HO
Cell density d16 [cells/ mL]					
H9	$1.7x10^5 \pm 1.5x10^4$	$2.3x10^5 \pm 1.5x10^4$ *	$2.2x10^5 \pm 8.5x10^4$	$4.0x10^5 \pm 2.3 \times 10^4$	$5.2x10^5 \pm 2.8x10^4$ * **
HES2	$1.5x10^5 \pm 1.0x10^4$	$2.2x10^5 \pm 5.0x10^3$ *	$3.1x10^5 \pm 3.2x10^4$	$4.3x10^5 \pm 2.0x10^4$ *	$6.3 x10^5 \pm 5.0x10^4$ * **
Contracting EBs d16 [%]					
H9	19.0 ± 2.3	20.6 ± 7.7	23.7 ± 3.7	48.3 ± 4.4 *	48.8 ± 2.8 *
HES2	17.5 ± 6.0	23.5 ± 8.0	25.3 ± 1.8	46.1 ± 9.7 *	50.5 ± 12.1 *

Table 3-II - Final cell densities (d16) and percentage of contracting EBs generated in uncontrolled and controlled conditions. Micropatterned EBs were cultured in dish and spinner culture under hypoxic (HO) and normoxic (NO) conditions compared to uncontrolled formed EBs cultured in an uncontrolled environment (UC, incubator). Numbers represent mean ± standard deviation from three independent experiments. Statistical significance at the $p<0.05$ level in comparison to control conditions (UC) is denoted by *. Statistical significance at the $p<0.05$ level in comparison to normoxic conditions (NO) is denoted by**.

Functional and phenotypic analysis of mesoderm and cardiac development on cells produced using the integrated bioprocess.

- **Hypoxia enhances cardiac-enriched genes**

As a next step we examined the differentiation program induced by hypoxic and normoxic conditions. Quantitative RT-PCR (qRT-PCR) was carried out on total RNA from differentiated cells generated in bioreactor cultures under hypoxic and normoxic conditions. Differences were determined in comparison to pooled RNA from human fetal heart tissue (FH), except for Oct4 expression, which was normalized to RNA from hESCs. RNA was analysed from H9 and HES2 experiments.

Oct4 analysis demonstrated that the initial ESC population differentiated in response to the inductive conditions employed (Fig. 3.5, Ai). QRT-PCR analyses for several mesodermal and cardiac markers were then performed. Our analysis revealed a temporal induction of differentiation, as expected, from mesendoderm and mesoderm markers to more definitive cardiac-associated genes. Mean expression of brachyury (T) increased in 4d EBs and was found to be significantly higher (4.4x; H9) under hypoxic conditions as compared to normoxic conditions, suggesting a supportive effect of low oxygen on mesendoderm differentiation (Fig.

3.5, Aii). Mesodermal markers Nkx2.5 and transcription factor Mesp1 were highly expressed on d4 of differentiation in all three conditions (Fig. 3.5, Aiii, Aiv). Brachyury and Mesp1 expression was found to be increased in hypoxia. Interestingly FOXC1 expression was upregulated on both d4 and d14 suggesting a role in early and late development as reported before (Beqqali, Kloots et al. 2006) (Fig. 3.5, Av). LIM domain homeobox gene Isl-1 (ISL1), which has been described as a marker for a cardiac progenitor cell population (Laugwitz, Moretti et al. 2005), was highly expressed under hypoxia on 4d, (Fig. 3.5, Avi). After 14d of differentiation up regulation of cardiac transcription factors T-box (Tbx)2, Tbx5 and Mef2c (Fig. 3.5, Avii, Aviii, Axi) was detected. Similarly known cardiac genes such as α-Actinin, Troponin T and Myosin light chain 2v (MLC2v; Fig. 3.5, Ax, Axi, Axii) were highly expressed on d14. Gene upregulation of cardiogenic markers was clearly effected by oxygen tension, e.g. Troponin T and α-Actinin expression was found to be significantly higher as compared to normoxic conditions: 3.2x (α-Actinin), 1.7x (Troponin T).

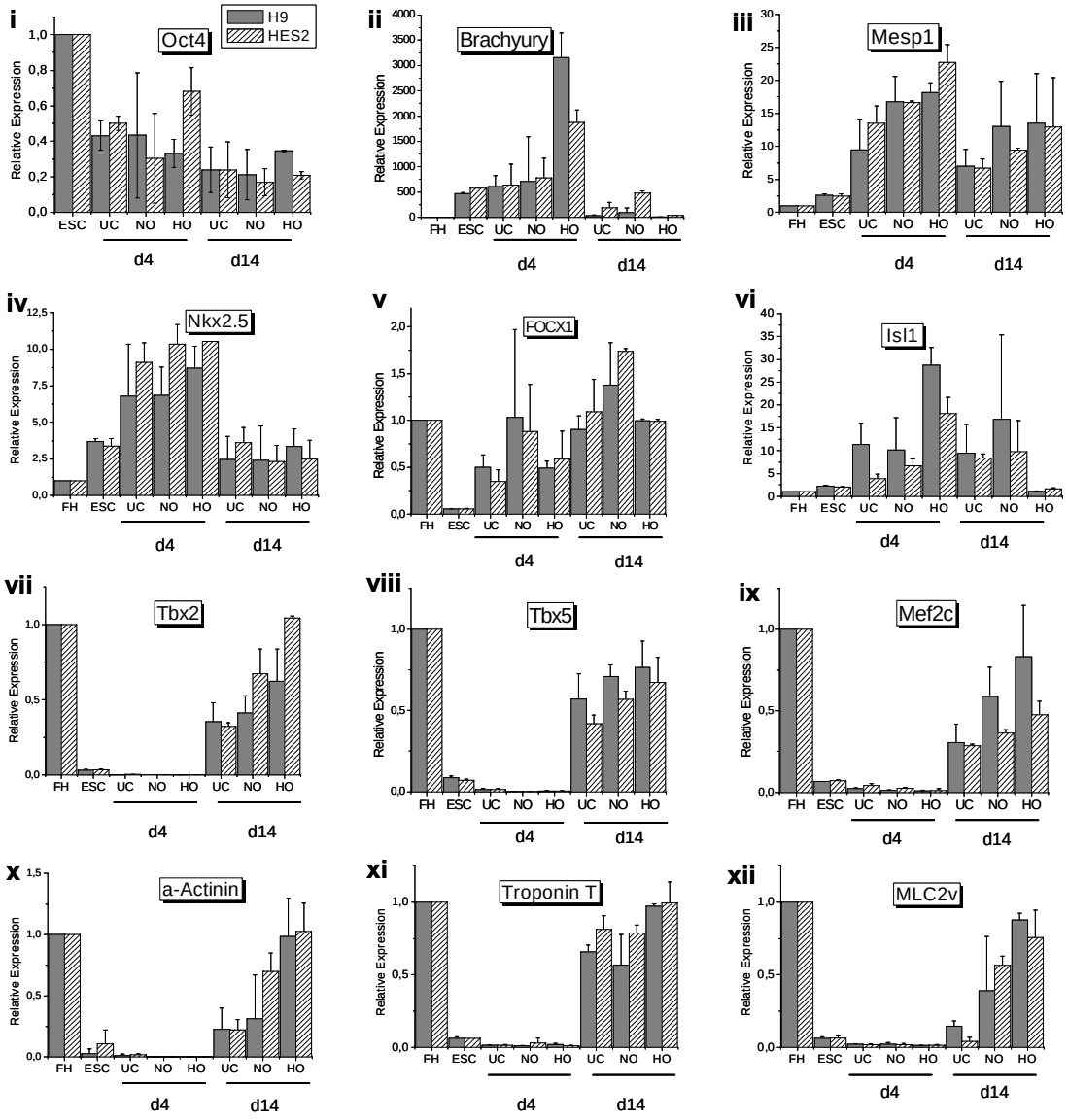

Figure 3.5: Micropatterned and oxygen controlled bioprocess-generated aggregates exhibit mesodermal and cardiac-related genes in an oxygen sensitive manner. Quantitative RT-PCR analysis of patterned H9 (filled columns) and HES2 (sparse columns) aggregates cultured under hypoxic (HO) and normoxic (NO) conditions, respectively. Conventionally formed EBs in uncontrolled spinner culture (UC) served as internal control. Expression was normalized to RNA from fetal heart tissue (FH), except Oct4 expression was normalized to RNA from hESCs. RNA was harvested from the initial ESC population and at d4 and d14 of differentiation. Data are reported from two independent experiments analysed in duplicates for each data point.

- **Bioprocess generated EBs exhibit cardiac specific morphology and functionality**

Immunocytochemistry was used to characterize cardiac cells. Aggregates were dissociated on 16d of differentiation and replated at a density enabling analysis of individual cells. On average

three to five percent of the seeded cells demonstrated a typical cardiac morphology with organized sarcomeric-actin and α-actinin structures (Fig. 3.6A).

In addition, analysis of the replated EBs was performed to explore the function and maturation stage of the bioprocess generated cells. Cells displaying prolonged action potentials may represent Purkinje-like cells or cells with primitive levels of expression of ion channels that regulate repolarisation (Vassalle, Bocchi et al. 2007). Our survey of the upstrokes of the recorded action potentials revealed that each cell analyzed appeared unique in its electrophysiological properties. This could suggest that cells of different conduction-system lineages (nodal vs. ventricular vs. atrial) were generated, or that cells varied between primitive and mature expression levels of sodium channels (Fig. 3.6B), although the number of beating areas analyzed (n= 15) is insufficient to make definitive conclusions at this time. To further assess physiological properties of these cardiomyocytes, we tested whether they could respond to the adrenergic stimulant norepinephrine (NE). As expected an increased rate of spontaneous depolarization, and a shortening of action potential duration was observed with NE infusion, suggesting intact physiological responses in these cells (Fig. 3.6C). In summary, these results suggest the generation of bona fide cardiomyocytes in our bioreactor process.

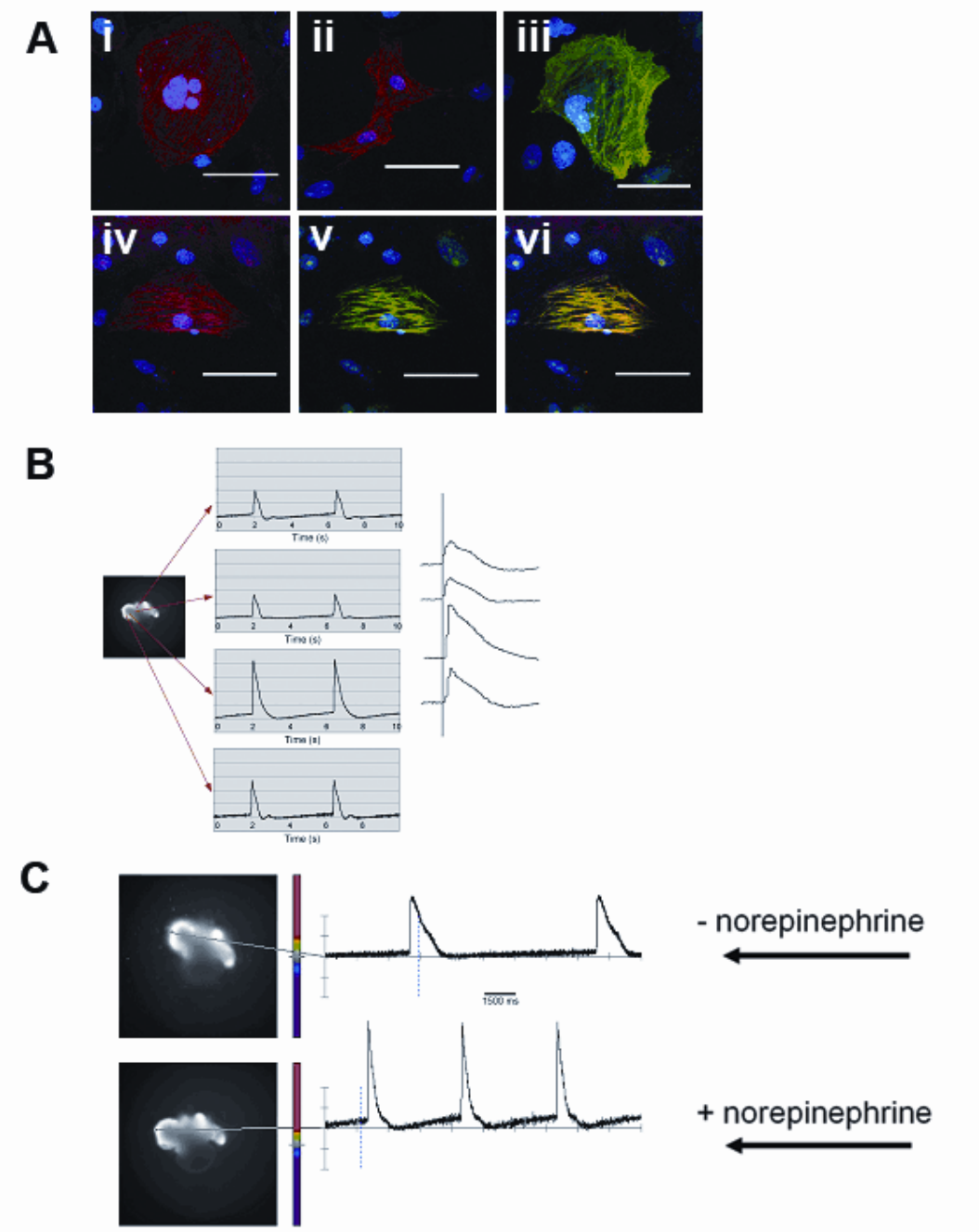

Figure 3.6: Immunohistochemistry and optical mapping studies demonstrate cardiac morphology and functionality generated from micropatterned aggregates in bioreactor culture. (A) Fluorescence labelling of bioreactor generated cells. d16 embryoid bodies were dissociated to single cells, plated on chamber slides and cultured for additional 3 days before staining. Cardiomyocytes within the cell population were detected by α-actinin **(i,ii; red)** and sarcomeric actin **(iii; green)**. Cells were double labelled for α-actinin **(iv; red)**, sarcomeric actin **(v; green)** and merged image **(vi)**. Nuclear staining appears blue (scale bars represent 50 μm). Figure **(B)** demonstrates d15 bioreactor produced aggregates are capable of generating spontaneously beating colonies of cells. Optical mapping reveal cells with varying action potential duration and shape. **(C)** Effects of norepinephrine on the physiology of the bioprocess generated aggregates. The two panels show action potentials recorded before (upper panel) and after (lower panel) administration of norepinephrine. The effect of the drug shows a shortening of the action potential duration (APD) and a decreased basic cycle length (BCL). APs were monitored over a period of 15s.

DISCUSSION

Cell replacement therapy, drug discovery and pharmacotoxicology are applications that require large numbers of pluripotent cell-derived cells. Well characterized cardiomyocytes and their progenitors would be a valuable resource of pre-clinical transplantation studies and drug screening and tissue engineering protocols.

Scalable dynamic culture systems, such as spinner flasks, stirred bioreactors and rotary culture have been used for the generation of differentiated cells from mESCs (Zandstra, Bauwens et al. 2003; Dang, Gerecht-Nir et al. 2004; Bauwens, Yin et al. 2005; Schroeder, Niebruegge et al. 2005; Carpenedo, Sargent et al. 2007; Niebruegge, Nehring et al. 2008). The beneficial effects of dynamic conditions on cell viability are well described and likely due to decreased events of EB agglomeration (Dang, Gerecht-Nir et al. 2004), increased circulation of exogenous factors (nutrients, soluble factors), increased physicochemical homogeneity (oxygen and pH) and, importantly, the reduction of endogenously produced inhibitory factors (both metabolites and cytokines) (Gerecht-Nir, Cohen et al. 2004; Schroeder, Niebruegge et al. 2005; Cameron, Hu et al. 2006; Carpenedo, Sargent et al. 2007; Niebruegge, Nehring et al. 2008). EB agglomeration is also directly related to initial EB and cell densities. For our bioprocess an inoculum of 40 EBs/mL (~100 000 cells/mL) was chosen based on previously published data for mESCs and hESCs (Bauwens, Yin et al. 2005; Cameron, Hu et al. 2006). For future studies it is worthy to further investigate the impact of initial cell density on hESC growth kinetics.

Importantly, although cell viability and differentiation is promoted by implementing mixing in three-dimensional systems, resulting EBs typically appear inconsistent in shape and size. Previously published work (Ng, Davis et al. 2005) has demonstrated a significant role of hEB size on differentiation outcomes, and we have shown that hESC self-renewal and differentiation is influenced by colony size (Peerani, Rao et al. 2007). Thus the ability to control the size of an aggregate, in a manner that can be incorporated into a scalable differentiation bioprocess, may contribute to a more homogeneous and synchronized cell production system. By incorporating the micropatterning technique into our bioreactor system we overcame two challenges. First, initial aggregates with more homogenous in shape and size distribution than conventionly formed EBs. Second, almost no evidence for oversized aggregates was detected during the

process, a likely consequence of both the serum-free "predifferentiation" EB induction step and the mixing in the stirred cultures.

Based on our previous findings with mESCs (Bauwens, Yin et al. 2005) we used the bioreactor system to evaluate the effect of hypoxia on the yield of hESC derivatives. The impact of oxygen on mesoderm and cardiac differentiation in the bioprocess was screened using quantitative gene expression analysis. The fact that differentiation was efficiently initiated from micropatterned aggregates was demonstrated by downregulated expression of self-renewal associated gene Oct4 as the culture progressed, followed by up regulation of several known mesodermal and cardiac markers (Mummery, Ward-van Oostwaard et al. 2003; Beqqali, Kloots et al. 2006). Hypoxic exposure resulted in enhanced expression of mesodermal and early cardiac genes such as brachyury, Mesp1 and Isl1 indicating the impact of hypoxia at early stages of differentiation. This data suggests that hypoxia may act to provide a mesoderm-inductive signal. Hypoxia was furthermore observed to significantly increase the expression of late cardiac genes such as α-actinin, Tbx2, Tbx5 and Troponin T.

Notably, compared to well-based EB culture approaches, our culture system combining aggregate size control with low oxygen tension resulted in a 3.5x increased cell output. A comparison of hypoxic and normoxic conditions in controlled culture demonstrate the benefits of hypoxic cultures: final cell numbers were significantly increased (Table 3-II).

Protein-based and functional analyses were also performed on bioreactor generated cells. Immunocytochemistry of dissociated EBs detected expression of typical cardiac morphology with highly organized α-actinin and sarcomeric actin structures; this analysis indicates that the suspension bioreactor and microcontact printing steps did not compromise the ability of the differentiated cells to re-adhere and express mature cardiac markers. Action potentials (APs) were recorded from plated EBs. This analysis revealed that APs indeed propagate from a central colony to the rest of the cells, suggesting that some of these cells may be pacemaker in origin. The drug responsiveness of the bioprocess generated cells also supports the possibility of their use in drug screening studies.

Importantly, although the reported bioprocess represents a next-generation technology for the production of pluripotent cell derivatives, further improvements are necessary to increase the yield of target cells. Under currently serum-induced differentiation conditions only a subset of

these cells are mesoderm and cardiac cells fated. We previously used genetic selection systems to enrich for target cells (Zandstra, Bauwens et al. 2003) and, certainly, with appropriately engineered hESC lines this strategy could work here. Alternately, incorporating the use of serum-free media and cytokine driven differentiation as demonstrated in recent developments in ESC differentiation protocols (Li, Powell et al. 2005; McDevitt, Laflamme et al. 2005; Passier, Oostwaard et al. 2005; Kattman, Huber et al. 2006; Xu, He et al. 2006; Kattman, Adler et al. 2007; Laflamme, Chen et al. 2007; Yang, Soonpaa et al. 2008; Zhang, Li et al. 2008) could improve the yield of target cells. An important aspect of transferring bioreactor systems to serum-free cytokine induced systems will be developing new bioengineering strategies to deliver recombinant molecules in a cost effective manner, and addressing the known (van der Pol and Tramper 1998) increased sensitivities of cells to shear in serum free systems.

In this paper we have focused on hESCs as a model system, but the described technology is broadly adaptable to other cell types, including pluripotent lines produced by iPS cells (Takahashi, Tanabe et al. 2007; Yu, Vodyanik et al. 2007). Overall, this study contributes towards the goal of generating pluripotent stem cell-derived cells in a scalable manner under controlled conditions; an important step in the technological and health-related use of these cells.

Chapter 4
Geometric Control of Cardiomyogenic Induction in Human Pluripotent Stem Cells

This chapter has been prepared for submission for publication. Co-authors include Mark Ungrin, Cheryle Seguin, and Peter W. Zandstra. Authorization to reproduce this work has been obtained from all co-authors.

ABSTRACT

Rationale: It has been widely observed that aggregate size affects cardiac differentiation efficiency of human pluripotent stem cells, but the cellular mechanisms underlying cardiomyogenesis are incompletely understood. **Objective:** To develop cellular and molecular mechanisms for the intrinsic control of human tissue development, we evaluated tissue-specific differentiation as a function of human embryonic stem cell (hESC) aggregate size, and examined the effect of manipulating expression of SOX7, a transcription factor required for extraembryonic endoderm (ExE) commitment, on cardiac development. **Methods and Results:** HESC aggregates were generated with either 100, 1000, or 4000 cells per aggregate. We observed that the frequency of endoderm marker (FoxA2 and GATA6) expressing cells decreased with increasing aggregate size during early differentiation. Cardiogenesis was maximized in aggregates initiated from 1000 cells, with 49.2% ± 5.8% (45.6-55.9%) of cells exhibiting a cardiac progenitor phenotype (KDR^{low}/$C\text{-}KIT^{neg}$) on day 5 (D5) and 23.6% ± 5.7% (17.1-27.7%) expressing cardiac troponin T on D16. A direct relationship between ExE and cardiac differentiation efficiency was established by forming aggregates with varying ratios of SOX7-overexpressing or knockdown hESCs to unmanipulated hESCs, wherein cardiomyocyte frequency (~27%) was maximized in aggregates formed with 10 to 25% SOX7 overexpressing cells. **Conclusions:** We demonstrate that cardiac differentiation efficiency is a function of ExE cell concentration, a parameter that can be directly modulated by controlling hESC aggregate size. This is the first presentation of a cellular mechanism to describe the effect of aggregate size on cardiac development, suggesting that a molecular mechanism may be based on endoderm-secreted factors.

INTRODUCTION

One of the most common techniques to induce human pluripotent stem cell (hPSC) differentiation is by forming three-dimensional cell aggregates (Doetschman, Eistetter et al. 1985). Within the developing aggregate, pluripotent stem cells differentiate to cell types belonging to each of the three germ layers (mesoderm, endoderm, and ectoderm) (Thomson, Itskovitz-Eldor et al. 1998). Differentiating aggregates are thought to mimic the environment of the peri-implantation embryo where interactions between various cell types facilitate inductive events. As in the embryo, one of the earliest events during aggregate-based stem cell differentiation is the organization of the cells into an outer epithelial layer of extraembryonic endoderm (ExE) cells surrounding an inner core of epiblast-like pluripotent cells (Coucouvanis and Martin 1995; Keller 1995; Abe, Niwa et al. 1996; Grabel, Becker et al. 1998; Coucouvanis and Martin 1999; Ungrin, Joshi et al. 2008; Carpenedo, Bratt-Leal et al. 2009). During embryonic development, precardiac mesoderm is in close contact with endoderm tissue which has been shown to play an inductive role as evidenced by the generation of beating cardiac tissue in cocultures of non-cardiogenic embryonic tissue explants and endodermal tissue (Orts Llorca 1963; Jacobson and Duncan 1968; Sugi and Lough 1994; Nascone and Mercola 1995; Schultheiss, Xydas et al. 1995). In differentiating PSCs, ExE and its derivatives, visceral and parietal endoderm, have also been shown to promote cardiomyocyte differentiation in co-culture and conditioned medium studies (Hogan, Taylor et al. 1981; Bader, Gruss et al. 2001; Mummery, Ward-van Oostwaard et al. 2003; Passier and Mummery 2005; Passier, Oostwaard et al. 2005; Bin, Sheng et al. 2006; Xu, Graichen et al. 2008).

One of the main challenges of aggregate-based hPSC differentiation is that heterogeneity and spatial disorganization leads to inefficient differentiation to specific cell types and a poor understanding of the mechanisms involved in lineage commitment. In studies addressing this challenge, two strategies have emerged. One involves exogenously controlling differentiation by delivering factors that are known or thought to be involved in specification, commitment and proliferation of the cell type of interest (Laflamme, Chen et al. 2007; Pick, Azzola et al. 2007; Yang, Soonpaa et al. 2008; Nakanishi, Kurisaki et al. 2009). The second strategy focuses on controlling physical parameters of aggregate formation, such as aggregate size and shape (Ng, Davis et al. 2005; Khademhosseini, Ferreira et al. 2006; Mohr, de Pablo et al. 2006; Burridge,

Anderson et al. 2007; Pick, Azzola et al. 2007; Bauwens, Peerani et al. 2008; Ungrin, Joshi et al. 2008; Niebruegge, Bauwens et al. 2009). We and others have previously reported the observation that human embryonic stem cell (hESC) aggregate size can be modulated to optimize cardiac induction efficiency (Burridge, Anderson et al. 2007; Bauwens, Peerani et al. 2008; Hwang, Chung et al. 2009; Mohr, Zhang et al. 2009; Niebruegge, Bauwens et al. 2009), however the cellular mechanism by which aggregate size and geometry impacts differentiation to specific cell types remains unclear. Given that the surface area to volume ratio of a sphere decreases with increasing sphere size, and that an ExE layer forms on the surface of the differentiating aggregate, we examined the possibility that this geometric relationship dictates ExE cellularity during early aggregate-based hESC differentiation and the implications of varying ExE concentration on cardiomyocyte differentiation efficiency.

One challenge in controlling hESC aggregate size has been that hESCs exhibit poor tolerance to single cell dissociation (Reubinoff, Pera et al. 2000; Burridge, Anderson et al. 2007). A number of techniques have been developed to address this challenge including forced aggregation of defined cell numbers (Ng, Davis et al. 2005; Burridge, Anderson et al. 2007; Ungrin, Joshi et al. 2008), or culturing hESCs in maintenance conditions as size specified colonies on micropatterned extracellular matrix (Bauwens, Peerani et al. 2008; Niebruegge, Bauwens et al. 2009) or as 3-D clumps in size-specified microwells (Khademhosseini, Ferreira et al. 2006; Mohr, de Pablo et al. 2006; Hwang, Chung et al. 2009; Mohr, Zhang et al. 2009) and then transferring these colonies or cell clumps to suspension in differentiation medium to induce aggregate differentiation. Since we previously observed that the status of the input population is a function of hESC colony size and significantly affects cardiac induction efficiency (Bauwens, Peerani et al. 2008), we tracked ExE and cardiac development in size specified aggregates formed using forced aggregation of a single cell suspension (Ungrin, Joshi et al. 2008) to eliminate heterogeneity of the input hESCs. To investigate the effect of ExE differentiation frequency on cardiomyocyte differentiation independently of aggregate size, we manipulated the expression of SOX7. SOX7 is a transcription factor that plays a crucial role in ExE development. SOX7 silencing leads to inhibition of ExE differentiation of pluripotent cells (Futaki, Hayashi et al. 2004) and SOX7 overexpression of hESCs leads to the development of an ExE progenitor phenotype (Seguin, Draper et al. 2008). It should be noted that this is the first report examining the effect of hESC aggregate size on cardiomyocyte differentiation under

defined conditions that promote cardiogenesis (Yang, Soonpaa et al. 2008). From the results presented here, we propose that varying hESC aggregate size leads to geometrically determined effects on the level of ExE development during early differentiation which subsequently impacts cardiac differentiation efficiency.

MATERIALS AND METHODS

Cell culture

The H9 (Israel Institute of Technology, WiCell Research Institute), HES2 (ES Cell International), and CA1 (Nagy Lab, Mount Sinai Hospital, University of Toronto) hESC cell lines used in these experiments were maintained and expanded as previously described (Bauwens, Peerani et al. 2008; Seguin, Draper et al. 2008; Yang, Soonpaa et al. 2008). Briefly, hESC colonies were maintained on mitotically inactivated mouse embryonic fibroblast (MEF) feeders in Dulbecco's Modified Eagle Medium: Nutrient Mixture F-12 (DMEM/F12, Invitrogen) supplemented with 10 to 20% Knockout^{TM} Serum Replacement (ko-SR, Invitrogen) and 20 ng/mL Basic Fibroblast Growth Factor (FGF-2, Peprotech). Cells were passaged by enzymatic dissociation. H9 passaging was performed every 4 days by dissociating the cells into small clumps using Collagenase type IV (2 mg/mL, Invitrogen), whereas CA1 and HES2 cells were passaged every 7 days by dissociating to single cells using TrypLE^{TM} (Invitrogen). SOX7 O/E cell lines were generated from CA1 cells as previously described (Seguin, Draper et al. 2008) and maintained in the same conditions as their parental CA1 cell line. Aggregate-based differentiation of hESCs was carried out using a protocol for serum-free directed differentiation to the cardiac lineage which has been previously described (Yang, Soonpaa et al. 2008). Briefly, hESC aggregates were cultured in base media composed of StemPro34 (Invitrogen) with 2 mM glutamine, 4×10^{-4} M monothioglycerol (MTG), 50 μg/ml ascorbic acid (Sigma), and 0.5 ng/ml BMP4. The following concentrations of factors were used for primitive-streak formation and for mesoderm induction and cardiac specification: BMP4, 10 ng/ml; human bFGF, 5 ng/ml; activin A, 3 ng/ml; human DKK1, 150 ng/ml; and human VEGF, 10 ng/ml. The factors were added with the following sequence: days 1–4, BMP4, bFGF and activin A; days 4–8, VEGF and DKK1; after day 8, VEGF, DKK1 and bFGF. All factors were purchased from R&D Systems. Cultures were maintained in a 5% CO_2/5% O_2/90% N_2 environment for the first 12 days and then transferred to a 5% CO_2/air environment. HESC aggregate size was controlled by forced

aggregation of defined cell concentrations in AggreWells (Stem Cell Technologies), poly(dimethylsiloxane) (PDMS) inserts containing a textured surface of micro-wells (Ungrin, Joshi et al. 2008).

Knockdown of SOX7 gene expression in hESCs by siRNA

The Dharmafect™ 1 (Dharmacon) delivery system was used to transfect hESCs with predesigned siRNA against SOX7 (100nM, SMARTpool, L-019017-01) according to the manufacturer's protocol in OptiMEM (Invitrogen) base medium. Control cells were similarly transfected with non-targeting siRNA (ON-TARGET*plus* Non-targeting Pool, D-001810-10-20). Cells were enzymatically dissociated to single cells with TrypLE, and seeded onto a Matrigel-coated surface in hESC maintenance medium plus the transfection medium. After 24 hours the cells were washed and re-fed with hESC maintenance medium alone. 48 hours following seeding, aggregates were formed by forced aggregation of varying ratios of SOX7 siRNA transfected HES2 cells and SOX7 O/E CA1 cells (hESC-derived ExE progenitors).

Flow cytometry

HESC colonies or aggregates were dissociated to single cells using the appropriate dissociation technique. For detection of intracellular proteins FoxA2 (R&D Systems), GATA6 (R&D Systems), and cardiac troponin T (cTnT, Lab Vision), cells were fixed and permeabilized with the IntraPrep fixation and permeabilization kit (Immunotech), then incubated in the presence of primary antibody (1:500 for FoxA2, 1:10 for GATA6, and 1:100 for cTnT) for 20 minutes at room temperature, followed by an incubation with secondary fluorophore-conjugated antibody (Molecular Probes) at a 1:100 dilution for 20 minutes at room temperature. For detecting the expression of surface proteins KDR and C-KIT, live cells were incubated on ice for 30 minutes in the presence of anti-KDR-PE (Phyco-erythrin; 1:10, R&D Systems) and anti-C-KIT-APC (Allophycocyanin; 1:100, R&D Systems). Cells were analyzed using a FACSCanto (BD Biosciences) flow cytometer. Positive staining was defined as the emission of a level of fluorescence that exceeded levels obtained by 99.5% of cells from the control population stained with only the secondary antibody.

Confocal microscopy

HESC aggregates were fixed and stained for confocal microscopy imaging at different stages in the differentiation culture using a protocol that has been previously described (Bauwens, Yin et al. 2005). The following antibodies were used: FoxA2 (1:1000), and secondary antibodies (1:200, Molecular Probes). Cell nuclei were detected by staining aggregates with Hoechst 33342 (Molecular Probes). Cells were imaged at the University Health Network's Advanced Optical Microscopy Facility using an Olympus FV1000 confocal laser microscope.

Immunostaining and Imaging

Fluorescent images of Sox7 (1:100, R&D Systems), Sox17 (1:100, R&D Systems), and GATA-6 (1:20, R&D Systems) protein expression were obtained with the Cellomics Arrayscan V^{TI} platform and quantitatively analyzed using the Target Activation assay algorithms available with the Cellomics Arrayscan V^{TI} platform (Cellomics).

Statistics

All data shown are the mean of three independent experiments with error bars on plots representing the standard deviation of the mean unless otherwise indicated. To evaluate differences between conditions, statistics were computed in Origin 7.5 using the the two sample t-test or one-way ANOVA as indicated at a significance level of $P < 0.5$.

RESULTS

Establishing optimal hESC aggregate size to maximize cardiomyocyte differentiation

Cardiac induction and differentiation was assessed in hESC aggregates formed with 100, 1000 and 4000 cells per aggregate (Figure 4.1A). It was previously reported that when conventional scraped EBs, cultured in the same defined conditions used for the studies presented here, were analyzed for expression of KDR and CKIT on day (D)5/6, three distinct populations emerged: $KDR^{high}/CKIT^{pos}$, $KDR^{low}/CKIT^{neg}$, and $KDR^{neg}/CKIT^{pos}$ (Yang, Soonpaa et al. 2008). In that report it was demonstrated that the $KDR^{low}/CKIT^{pos}$ population expressed high levels of genes involved in cardiac development and that these cells subsequently gave rise to an enriched

population of cells expressing mature cardiac differentiation markers (Yang, Soonpaa et al. 2008). We therefore assayed the same markers to assess the influence of aggregate size on cardiac induction. Representative flow cytometry dot plots are presented in Figure 4.1B. The results of the KDR/CKIT flow cytometry analysis demonstrate that the large (4000 cells) and small (100 cells) aggregate sizes we tested were not optimal for cardiac induction, and that the highest frequency of $KDR^{low}/CKIT^{neg}$ cells were detected in the mid- size condition (1000 cells) (Figure 4.1C). This observation is consistent with previously published findings that varying aggregate size modulates the level of cardiac induction during hESC differentiation (Burridge, Anderson et al. 2007; Bauwens, Peerani et al. 2008; Hwang, Chung et al. 2009; Mohr, Zhang et al. 2009).

By day 12 of differentiation, spontaneous contractions were observed in the majority of EBs under all size conditions. Mature cardiac differentiation was assessed by measuring the frequency of cardiac troponin T (cTnT) expressing cells in D16 size-specified aggregates using flow cytometry (representative flow cytometry histograms are presented in Figure 4.1D). Corresponding to the results of the cardiac induction analysis, the highest percentage (approximately 25%) of cTnT expressing cells was detected in aggregates initiated with 1000 cells (Figure 4.1E). Aggregates formed with 100 and 4000 cells exhibited lower frequencies of cTnT expression by D16, ranging between 5 to 10% (Figure 4.1E). This data demonstrates that controlling aggregate size with respect to the number of cells per aggregate influences cardiac induction and differentiation even in defined medium that contains factors that specify cardiac commitment and expansion.

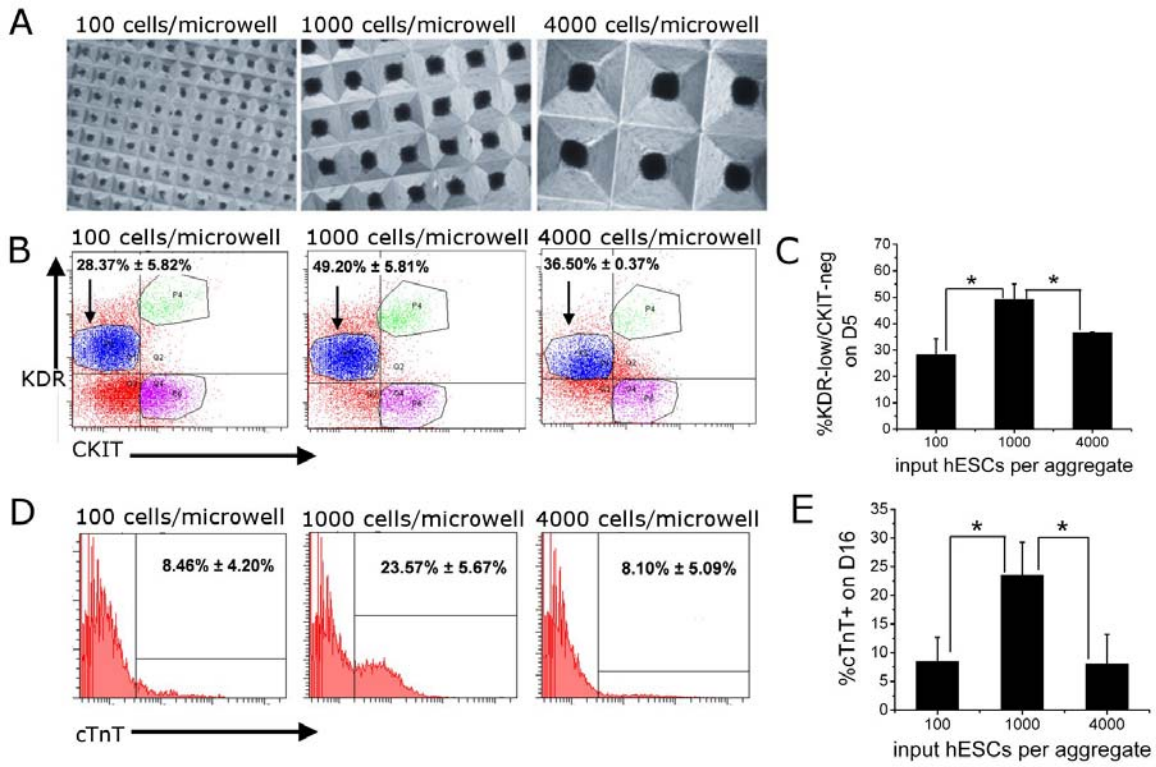

Figure 4.1: Of the three EB sizes investigated, cardiac induction is maximized in EBs generated from 1000 cells. (A) Phase contrast microscopy images of size controlled aggregates initiated with 100, 1000, or 4000 cells per aggregate. **(B)** Representative flow cytometry dot plots for the cardiac progenitor analysis examining KDR and C-KIT protein expression. The population identified as not expressing C-KIT and expressing KDR protein at low levels is recognized as a cardiac progenitor enriched population. **(C)** Bar graph displaying the frequency of KDR^{low}/C-KIT^{-} cells in D5 size-controlled EBs. * indicates significantly different values as determined by a two sample t-test. **(D)** Representative flow cytometry histograms for the expression of cardiac marker cTnT in d16 size-controlled EBs. **(E)** Bar graph displaying the frequency $cTnT^{+}$ cells in D16 size-controlled EBs. * indicates significantly different values as determined by a two sample t-test.

Emergence and spatial organization of endoderm cells in size-controlled aggregates

We next evaluated spatial organization in differentiating hESC aggregates to confirm that endoderm cells develop on the surface of the spheroid during early differentiation. Figure 4.2A outlines the relationship between the surface area and volume of a sphere as sphere radius doubles. With each radius doubling, the surface area to volume ratio of a sphere is halved. If an inverse relationship also applies to the development of the ExE layer on the surface of a differentiating hESC aggregate, then ExE frequency during early differentiation decreases with increasing aggregate size. Confocal imaging revealed the spatial expression of the endoderm protein marker FoxA2 was mainly localized to the surface of D4 aggregates (Figure 4.2B). This

analysis suggested that spatial organization of endoderm cells to the aggregate surface occurs in hESC aggregates formed by forced aggregation in the Aggrewell™ system.

The capacity for hESC differentiation along the endoderm lineage increases with decreasing aggregate size

To directly evaluate the effect of aggregate size on endoderm concentration during early differentiation, size specified aggregates were assessed at D0, D1, D3, and D6 of differentiation for frequency of cells expressing the endoderm protein markers FoxA2 and GATA6 by flow cytometry (Figure 4.2C, D). Figure 4.2C depicts representative dot plots from the flow cytometry analysis. A trend emerged in which the frequency of $FoxA2^+$ and $GATA6^+$ cells increased with decreasing aggregate size at each timepoint, with the smallest aggregates that were formed at an initial size of 100 cells consistently exhibiting the highest frequency of endoderm marker-expressing cells (Figure 4.2D). Similar protein expression profiles were observed for both endoderm markers tested at all three aggregate sizes, with maximum frequencies generally reached by D3 of the timepoints that were analyzed. FoxA2 expression reached a maximum level of 7.30% ± 1.30% in the smallest aggregate condition (initiated with 100 cells) on D3, whereas the largest aggregates (formed with 4000 cells) consistently displayed the lowest frequencies of $FoxA2^+$ cells never exceeding 3% (Figure 4.2Di). Maximum expression frequencies for GATA6 were also observed on D3, where the highest levels of cells expressing the protein (11.93% ± 1.32% of cells) was observed in the smallest aggregate size condition (initiated with 100 cells) and the lowest levels (6.40% ± 0.71%) in the largest aggregates (initiated with 4000 cells) (Figure 4.2Dii).

D3 aggregate diameters were measured by analyzing phase contrast microscope images of the aggregates and these values were then used to estimate the ratio of the volume of the outer layer of cells (OV) to the total aggregate volume (TV). To estimate the outer cell layer volume, the diameter of a single cell was assumed to equal 10 μm(Sharma, Cabana et al. 2008). The OV/TV ratios for aggregates generated with 100, 1000 and 4000 cells are presented in Figure 4.2E. Under all aggregate size conditions, the OV/TV ratios decreased with increasing aggregates size similar to the trend observed in tracking $FoxA2^+$ and $GATA6^+$ cells on D3, and consistent with our hypothesis. In all cases, the OV/TV ratios were higher than the corresponding $FoxA2^+$ and $GATA6^+$ cell frequencies (100 cell aggregates: OV/TV ~ 0.6, $FoxA2^+$ ~ 0.07, $GATA6^+$ ~ 0.12;

1000 cell aggregates: OV/TV ~ 0.3, FoxA2^{+} ~ 0.05, GATA6^{+} ~ 0.09; 4000 cell aggregates: OV/TV ~ 0.2, FoxA2^{+} ~ 0.03, GATA6^{+} ~ 0.06), indicating that either endoderm cells do not make up a complete layer surrounding the aggregate, cells in the outer layer may not be as densely packed as cells located in the interior of the aggregate, or may vary in size from inner cells. It can be observed in the confocal images (Figure 4.2B) that not all aggregates contain an outer layer of endoderm cells and that in many aggregates endoderm cells do not make up the full layer of outer cells.

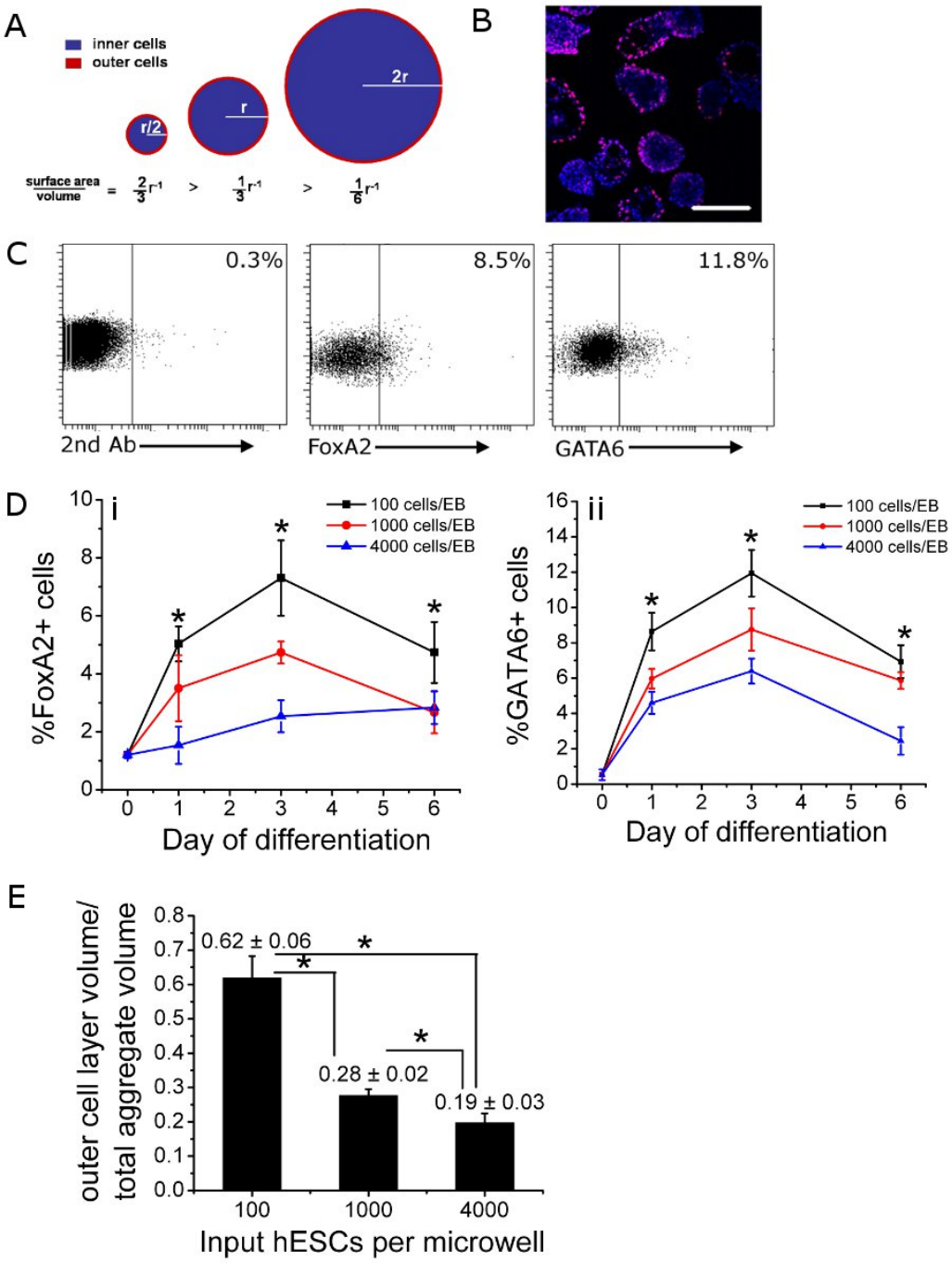

Figure 4.2: Endoderm cells develop on the surface of size-specified hESC aggregates formed by forced aggregation and endoderm differentiation frequency decreases with increasing hESC aggregate size. (A) An illustration of the underlying concept behind the hypothesis that the level of extraembryonic endoderm differentiation is inversely proportional to EB size. **(B)** Confocal microscopy image of aggregates demonstrating protein expression of FoxA2 (red, blue = Hoechst nuclear staining) in D4 EBs generated from 1000 cells. Scale bar = 250 μm. **(C)** Representative flow cytometry dot plots for FoxA2 and GATA6 protein expression. **(D)** Kinetics of the frequency of cells expressing endoderm-associated proteins FoxA2 (i) and GATA6 (ii) in aggregates generated from 100, 1000, and 4000 cells. * represents significant differences between the values at each time point as determined by ANOVA analysis. **(E)** The ratio of the volumes of the outer layer of cells to the total aggregate of D3 aggregates generated with 100, 1000, and 4000 cells per aggregate, determined by image analysis of phase contrast microscope images. * indicates significantly different values as determined by a two sample t-test.

Varying the frequency of ExE progenitor cells in hESC aggregates influences cardiac differentiation efficiency in size controlled hESC aggregates independently of aggregate size

As it was observed that cardiac induction and differentiation could be modulated by varying hESC aggregate size and that there was an inverse relationship between aggregate size and the frequency of endoderm cells present during the first six days of differentiation, we next examined the possibility that the frequency of endoderm cells can be optimized to maximize cardiomyocyte differentiation efficiency. To vary ExE frequency independently from aggregate size, we manipulated the expression of SOX7, a transcription factor that is required for ExE differentiation (Futaki, Hayashi et al. 2004; Seguin, Draper et al. 2008), in the input hESC population (Figure 4.3A). To study the effect of increasing ExE frequency, 1000 cell aggregates were generated with varying ratios of normal hESCs to SOX7-overexpressing (O/E) hESCs (ExE progenitors) (Figure 4.3Bi). Conversely, the effect of reducing ExE frequency was examined by generating 1000 cell aggregates with varying ratios of normal hESCs to knockdown SOX7 hESCs (kd-SOX7) (Figure 4.3Bii). SOX7 expression was induced in genetically engineered CA1 hESC lines (SOX7 O/E) following transient expression of Cre recombinase. An ExE progenitor phenotype in transgenic cell lines was confirmed by expression of SOX7, GATA6 and SOX17 proteins, markers that are associated with an ExE phenotype (Supplementary Figure S3-1). SiRNA transfection was employed to silence SOX7 expression in hESCs. SOX7 siRNA transfection was validated by demonstrating SOX7 protein knockdown in the SOX7 O/E cells that were transfected with the siRNA (Supplementary Figure S3-2).

The frequency of $cTnT^+$ cells on D16 was measured to track cardiomyocyte differentiation frequency with respect to input ExE progenitor (SOX7 O/E hESC) or kd-SOX7 hESC frequency. Parallel controls that were carried out included the parental non-Cre-transfected CA1 cells in place of SOX7 O/E hESCs or non-targeting siRNA-transfected hESCs in place of kd-SOX7 hESCs. It was observed that cardiomyocyte differentiation efficiency varied in response to different input levels of ExE progenitors (Figure 4.3Ci). Maximum cardiac differentiation (27.55% ± 4.74% and 27.50% ± 1.90%) was observed in aggregates generated with 10% to 25% SOX7 O/E hESCs (Figure 4.3Ci). In the condition initiated with 50% input ExE progenitors, cardiomyocyte differentiation efficiency returned to control levels (13.4%). As expected, in aggregates initiated with 100% ExE progenitors, cardiomyocyte differentiation was drastically

reduced (3.1%) from control levels. A negative response to increasing frequencies of kd-SOX7 hESCs was observed with respect to cardiomyocyte differentiation efficiency (Figure 4.3Cii), wherein all aggregates containing kd-SOX7 hESCs exhibited reduced cardiomyocyte frequencies compared to the control condition reaching a minimum of 2.5% $cTnT^{+}$ in aggregates generated with 100% kd-SOX7 hESCs, indicating that although SOX7-expressing cells do not efficiently differentiate towards the cardiac lineage their presence promotes cardiogenesis. From these findings it was concluded that by manipulating the input frequencies of ExE progenitors, cardiomyocyte differentiation could be attenuated or increased even in the presence of growth factors that specifically direct cardiac commitment and expansion, suggesting that ExE cells exert a cell non autonomous effect on differentiating hESCs.

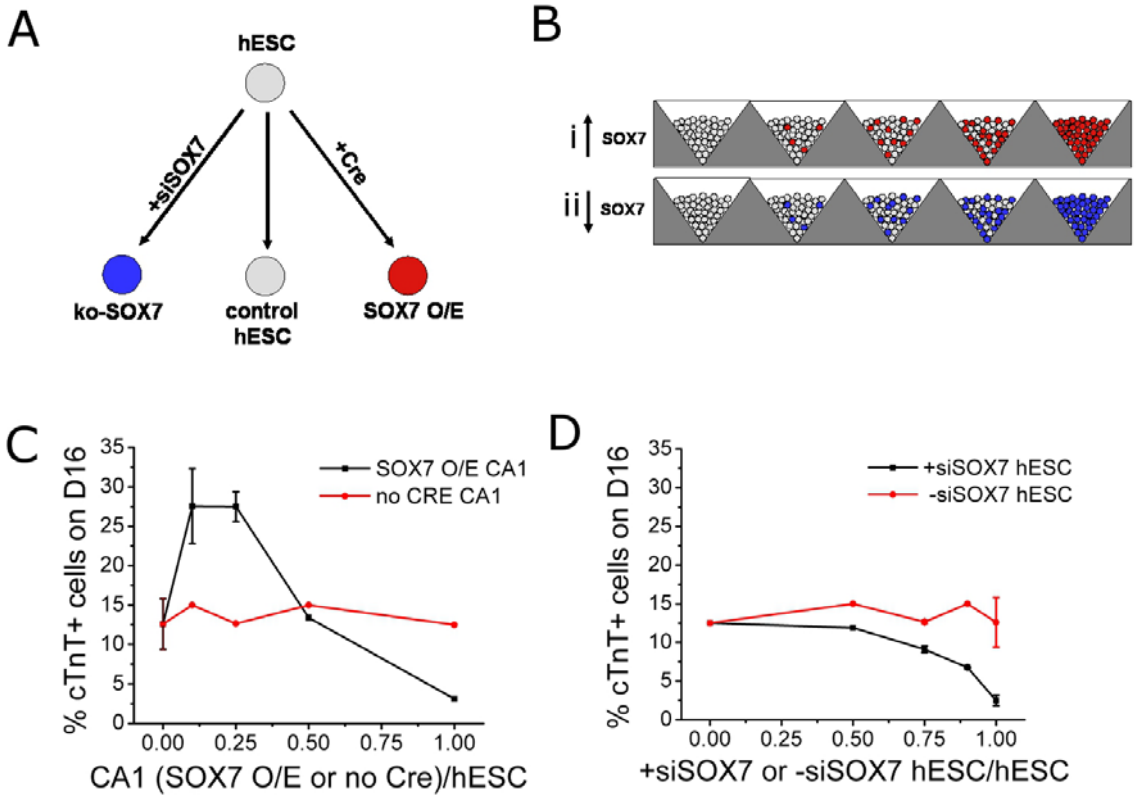

Figure 4.3: The frequency of input ExE cells has an aggregate size independent effect on cardiomyocyte differentiation efficiency. (A) ExE differentiation is blocked by transfecting cells with siRNA that silences SOX7 transcription factor (ko-SOX7) and promoted in genetically engineered cells that over-express SOX7 upon transfection with Cre (SOX7 O/E). **(B)** Size controlled EBs are formed at controlled ratios of SOX7 O/E and ko-SOX7. **(C)** Frequency of cardiomyocytes ($cTnT^{pos}$) in D16 EBs generated with varying frequencies of SOX7 O/E cells or **(D)** siSOX7-transfected cells (N=2).

DISCUSSION

Using a variety of methods to control aggregate size, a number of reports have demonstrated that this parameter influences hPSC differentiation along the cardiac lineage (Burridge, Anderson et al. 2007; Bauwens, Peerani et al. 2008; Mohr, Zhang et al. 2009; Niebruegge, Bauwens et al. 2009). A significant observation that has been made consistently across these studies is that there is a specific range of aggregate sizes, usually defined by aggregate diameter, in which the frequency of contracting aggregates and cardiac-associated gene expression is maximized. In aggregates generated by either forced aggregation (Burridge, Anderson et al. 2007) or in microwells (Mohr, Zhang et al. 2009), it has been shown that the frequency of contracting aggregates and expression of cardiac-associated genes was maximized in aggregates with diameters in the 250 to 350 μm range, and decreased in smaller and larger aggregates. Even under conditions in which aggregate size has been optimized however, cardiac differentiation efficiency appears to be quite low in these studies, with observed frequency of contracting aggregates typically less than 25% (Burridge, Anderson et al. 2007; Mohr, Zhang et al. 2009), and in the few cases where cardiomyocyte differentiation frequency was evaluated, less than 5% of cells expressed cardiac-specific proteins (Bauwens, Peerani et al. 2008; Mohr, Zhang et al. 2009).

The present study is the first report investigating the effect of hESC aggregate size on cardiomyocyte differentiation under defined conditions that promote cardiogenesis. In addition, more robust metrics for aggregate size and cardiac differentiation efficiency were employed than in the previously described reports. Aggregate size was defined in terms of the number of input cells per aggregate, not aggregate diameter which can represent slightly different cell numbers between runs depending on cell density. To more accurately determine cardiomyocyte differentiation efficiency we analyzed the frequency of cells expressing cardiac progenitor and mature cardiac markers, instead of counting the frequency of beating aggregates or determining relative gene expression levels of cardiac markers. Similar to previous reports, we observed a trend wherein cardiomyocyte induction and differentiation was attenuated in aggregates that were too small or too large even in the presence of growth factors that specify the cardiac lineage, and mid-size aggregates (initiated with 1000 cells) produced the highest levels of D5 cardiac progenitors (~50%) and D16 cardiomyocytes (~25%). While the trend we observed was similar to previous studies, under defined conditions that specify cardiac induction we achieved

significantly higher levels of cardiomyocyte differentiation in hESC size-controlled aggregates than in any prior reports.

From the findings presented here we propose a cellular mechanism to describe how aggregate size affects cardiomyocyte differentiation efficiency. We reasoned that aggregate size determined the level of cardiac-promoting ExE that developed by a simple geometric relationship; that the ratio of the surface area to volume of a sphere decreased with increasing sphere diameter. In this case, aggregate size could be varied to directly control the frequency of ExE differentiation which subsequently could impact the efficiency of cardiac differentiation. Tracking endoderm frequency over the first 6 days in size-specified aggregates, we observed a relationship in which the level of endoderm cell development decreased with increasing aggregate size, supporting the hypothesis that the level of endoderm differentiation is related to the ratio of outer cells to inner cells in the cell spheroid. A direct relationship between frequency of ExE cells during aggregate formation and cardiomyocyte differentiation efficiency was confirmed by monitoring cardiomyocyte frequency in size-specified hESC aggregates that were generated with controlled frequencies of cells that either overexpressed SOX7 transcription factor or were transfected with siRNA blocking SOX7 transcription. Our findings support the concept that there is a geometric relationship between hESC aggregate size and the extent of ExE development during early differentiation that subsequently impacts cardiac induction and differentiation efficiency.

It has been suggested that the effect of hESC aggregate size on cardiac differentiation is influenced by the diffusion of critical substrates and growth factors throughout the aggregate (Mohr, Zhang et al. 2009). Certainly, during embryogenesis spatial gradients of several signaling molecules are involved in guiding cardiac development, many originating from ExE cells as previously described. The inductive characteristic of the endoderm has been attributed to TGF-β superfamily and FGF family growth factors that have been reported to be involved in cardiac differentiation (Sugi and Lough 1994; Schultheiss, Xydas et al. 1995; Sugi and Lough 1995; Schultheiss, Burch et al. 1997; Schultheiss and Lassar 1997). It has been shown using mouse (m)ESCs that inhibition of primitive endoderm with diffusible leukemia inhibitory factor (LIF) during cell aggregation attenuates cardiomyocyte differentiation and that cardiomyogenesis could be rescued with parietal endoderm conditioned medium (Bader, Gruss et al. 2001), suggesting that the primitive endoderm secretes factors that contribute to cardiac

commitment in a paracrine, LIF independent manner. In mESC aggregates generated by mixing different ratios of Dox-inducible GATA4 overexpressing mESCs with the untransfected parental cell line (Holtzinger, Rosenfeld et al. 2010), GATA4 overexpressing cells develop into $SOX17^{+}$ cells that secrete BMPs and DKK to promote cardiac induction in the non-GATA4 overexpressing cells. It has been recently observed in the mESC system that Wnt5A gene expression is modulated in an aggregate size dependent manner wherein lower gene expression in larger aggregates (generated from 450 μm diameter microwells) corresponded to enhanced cardiogenesis based on frequency of beating aggregates and cardiac gene expression (Hwang, Chung et al. 2009). In the same study it was shown that GATA4 mRNA was highly expressed in larger aggregates. It may be that the GATA4-expressing cells secrete enough DKK to inhibit Wnt5A in the larger aggregate condition. SPARC (Secreted Protein, Acidic, Rich in Cysteine), a matricellular glycoprotein that is highly expressed in the developing heart (Holland, Harper et al. 1987; Brekken and Sage 2001), is another candidate molecule secreted by parietal endoderm that has been shown to promote early myocardial differentiation in mESC aggregates (Stary, Pasteiner et al. 2005; Hrabchak, Ringuette et al. 2008). Mouse ESC aggregates cultured in parietal endoderm conditioned medium exhibit enhanced cardiac differentiation (Stary, Pasteiner et al. 2005); an effect which is abrogated with the addition of anti-SPARC antibodies in a concentration-dependent manner.

In conclusion, we have established a robust system for hESC aggregate-size controlled cardiac induction and differentiation. Using this system, it was determined that aggregate size influences endoderm differentiation efficiency, and that the concentration of ExE in size controlled aggregates directly influences cardiac differentiation efficiency. This system establishes a basis to examine the effect of endoderm-secreted factors on cardiogenesis in aggregate size-controlled hPSC aggregates.

Chapter 5
Discussion and Future Work

THE MECHANISM UNDERLYING THE EFFECT OF HPSC AGGREGATE SIZE ON CARDIOMYOGENESIS

As demonstrated here and widely reported by others, aggregate size is a parameter that can be varied to influence pluripotent stem cell differentiation along the cardiac lineage (Burridge, Anderson et al. 2007; Bauwens, Peerani et al. 2008; Mohr, Zhang et al. 2009; Niebruegge, Bauwens et al. 2009). What remained to be determined was the mechanism underlying this observation. Herein, we have revealed a cellular mechanism to describe how aggregate size influences cardiac induction by modulating the frequency of cardiac-promoting ExE cells which form an epithelial layer surrounding the differentiating aggregate. Interestingly, a recent report has suggested that spatial organization in hESC-derived EBs differs from mESC-derived EBs, wherein the outer layer is composed of $OCT4^+$ ectoderm, and primitive endoderm cells are located in the interior of the aggregate based on expression of erythropoietin receptor (EPOR) (Kopper, Giladi et al. 2010). The authors suggested that the $EPOR^+$ cells may represent primitive endoderm because this marker is also expressed in the yolk sac of 7 day old embryos. This report appears to contradict our own observations that ExE cells are located on the aggregate surface based on the expression of FoxA2 and GATA6 (Ungrin, Joshi et al. 2008). It has been previously reported that primitive endoderm cells do not originate at the EB surface but first appear throughout the EB and subsequently migrate to the surface to form an epithelial layer (Rula, Cai et al. 2007; Moore, Cai et al. 2009). Early aggregates of F9 embryonal carcinoma cells (1 and 2 days old) are largely made up of undifferentiated cells but do contain a few primitive endoderm cells, detected by the expression of GATA4 and the cytoplasmic endocytic adaptor Dab2 (Rula, Cai et al. 2007), which are mainly located in the interior of some of the spheroids with some also present on the surface. By day 4 and 7 of aggregate culture primitive endoderm cells are located on the outer layer of the aggregates, probably by migration, and only a few differentiated cells are located in the interior. Therefore the discrepancy between our observations and those made by Koppler et al may be attributed to the timing of aggregate analysis. Koppler et al analyzed 2 and 3 day old EBs, while we only observe a surface layer of endoderm cells starting at day 4 of aggregate culture (Figure 4.2). Interesting future studies in our system could include tracking the endoderm population during the course of differentiation and tracking the SOX7 O/E hESC population in our EB co-cultures.

An important observation made in these studies is that cell-cell interactions can override exogenous signals during hESC maintenance and differentiation. The development of protocols designed to either maintain pluripotent stem cell populations in the undifferentiated state or differentiate pluripotent stem cells along specific lineages has been largely based on bulk addition of exogenous factors to the culture medium. In the case of hESC maintenance this strategy has consisted of culturing colonies in the presence of saturating concentrations of TGF-β and bFGF. As illustrated in Chapter 2, however, gene expression profiles for hESCs cultured under these conditions vary widely from run to run and it was observed that cell interactions, manipulated by controlling colony size, have a tremendous impact on gene and protein expression status and the subsequent differentiation trajectory of hESCs. These findings, along with previous work published by our lab (Peerani, Rao et al. 2007), suggest that manipulating the physical arrangement of cells in these cultures may influence hESC fate despite the addition of exogenous factors to the medium (Peerani, Rao et al. 2007; Bauwens, Peerani et al. 2008). Similarly, protocols for hESC differentiation to cardiomyocytes typically rely on exogenous factors that are either provided by serum (Kehat, Kenyagin-Karsenti et al. 2001; Xu, Police et al. 2002), secretions from an inductive cell type (Mummery, Ward-van Oostwaard et al. 2003; Passier, Oostwaard et al. 2005), or directly added in a manner meant to mimic the timing and secretion of growth factors during gastrulation in the embryo (Yang, Soonpaa et al. 2008). It was demonstrated in Chapters 2 through 4 that cardiac differentiation efficiency in hEBs cultured in the presence of exogenous factors that specify the cardiac lineage could be further influenced by manipulating aggregate size. Indeed, examining the frequency of cardiomyocytes produced in aggregates generated from 100, 1000, and 4000 cells per aggregate, it appears that in small and large aggregates, cardiac induction is hindered despite the presence of growth factors that are supposed to promote cardiac specification and commitment.

We have collected data that describes a cellular mechanism behind the effect of hESC aggregate size on cardiomyogenesis, however the molecular basis for the effect of aggregate size on cardiogenesis has still not been explored. Now that it has been established that endoderm differentiation can be regulated by manipulating aggregate size and that ExE frequency directly affects cardiac differentiation efficiency, future studies can focus on examining the role of factors secreted by SOX7 O/E hESCs on cardiac development. There are a number of candidate cardiogenic molecules originating from extraembryonic endoderm cells. One of the only

published studies examining the underlying biology behind the effect of (mESC) aggregate size on cardiac induction demonstrated that Wnt11 expression along with lower levels of Wnt5A gene expression in larger EBs (generated from 450 μm diameter microwells) corresponded with enhanced cardiogenesis based on frequency of beating EBs and cardiac gene expression (Hwang, Chung et al. 2009). In the same study it was shown that GATA4 mRNA was highly expressed in larger EBs. GATA4-expressing endoderm cells have been shown to secrete DKK, a Wnt inhibitor (Holtzinger, Rosenfeld et al. 2010). SPARC (Secreted Protein, Acidic, Rich in Cysteine) is another candidate molecule secreted by parietal endoderm that has been shown to promote early myocardial differentiation in mouse EBs (Stary, Pasteiner et al. 2005; Hrabchak, Ringuette et al. 2008). SPARC is a matricellular glycoprotein that is highly expressed in the developing heart (Holland, Harper et al. 1987; Brekken and Sage 2001). Mouse EBs cultured in parietal endoderm conditioned medium exhibit enhanced cardiac differentiation (Stary, Pasteiner et al. 2005); an effect which is abrogated with the addition of anti-SPARC antibodies in a concentration-dependent manner. Additionally TGF- and FGF-family proteins are known to promote PS formation and exogenously added to hESC differentiation cultures to direct cardiac development (Kattman, Adler et al. 2007; Laflamme, Chen et al. 2007; Yang, Soonpaa et al. 2008).

A direct link between SOX7 expression and cardiogenesis has been previously examined (Nelson, Chiriac et al. 2009). SOX family transcription factors have been implicated in the regulation of cardiac and/or vascular fate selection during early embryonic development (Naito, Shiojima et al. 2006; Nelson, Chiriac et al. 2009). Bioinformatics analysis has revealed that the Wnt/β-catenin signaling pathway, which has been demonstrated to drive early progenitor cells into mature cardiomyocytes, is a target of SOX transcription factors (Faustino, Behfar et al. 2008). Differential SOX7 expression has been associated with cardiovascular lineage specification in Flk-1^{+} PS-like cells (Nelson, Chiriac et al. 2009). It has also been reported that SOX7 can inhibit the Wnt/β-catenin pathway (Takash, Canizares et al. 2001), which as discussed in Chapter 1, is involved in commitment of mesoderm towards the vascular and hematopoietic lineages but inhibits cardiac induction (Naito, Shiojima et al. 2006). Therefore, investigating downstream SOX7 signalling may also provide insights into the molecular mechanism behind the role of ExE in promotoing cardiogenesis.

DEFINITIVE ENDODERM (DE) VERSUS EXE: PROMOTING SPECIFIC CARDIAC CELL TYPES

In Chapter 4, the investigation into the effect of aggregate size on endoderm differentiation showed that the frequency of cells expressing the pan-endodermal markers FoxA2 and GATA6 decreased with increasing aggregate size during the first 6 days of differentiation. The subsequent analysis assaying the effect of SOX7 O/E hESC frequency on cardiac differentiation indicated that ExE cells specifically promote cardiogenesis but did not eliminate the possibility that definitive endoderm (DE) cells also contribute to the aggregate size effect observed. Reports specifically examining the effect of DE on cardiac development have been sparse and contradictory. In zebrafish, although heart morphogenesis is severely disrupted when endoderm formation is impaired following inactivation of a Sox-related transcription factor (Kikuchi, Agathon et al. 2001) cardiac tissue still forms (Alexander, Rothenberg et al. 1999; Latinkic, Kotecha et al. 2003). Therefore it appears that induction of cardiac tissue can occur in the absence of endoderm. In xenopus, ectopic expression of GATA4 in animal pole explants results in the formation of DE tissues such as gut (Weber, Symes et al. 2000) and liver. However, it was observed that GATA4-mediated cardiac induction was not dependent on the presence of endoderm in these explants. In fact inhibition of endoderm differentiation by a dominant-negative form of the endoderm transcription factor SOX17β actually led to increased formation of cardiac tissue (Latinkic, Kotecha et al. 2003). These findings appear to suggest that in xenopus the formation of DE may in fact antagonize cardiogenesis, or that inhibition of SOX17 expression may shift cell fate from endoderm to mesoderm (Clements and Woodland 2000). Reports on the role of SOX17 on cardiac mesoderm specification in mESCs appear to contradict what has been observed in xenopus (Liu, Asakura et al. 2007). RNA interference of SOX17 using short hairpin RNA (shRNA) did not impair mesendoderm formation but suppressed Mesp1 and Mesp2 transcription factors that are required for cardiac induction (Kitajima, Takagi et al. 2000). Suppression of SOX17 by either shRNA or treatment with Noggin and sFz8 was followed by suppression of transcription factors for endoderm (FoxA1 and FoxA2) and cardiac differentiation (Nkx2.5, Tbx5, Mef2c, and Myocd). Further indications of impaired cardiac differentiation in mESC-derived EBs were the lack of sarcomeric proteins and spontaneous contractions as cultures progressed. Inhibition of SOX17 did not appear to impair mesendoderm formation, as Oct4 pluripotency marker was downregulated upon initiating differentiation and PS

markers, brachyury and Gsc, as well as hematopoietic marker Runx1 were upregulated. Flk1, a mesoderm marker expressed by both hematopoietic and cardiac muscle progenitors, expression was impaired in 4 to 5 day old EBs however (Liu, Asakura et al. 2007). In mouse EBs generated by mixing different ratios of Dox-inducible GATA4 overexpressing mESCs with the untransfected parental cell line (Holtzinger, Rosenfeld et al. 2010), GATA4 overexpressing cells develop into $SOX17^+$ cells that secrete BMPs and DKK to promote cardiac induction in the non-GATA4 overexpressing cells.

From the conflicting results of these studies, the effect of DE on cardiac specification during embryogenesis is still unclear. It was suggested that impaired cardiac development upon inhibiting SOX17 in mESCs occurred because SOX proteins interfere with canonical Wnt signaling while expression of cardiogenic Wnt11 was impaired following suppression of SOX17 (Liu, Asakura et al. 2007). It should also be noted that SOX17 expression is not exclusive to DE, but is also expressed by ExE during embryogenesis (Hudson, Clements et al. 1997; Kanai-Azuma, Kanai et al. 2002). Previous reports suggest that Sox17 contributes to later differentiation of the visceral and parietal endoderm (Shimoda, Kanai-Azuma et al. 2007). Therefore, in these studies it may still be unclear whether it is the lack of DE or ExE that is affecting cardiogenesis.

Using the system developed herein, it would be relatively simple to test the effect of DE on cardiac induction and differentiation. Similar to the SOX7 O/E hESC cell lines used here in the studies presented in Chapter 4, hESCs have also been genetically engineered to overexpress SOX17 in CA1 and CA2 cell lines (Seguin, Draper et al. 2008). SOX17 O/E hESCs were analyzed after being exposed to either BMP, which is used to induce ExE and trophectoderm differentiation from hESCs (Xu, Chen et al. 2002; Pera, Andrade et al. 2004), or activin A which promotes DE differentiation (D'Amour, Agulnick et al. 2005). Activin A treatment increased expression of the DE markers CXCR4, CER, GSC, and DLX5 in SOX17 O/E hESCs compared to control hESCs, while ExE genes were not expressed in BMP4-treated SOX17 O/E hESCs. Furthermore, BMP4 treatment of SOX17 O/E hESCs actually induced DE markers, indicating that SOX17 O/E hESCs are DE progenitor cells exclusively and incapable of ExE differentiation. Therefore, the effect of DE cells on cardiac commitment during hESC differentiation can be examined by generating EB cocultures containing hESCs and SOX17 O/E cells similar to the experiments presented in Chapter 4 using SOX7 O/E hESCs.

It would be of particular interest to contrast the effects of DE and ExE on different cardiac cell types. In the early streak mouse embryo, a sheet of visceral endoderm is located on the anterior embryonic surface, whereas definitive endoderm develops in the medial regions of the embryo (Figure 5.1A) (Lewis and Tam 2006). Heart mesoderm progenitors arise in the posterior region of the embryo and migrate towards the anterior and medial regions (Figure 5.1B) (Kinder, Loebel et al. 2001). During gastrulation, cardiogenesis occurs in two separate progenitor cell populations that arise from a common progenitor (Garry and Olson 2006). The first cardiac progenitors are specified in the anterior lateral plate mesoderm to form the primary heart field and subsequently give rise to cardiomyocytes belonging to the left ventricle and atria. The first heart field is characterized by the unique expression of Tbx-5 and Hand1 (heart and neural crest derivatives expressed protein-1) transcription factors (Cai, Liang et al. 2003). Pharyngeal mesoderm cells give rise to the secondary heart field which is located medial to the primary heart field. Cells in the secondary heart field express the transcription factors Islet-1 (Isl1) and FGF-10 (Kelly, Brown et al. 2001; Cai, Liang et al. 2003) and contribute to the right ventricle and outflow tract of the heart. Given that there is evidence for both ExE and DE promotion of cardiogenesis and that the two heart fields arise at different times and locations in the embryo, it may be that ExE cells play a role in specifying cardiac induction in the primary heart field while DE cells are involved in guiding commitment of the secondary heart field.

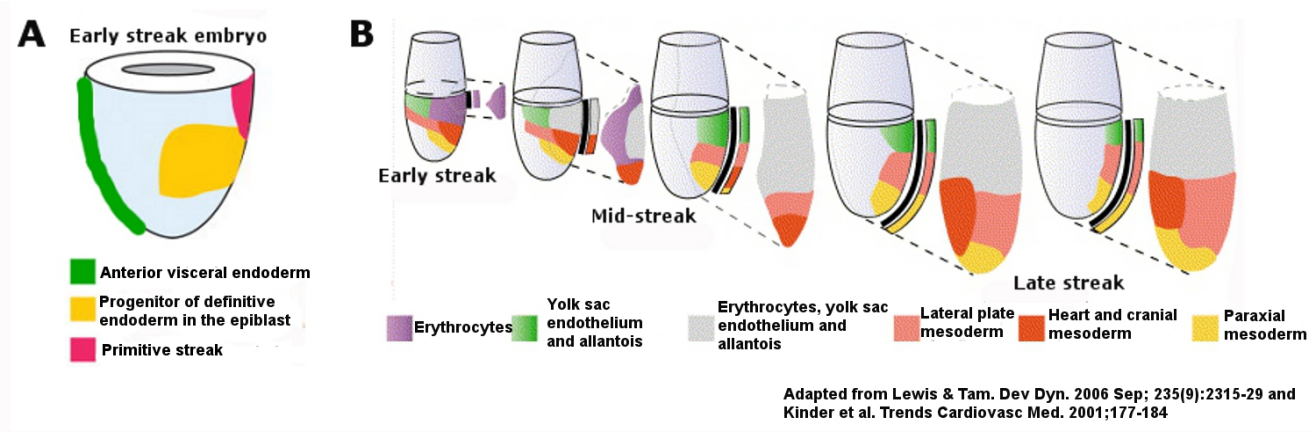

Figure 5.1: Emerging cardiac tissue in relation to extraembryonic endoderm and definitive endoderm. (A) The regionalization of the anterior visceral endoderm and progenitors of the definitive endoderm in the epiblast of the early streak embryo (Lawson, Meneses et al. 1991). **(B)** Localization of mesodermal tissue progenitors in the epiblast/ ectoderm (light blue), the primitive streak (PS, black bar) and the mesoderm (pulled-away layer). Mesoderm tissue composition reflects the types of progenitors that have been recruited from the epiblast through the PS in the immediately preceding developmental stage, not those that are currently ingressing into the PS.

INSIGHTS INTO THE DEVELOPMENT OF A BIOPROCESS FOR EFFICIENT, LARGE SCALE PRODUCTION OF CARDIOMYOCYTES

While examining the effect of hESC aggregate size on cardiac induction provides insights into the mechanisms of embryonic development and cell-cell interactions that guide cardiac commitment, these studies also provide valuable information towards optimizing cardiac production for large scale cell generation. Cell replacement therapy, drug discovery and pharmacotoxicology are applications that require large numbers of pluripotent cell-derived cells. We demonstrated that bioreactor cultures inoculated with micropatterned, size-controlled hESC aggregates contain higher cell expansions (2 to 3 times) and frequency of beating aggregates (2 to 5 times) than bioreactors inoculated with non-size-controlled EBs (Niebruegge, Bauwens et al. 2009). Interestingly, the effect of controlling aggregate size exerted a greater influence on cell expansion and frequency of beating aggregates than the effect of controlling oxygen tension in the bioreactors which only improved yield by approximated 1.7 times under hypoxic conditions and 1.4 times in normoxic conditions compared to uncontrolled oxygen conditions and suggests that in aggregate-based differentiation the endogenous interactions between cells may have a greater impact on cell fate than controlling external parameters such as oxygen concentration.

Controlling hESC aggregate size in an oxygen-controlled stirred suspension bioreactor was a first step in developing robust scalable protocols for efficient cardiac generation. While controlling aggregate size in the studies described in Chapter 3 did lead to a significant improvement in cell expansion which corresponds to improved cardiomyocyte yield, cardiac differentiation efficiency was still very low due to the serum-based induction used in these studies. Many improvements can readily be enabled in this bioprocess. For instance, since performing those experiments, we have established a protocol for cardiac differentiation in size-controlled hESC aggregates under defined conditions (serum-free) (Yang, Soonpaa et al. 2008). Additionally, instead of micropatterning hESC aggregates, a system in which the effects of colony size and aggregate size can not be separated, size controlled aggregates can be formed by centrifuging a single cell suspension of hESCs in Aggrewells (Ungrin, Joshi et al. 2008), thereby enabling us to screen the cardiogenic capacity of aggregates of varying size from one consistent input hESC population. Using forced aggregation also allows for the production of aggregate cocultures containing hESCs and inductive cell types (such as SOX7 O/E hESCs), which we demonstrated in Chapter 4 could further enhance cardiac induction and maximize cardiomyocyte

yield per input hESC in a scalable system. By combining the elements of independent control of hESC colony and aggregate size, consistent input hESC populations, hESC aggregate cocultures containing inductive cell types, and defined conditions that drive cardiac induction in a stirred suspension controlled bioreactor, there is a strong potential of developing a robust system for large scale, efficient production of cardiomyocytes.

SUMMARY AND CONCLUSIONS

The methods developed to control hESC aggregate size revealed that there is a viable range of aggregate sizes for cardiac induction. Furthermore, the newly developed systems for controlling aggregate size were used to elucidate a mechanism for the effect of aggregate size on cardiac induction. Chapter 2 described the establishment of a micropatterning technique for robust generation of uniform hESC aggregates of controlled size that were capable of cardiac differentiation. Further it was demonstrated that differentiation trajectory in size-controlled hESC aggregates was influenced by both MP-hESC colony and aggregate size. These findings demonstrate the importance of controlling input hESC populations for efficient and reproducible differentiation cultures. Specifically, reproducible, efficient (endogenous) mesoderm/cardiac induction is dependent on the ratio of endoderm to neural precursors in the input hESC population, which can be modulated by controlling hESC colony size, as well as on aggregate size. In Chapter 3, it was demonstrated that large-scale differentiation of cardiomyocytes in stirred suspension was enhanced by incorporating MP-hESC aggregates, evidenced by higher cell expansions (2 to 3 times) and frequency of beating aggregates (2 to 5 times) compared to stirred suspension differentiation of non-size controlled aggregates. Finally, in Chapter 3, a direct link between hESC aggregate size, endoderm differentiation efficiency and cardiac yield was established. Using a serum-free, forced aggregation based system for cardiac induction in size controlled hESC aggregates, an inverse relationship between endoderm frequency and hESC aggregate size was observed during the first 6 days of differentiation. In aggregate cocultures, generated by forming aggregates from a mixture of SOX7 O/E ExE progenitor cells and hESCs, it was confirmed that varying the ratio of ExE progenitors directly affects cardiac differentiation efficiency.

Our findings suggest that there is a geometric relationship between hESC aggregate size and the extent of endoderm development during early differentiation that subsequently impacts cardiac

induction and differentiation efficiency, probably via the level of expression of signaling molecules (DKK, SPARC, BMP, Wnt) originating from these ExE cells. These findings are an important step in understanding endogenous control of cell fate through cell-cell interactions in the hESC aggregate, and also provide insights into improving cardiac yields in large scale cultures.

References

Abdel-Latif, A., R. Bolli, et al. (2007). "Adult bone marrow-derived cells for cardiac repair: a systematic review and meta-analysis." Arch Intern Med **167**(10): 989-97.

Abe, K., H. Niwa, et al. (1996). "Endoderm-specific gene expression in embryonic stem cells differentiated to embryoid bodies." Exp Cell Res **229**(1): 27-34.

Ahlquist, P. (2002). "RNA-dependent RNA polymerases, viruses, and RNA silencing." Science **296**(5571): 1270-3.

Alexander, J., M. Rothenberg, et al. (1999). "casanova plays an early and essential role in endoderm formation in zebrafish." Dev Biol **215**(2): 343-57.

Amit, M., M. K. Carpenter, et al. (2000). "Clonally derived human embryonic stem cell lines maintain pluripotency and proliferative potential for prolonged periods of culture." Dev Biol **227**(2): 271-8.

Amit, M., C. Shariki, et al. (2004). "Feeder layer- and serum-free culture of human embryonic stem cells." Biol Reprod **70**(3): 837-45.

Antin, P. B., T. Yatskievych, et al. (1996). "Regulation of avian precardiac mesoderm development by insulin and insulin-like growth factors." J Cell Physiol **168**(1): 42-50.

Attisano, L. and E. Labbe (2004). "TGFbeta and Wnt pathway cross-talk." Cancer Metastasis Rev **23**(1-2): 53-61.

Attisano, L. and J. L. Wrana (2000). "Smads as transcriptional co-modulators." Curr Opin Cell Biol **12**(2): 235-43.

Attisano, L. and J. L. Wrana (2002). "Signal transduction by the TGF-beta superfamily." Science **296**(5573): 1646-7.

Bader, A., A. Gruss, et al. (2001). "Paracrine promotion of cardiomyogenesis in embryoid bodies by LIF modulated endoderm." Differentiation **68**(1): 31-43.

Balsam, L. B., A. J. Wagers, et al. (2004). "Haematopoietic stem cells adopt mature haematopoietic fates in ischaemic myocardium." Nature **428**(6983): 668-73.

Barron, M., M. Gao, et al. (2000). "Requirement for BMP and FGF signaling during cardiogenic induction in non-precardiac mesoderm is specific, transient, and cooperative." Dev Dyn **218**(2): 383-93.

Bauwens, C., T. Yin, et al. (2005). "Development of a perfusion fed bioreactor for embryonic stem cell-derived cardiomyocyte generation: oxygen-mediated enhancement of cardiomyocyte output." Biotechnol Bioeng **90**(4): 452-61.

Bauwens, C. L., R. Peerani, et al. (2008). "Control of human embryonic stem cell colony and aggregate size heterogeneity influences differentiation trajectories." Stem Cells **26**(9): 2300-10.

Behfar, A., L. V. Zingman, et al. (2002). "Stem cell differentiation requires a paracrine pathway in the heart." Faseb J **16**(12): 1558-66.

Beqqali, A., J. Kloots, et al. (2006). "Genome-wide transcriptional profiling of human embryonic stem cells differentiating to cardiomyocytes." Stem Cells **24**(8): 1956-67.

Bettiol, E., L. Sartiani, et al. (2007). "Fetal bovine serum enables cardiac differentiation of human embryonic stem cells." Differentiation **75**(8): 669-81.

Bin, Z., L. G. Sheng, et al. (2006). "Efficient cardiomyocyte differentiation of embryonic stem cells by bone morphogenetic protein-2 combined with visceral endoderm-like cells." Cell Biol Int **30**(10): 769-76.

Binah, O., K. Dolnikov, et al. (2007). "Functional and developmental properties of human embryonic stem cells-derived cardiomyocytes." J Electrocardiol **40**(6 Suppl): S192-6.

Brekken, R. A. and E. H. Sage (2001). "SPARC, a matricellular protein: at the crossroads of cell-matrix communication." Matrix Biol **19**(8): 816-27.

Bruneau, B. G., G. Nemer, et al. (2001). "A murine model of Holt-Oram syndrome defines roles of the T-box transcription factor Tbx5 in cardiogenesis and disease." Cell **106**(6): 709-21.

Buggisch, M., B. Ateghang, et al. (2007). "Stimulation of ES-cell-derived cardiomyogenesis and neonatal cardiac cell proliferation by reactive oxygen species and NADPH oxidase." J Cell Sci **120**(Pt 5): 885-94.

Burridge, P. W., D. Anderson, et al. (2007). "Improved human embryonic stem cell embryoid body homogeneity and cardiomyocyte differentiation from a novel V-96 plate aggregation system highlights interline variability." Stem Cells **25**(4): 929-38.

Cabrita, G. J., B. S. Ferreira, et al. (2003). "Hematopoietic stem cells: from the bone to the bioreactor." Trends Biotechnol **21**(5): 233-40.

Cai, C. L., X. Liang, et al. (2003). "Isl1 identifies a cardiac progenitor population that proliferates prior to differentiation and contributes a majority of cells to the heart." Dev Cell **5**(6): 877-89.

Cameron, C. M., W. S. Hu, et al. (2006). "Improved development of human embryonic stem cell-derived embryoid bodies by stirred vessel cultivation." Biotechnol Bioeng **94**(5): 938-48.

Candia, A. F., T. Watabe, et al. (1997). "Cellular interpretation of multiple TGF-beta signals: intracellular antagonism between activin/BVg1 and BMP-2/4 signaling mediated by Smads." Development **124**(22): 4467-80.

Carpenedo, R. L., A. M. Bratt-Leal, et al. (2009). "Homogeneous and organized differentiation within embryoid bodies induced by microsphere-mediated delivery of small molecules." Biomaterials **30**(13): 2507-15.

Carpenedo, R. L., C. Y. Sargent, et al. (2007). "Rotary suspension culture enhances the efficiency, yield, and homogeneity of embryoid body differentiation." Stem Cells **25**(9): 2224-34.

Carpenter, M. K., M. S. Inokuma, et al. (2001). "Enrichment of neurons and neural precursors from human embryonic stem cells." Exp Neurol **172**(2): 383-97.

Caspi, O., I. Huber, et al. (2007). "Transplantation of human embryonic stem cell-derived cardiomyocytes improves myocardial performance in infarcted rat hearts." J Am Coll Cardiol **50**(19): 1884-93.

Christman, K. L., A. J. Vardanian, et al. (2004). "Injectable fibrin scaffold improves cell transplant survival, reduces infarct expansion, and induces neovasculature formation in ischemic myocardium." J Am Coll Cardiol **44**(3): 654-60.

Clements, D. and H. R. Woodland (2000). "Changes in embryonic cell fate produced by expression of an endodermal transcription factor, Xsox17." Mech Dev **99**(1-2): 65-70.

Climent, S., M. Sarasa, et al. (1995). "Neurogenic cells inhibit the differentiation of cardiogenic cells." Dev Biol **171**(1): 130-48.

Collins, P. C., W. M. Miller, et al. (1998). "Stirred culture of peripheral and cord blood hematopoietic cells offers advantages over traditional static systems for clinically relevant applications." Biotechnol Bioeng **59**(5): 534-43.

Conlon, F. L., K. M. Lyons, et al. (1994). "A primary requirement for nodal in the formation and maintenance of the primitive streak in the mouse." Development **120**(7): 1919-28.

Coucouvanis, E. and G. R. Martin (1995). "Signals for death and survival: a two-step mechanism for cavitation in the vertebrate embryo." Cell **83**(2): 279-87.

Coucouvanis, E. and G. R. Martin (1999). "BMP signaling plays a role in visceral endoderm differentiation and cavitation in the early mouse embryo." Development **126**(3): 535-46.

D'Amour, K. A., A. D. Agulnick, et al. (2005). "Efficient differentiation of human embryonic stem cells to definitive endoderm." Nat Biotechnol **23**(12): 1534-41.

Dai, W., L. J. Field, et al. (2007). "Survival and maturation of human embryonic stem cell-derived cardiomyocytes in rat hearts." J Mol Cell Cardiol **43**(4): 504-16.

Dang, S. M., S. Gerecht-Nir, et al. (2004). "Controlled, scalable embryonic stem cell differentiation culture." Stem Cells **22**(3): 275-82.

Dang, S. M., M. Kyba, et al. (2002). "Efficiency of embryoid body formation and hematopoietic development from embryonic stem cells in different culture systems." Biotechnol Bioeng **78**(4): 442-53.

Dang, S. M. and P. W. Zandstra (2005). "Scalable production of embryonic stem cell-derived cells." Methods Mol Biol **290**: 353-64.

Dimmeler, S., A. M. Zeiher, et al. (2005). "Unchain my heart: the scientific foundations of cardiac repair." J Clin Invest **115**(3): 572-83.

Doetschman, T. C., H. Eistetter, et al. (1985). "The in vitro development of blastocyst-derived embryonic stem cell lines: formation of visceral yolk sac, blood islands and myocardium." J Embryol Exp Morphol **87**: 27-45.

Dvash, T. and N. Benvenisty (2004). "Human embryonic stem cells as a model for early human development." Best Pract Res Clin Obstet Gynaecol **18**(6): 929-40.

Ebelt, H., M. Jungblut, et al. (2007). "Cellular cardiomyoplasty: improvement of left ventricular function correlates with the release of cardioactive cytokines." Stem Cells **25**(1): 236-44.

Evans, M. J. and M. H. Kaufman (1981). "Establishment in culture of pluripotential cells from mouse embryos." Nature **292**(5819): 154-6.

Faustino, R. S., A. Behfar, et al. (2008). "Genomic chart guiding embryonic stem cell cardiopoiesis." Genome Biol **9**(1): R6.

Figallo, E., C. Cannizzaro, et al. (2007). "Micro-bioreactor array for controlling cellular microenvironments." Lab Chip **7**(6): 710-9.

Fok, E. Y. and P. W. Zandstra (2005). "Shear-controlled single-step mouse embryonic stem cell expansion and embryoid body-based differentiation." Stem Cells **23**(9): 1333-42.

Forsyth, N. R., A. Musio, et al. (2006). "Physiologic oxygen enhances human embryonic stem cell clonal recovery and reduces chromosomal abnormalities." Cloning Stem Cells **8**(1): 16-23.

Freund, C., D. Ward-van Oostwaard, et al. (2008). "Insulin redirects differentiation from cardiogenic mesoderm and endoderm to neuroectoderm in differentiating human embryonic stem cells." Stem Cells **26**(3): 724-33.

Furusawa, T., K. Ohkoshi, et al. (2004). "Embryonic stem cells expressing both platelet endothelial cell adhesion molecule-1 and stage-specific embryonic antigen-1 differentiate predominantly into epiblast cells in a chimeric embryo." Biol Reprod **70**(5): 1452-7.

Futaki, S., Y. Hayashi, et al. (2004). "Sox7 plays crucial roles in parietal endoderm differentiation in F9 embryonal carcinoma cells through regulating Gata-4 and Gata-6 expression." Mol Cell Biol **24**(23): 10492-503.

Gadue, P., T. L. Huber, et al. (2005). "Germ layer induction from embryonic stem cells." Exp Hematol **33**(9): 955-64.

Gadue, P., T. L. Huber, et al. (2006). "Wnt and TGF-beta signaling are required for the induction of an in vitro model of primitive streak formation using embryonic stem cells." Proc Natl Acad Sci U S A **103**(45): 16806-11.

Garry, D. J. and E. N. Olson (2006). "A common progenitor at the heart of development." Cell **127**(6): 1101-4.

Gassmann, M., J. Fandrey, et al. (1996). "Oxygen supply and oxygen-dependent gene expression in differentiating embryonic stem cells." Proc Natl Acad Sci U S A **93**(7): 2867-72.

Gerecht-Nir, S., S. Cohen, et al. (2004). "Bioreactor cultivation enhances the efficiency of human embryoid body (hEB) formation and differentiation." Biotechnol Bioeng **86**(5): 493-502.

Gerecht-Nir, S., B. Fishman, et al. (2004). "Cardiovascular potential of embryonic stem cells." Anat Rec A Discov Mol Cell Evol Biol **276**(1): 58-65.

Gerecht, S., J. A. Burdick, et al. (2007). "Hyaluronic acid hydrogel for controlled self-renewal and differentiation of human embryonic stem cells." Proc Natl Acad Sci U S A **104**(27): 11298-303.

Gibbons, J., E. Hewitt, et al. (2006). "Effects of oxygen tension on the establishment and lactate dehydrogenase activity of murine embryonic stem cells." Cloning Stem Cells **8**(2): 117-22.

Grabel, L., S. Becker, et al. (1998). "Using EC and ES cell culture to study early development: recent observations on Indian hedgehog and Bmps." Int J Dev Biol **42**(7): 917-25.

Hakuno, D., T. Takahashi, et al. (2005). "Focal adhesion kinase signaling regulates cardiogenesis of embryonic stem cells." J Biol Chem **280**(47): 39534-44.

Hart, A. H., L. Hartley, et al. (2002). "Mixl1 is required for axial mesendoderm morphogenesis and patterning in the murine embryo." Development **129**(15): 3597-608.

Harvey, R. P. (2002). "Patterning the vertebrate heart." Nat Rev Genet **3**(7): 544-56.

He, J. Q., Y. Ma, et al. (2003). "Human embryonic stem cells develop into multiple types of cardiac myocytes: action potential characterization." Circ Res **93**(1): 32-9.

Henderson, J. K., J. S. Draper, et al. (2002). "Preimplantation human embryos and embryonic stem cells show comparable expression of stage-specific embryonic antigens." Stem Cells **20**(4): 329-37.

Hiroi, Y., S. Kudoh, et al. (2001). "Tbx5 associates with Nkx2-5 and synergistically promotes cardiomyocyte differentiation." Nat Genet **28**(3): 276-80.

Hogan, B. L. (1996). "Bone morphogenetic proteins in development." Curr Opin Genet Dev **6**(4): 432-8.

Hogan, B. L., A. R. Cooper, et al. (1980). "Incorporation into Reichert's membrane of laminin-like extracellular proteins synthesized by parietal endoderm cells of the mouse embryo." Dev Biol **80**(2): 289-300.

Hogan, B. L., A. Taylor, et al. (1981). "Cell interactions modulate embryonal carcinoma cell differentiation into parietal or visceral endoderm." Nature **291**(5812): 235-7.

Holland, P. W., S. J. Harper, et al. (1987). "In vivo expression of mRNA for the Ca++-binding protein SPARC (osteonectin) revealed by in situ hybridization." J Cell Biol **105**(1): 473-82.

Holtzinger, A., G. E. Rosenfeld, et al. (2010). "Gata4 directs development of cardiac-inducing endoderm from ES cells." Dev Biol **337**(1): 63-73.

Hrabchak, C., M. Ringuette, et al. (2008). "Recombinant mouse SPARC promotes parietal endoderm differentiation and cardiomyogenesis in embryoid bodies." Biochem Cell Biol **86**(6): 487-99.

Huber, I., I. Itzhaki, et al. (2007). "Identification and selection of cardiomyocytes during human embryonic stem cell differentiation." Faseb J **21**(10): 2551-63.

Hudson, C., D. Clements, et al. (1997). "Xsox17alpha and -beta mediate endoderm formation in Xenopus." Cell **91**(3): 397-405.

Hwang, Y. S., B. G. Chung, et al. (2009). "Microwell-mediated control of embryoid body size regulates embryonic stem cell fate via differential expression of WNT5a and WNT11." Proc Natl Acad Sci U S A **106**(40): 16978-83.

Itskovitz-Eldor, J., M. Schuldiner, et al. (2000). "Differentiation of human embryonic stem cells into embryoid bodies compromising the three embryonic germ layers." Mol Med **6**(2): 88-95.

Iyer, R. K., M. Radisic, et al. (2007). "Synthetic oxygen carriers in cardiac tissue engineering." Artif Cells Blood Substit Immobil Biotechnol **35**(1): 135-48.

Jacobson, A. G. and J. T. Duncan (1968). "Heart induction in salamanders." J Exp Zool **167**(1): 79-103.

Johnson, M. H. and C. A. Ziomek (1981). "Induction of polarity in mouse 8-cell blastomeres: specificity, geometry, and stability." J Cell Biol **91**(1): 303-8.

Kanai-Azuma, M., Y. Kanai, et al. (2002). "Depletion of definitive gut endoderm in Sox17-null mutant mice." Development **129**(10): 2367-79.

Kattman, S. J., E. D. Adler, et al. (2007). "Specification of multipotential cardiovascular progenitor cells during embryonic stem cell differentiation and embryonic development." Trends Cardiovasc Med **17**(7): 240-6.

Kattman, S. J., T. L. Huber, et al. (2006). "Multipotent flk-1+ cardiovascular progenitor cells give rise to the cardiomyocyte, endothelial, and vascular smooth muscle lineages." Dev Cell **11**(5): 723-32.

Kawai, T., T. Takahashi, et al. (2004). "Efficient cardiomyogenic differentiation of embryonic stem cell by fibroblast growth factor 2 and bone morphogenetic protein 2." Circ J **68**(7): 691-702.

Kehat, I., A. Gepstein, et al. (2002). "High-resolution electrophysiological assessment of human embryonic stem cell-derived cardiomyocytes: a novel in vitro model for the study of conduction." Circ Res **91**(8): 659-61.

Kehat, I., D. Kenyagin-Karsenti, et al. (2001). "Human embryonic stem cells can differentiate into myocytes with structural and functional properties of cardiomyocytes." J Clin Invest **108**(3): 407-14.

Kehat, I., L. Khimovich, et al. (2004). "Electromechanical integration of cardiomyocytes derived from human embryonic stem cells." Nat Biotechnol **22**(10): 1282-9.

Keller, G. (2005). "Embryonic stem cell differentiation: emergence of a new era in biology and medicine." Genes Dev **19**(10): 1129-55.

Keller, G. M. (1995). "In vitro differentiation of embryonic stem cells." Curr Opin Cell Biol **7**(6): 862-9.

Kelly, R. G., N. A. Brown, et al. (2001). "The arterial pole of the mouse heart forms from Fgf10-expressing cells in pharyngeal mesoderm." Dev Cell **1**(3): 435-40.

Khademhosseini, A., G. Eng, et al. (2007). "Microfluidic patterning for fabrication of contractile cardiac organoids." Biomed Microdevices **9**(2): 149-57.

Khademhosseini, A., L. Ferreira, et al. (2006). "Co-culture of human embryonic stem cells with murine embryonic fibroblasts on microwell-patterned substrates." Biomaterials **27**(36): 5968-77.

Kikuchi, Y., A. Agathon, et al. (2001). "casanova encodes a novel Sox-related protein necessary and sufficient for early endoderm formation in zebrafish." Genes Dev **15**(12): 1493-505.

Kinder, S. J., D. A. Loebel, et al. (2001). "Allocation and early differentiation of cardiovascular progenitors in the mouse embryo." Trends Cardiovasc Med **11**(5): 177-84.

Kispert, A. and B. G. Herrmann (1994). "Immunohistochemical analysis of the Brachyury protein in wild-type and mutant mouse embryos." Dev Biol **161**(1): 179-93.

Kitajima, S., A. Takagi, et al. (2000). "MesP1 and MesP2 are essential for the development of cardiac mesoderm." Development **127**(15): 3215-26.

Kitsberg, D. (2007). "Human embryonic stem cells for tissue engineering." Methods Mol Med **140**: 33-65.

Klug, M. G., M. H. Soonpaa, et al. (1996). "Genetically selected cardiomyocytes from differentiating embronic stem cells form stable intracardiac grafts." J Clin Invest **98**(1): 216-24.

Kolodziejska, K. M., H. N. Ashraf, et al. (2008). "c-Myb Dependent Smooth Muscle Cell Differentiation." Circ Res.

Kolossov, E., T. Bostani, et al. (2006). "Engraftment of engineered ES cell-derived cardiomyocytes but not BM cells restores contractile function to the infarcted myocardium." J Exp Med **203**(10): 2315-27.

Kopper, O., O. Giladi, et al. (2010). "Characterization of gastrulation-stage progenitor cells and their inhibitory crosstalk in human embryoid bodies." Stem Cells **28**(1): 75-83.

Kurosawa, H., T. Imamura, et al. (2003). "A simple method for forming embryoid body from mouse embryonic stem cells." J Biosci Bioeng **96**(4): 409-11.

Kwon, J., B. S. Kim, et al. (2003). "Suspension culture of hematopoietic stem cells in stirred bioreactors." Biotechnol Lett **25**(2): 179-82.

Ladd, A. N., T. A. Yatskievych, et al. (1998). "Regulation of avian cardiac myogenesis by activin/TGFbeta and bone morphogenetic proteins." Dev Biol **204**(2): 407-19.

Laflamme, M. A., K. Y. Chen, et al. (2007). "Cardiomyocytes derived from human embryonic stem cells in pro-survival factors enhance function of infarcted rat hearts." Nat Biotechnol **25**(9): 1015-24.

Laflamme, M. A., J. Gold, et al. (2005). "Formation of human myocardium in the rat heart from human embryonic stem cells." Am J Pathol **167**(3): 663-71.

Laflamme, M. A. and C. E. Murry (2005). "Regenerating the heart." Nat Biotechnol **23**(7): 845-56.

Laflamme, M. A., S. Zbinden, et al. (2007). "Cell-based therapy for myocardial ischemia and infarction: pathophysiological mechanisms." Annu Rev Pathol **2**: 307-39.

Lagna, G., A. Hata, et al. (1996). "Partnership between DPC4 and SMAD proteins in TGF-beta signalling pathways." Nature **383**(6603): 832-6.

Latinkic, B. V., S. Kotecha, et al. (2003). "Induction of cardiomyocytes by GATA4 in Xenopus ectodermal explants." Development **130**(16): 3865-76.

Laugwitz, K. L., A. Moretti, et al. (2005). "Postnatal isl1+ cardioblasts enter fully differentiated cardiomyocyte lineages." Nature **433**(7026): 647-53.

Lawson, K. A., J. J. Meneses, et al. (1991). "Clonal analysis of epiblast fate during germ layer formation in the mouse embryo." Development **113**(3): 891-911.

Lee, J., H. K. Kim, et al. (2006). "The human OCT-4 isoforms differ in their ability to confer self-renewal." J Biol Chem **281**(44): 33554-65.

Lee, L. H., R. Peerani, et al. (2009). "Micropatterning of human embryonic stem cells dissects the mesoderm and endoderm lineages." Stem Cell Res **2**(2): 155-62.

Leor, J., S. Gerecht, et al. (2007). "Human embryonic stem cell transplantation to repair the infarcted myocardium." Heart **93**(10): 1278-84.

Lewis, S. L. and P. P. Tam (2006). "Definitive endoderm of the mouse embryo: formation, cell fates, and morphogenetic function." Dev Dyn **235**(9): 2315-29.

Li, M., L. Pevny, et al. (1998). "Generation of purified neural precursors from embryonic stem cells by lineage selection." Curr Biol **8**(17): 971-4.

Li, Y., S. Powell, et al. (2005). "Expansion of human embryonic stem cells in defined serum-free medium devoid of animal-derived products." Biotechnol Bioeng **91**(6): 688-98.

Lien, C. L., J. McAnally, et al. (2002). "Cardiac-specific activity of an Nkx2-5 enhancer requires an evolutionarily conserved Smad binding site." Dev Biol **244**(2): 257-66.

Lindsley, R. C., J. G. Gill, et al. (2006). "Canonical Wnt signaling is required for development of embryonic stem cell-derived mesoderm." Development **133**(19): 3787-96.

Liu, P., M. Wakamiya, et al. (1999). "Requirement for Wnt3 in vertebrate axis formation." Nat Genet **22**(4): 361-5.

Liu, Y., M. Asakura, et al. (2007). "Sox17 is essential for the specification of cardiac mesoderm in embryonic stem cells." Proc Natl Acad Sci U S A **104**(10): 3859-64.

Lough, J., M. Barron, et al. (1996). "Combined BMP-2 and FGF-4, but neither factor alone, induces cardiogenesis in non-precardiac embryonic mesoderm." Dev Biol **178**(1): 198-202.

Ludwig, T. E., V. Bergendahl, et al. (2006). "Feeder-independent culture of human embryonic stem cells." Nat Methods **3**(8): 637-46.

Madlambayan, G. J., I. Rogers, et al. (2001). "Controlling culture dynamics for the expansion of hematopoietic stem cells." J Hematother Stem Cell Res **10**(4): 481-92.

Magyar, J. P., M. Nemir, et al. (2001). "Mass production of embryoid bodies in microbeads." Ann N Y Acad Sci **944**: 135-43.

Marchetti, S., C. Gimond, et al. (2002). "Endothelial cells genetically selected from differentiating mouse embryonic stem cells incorporate at sites of neovascularization in vivo." J Cell Sci **115**(Pt 10): 2075-85.

Martens, T. P., A. F. Godier, et al. (2009). "Percutaneous cell delivery into the heart using hydrogels polymerizing in situ." Cell Transplant **18**(3): 297-304.

Marvin, M. J., G. Di Rocco, et al. (2001). "Inhibition of Wnt activity induces heart formation from posterior mesoderm." Genes Dev **15**(3): 316-27.

Mason, I. J., A. Taylor, et al. (1986). "Evidence from molecular cloning that SPARC, a major product of mouse embryo parietal endoderm, is related to an endothelial cell 'culture shock' glycoprotein of Mr 43,000." Embo J **5**(7): 1465-72.

Massague, J. and Y. G. Chen (2000). "Controlling TGF-beta signaling." Genes Dev **14**(6): 627-44.

McDevitt, T. C., M. A. Laflamme, et al. (2005). "Proliferation of cardiomyocytes derived from human embryonic stem cells is mediated via the IGF/PI 3-kinase/Akt signaling pathway." J Mol Cell Cardiol **39**(6): 865-73.

McDevitt, T. C., K. A. Woodhouse, et al. (2003). "Spatially organized layers of cardiomyocytes on biodegradable polyurethane films for myocardial repair." J Biomed Mater Res A **66**(3): 586-95.

Menard, C., C. Grey, et al. (2004). "Cardiac specification of embryonic stem cells." J Cell Biochem **93**(4): 681-7.

Menard, C., C. Grey, et al. (2004). "Cardiac specification of embryonic stem cells." J Cell Biochem **93**(4): 681-7.

Menard, C., A. A. Hagege, et al. (2005). "Transplantation of cardiac-committed mouse embryonic stem cells to infarcted sheep myocardium: a preclinical study." Lancet **366**(9490): 1005-12.

Menasche, P. (2003). "Myoblast-based cell transplantation." Heart Fail Rev **8**(3): 221-7.

Menasche, P. (2004). "Skeletal myoblast transplantation for cardiac repair." Expert Rev Cardiovasc Ther **2**(1): 21-8.

Menasche, P. (2008). "Skeletal myoblasts and cardiac repair." J Mol Cell Cardiol **45**(4): 545-53.

Meyer, G. P., K. C. Wollert, et al. (2006). "Intracoronary bone marrow cell transfer after myocardial infarction: eighteen months' follow-up data from the randomized, controlled BOOST (BOne marrOw transfer to enhance ST-elevation infarct regeneration) trial." Circulation **113**(10): 1287-94.

Mima, T., H. Ueno, et al. (1995). "Fibroblast growth factor receptor is required for in vivo cardiac myocyte proliferation at early embryonic stages of heart development." Proc Natl Acad Sci U S A **92**(2): 467-71.

Mohr, J. C., J. J. de Pablo, et al. (2006). "3-D microwell culture of human embryonic stem cells." Biomaterials **27**(36): 6032-42.

Mohr, J. C., J. Zhang, et al. (2009). "The microwell control of embryoid body size in order to regulate cardiac differentiation of human embryonic stem cells." Biomaterials **31**(7): 1885-93.

Moon, S. Y., Y. B. Park, et al. (2006). "Generation, culture, and differentiation of human embryonic stem cells for therapeutic applications." Mol Ther **13**(1): 5-14.

Moore, R., K. Q. Cai, et al. (2009). "Cell adhesive affinity does not dictate primitive endoderm segregation and positioning during murine embryoid body formation." Genesis **47**(9): 579-89.

Moustakas, A., S. Souchelnytskyi, et al. (2001). "Smad regulation in TGF-beta signal transduction." J Cell Sci **114**(Pt 24): 4359-69.

Mummery, C., D. Ward-van Oostwaard, et al. (2003). "Differentiation of human embryonic stem cells to cardiomyocytes: role of coculture with visceral endoderm-like cells." Circulation **107**(21): 2733-40.

Murry, C. E. and G. Keller (2008). "Differentiation of embryonic stem cells to clinically relevant populations: lessons from embryonic development." Cell **132**(4): 661-80.

Murry, C. E., H. Reinecke, et al. (2006). "Regeneration gaps: observations on stem cells and cardiac repair." J Am Coll Cardiol **47**(9): 1777-85.

Murry, C. E., M. H. Soonpaa, et al. (2004). "Haematopoietic stem cells do not transdifferentiate into cardiac myocytes in myocardial infarcts." Nature **428**(6983): 664-8.

Naito, A. T., I. Shiojima, et al. (2006). "Developmental stage-specific biphasic roles of Wnt/beta-catenin signaling in cardiomyogenesis and hematopoiesis." Proc Natl Acad Sci U S A **103**(52): 19812-7.

Nakanishi, M., A. Kurisaki, et al. (2009). "Directed induction of anterior and posterior primitive streak by Wnt from embryonic stem cells cultured in a chemically defined serum-free medium." Faseb J **23**(1): 114-22.

Nascone, N. and M. Mercola (1995). "An inductive role for the endoderm in Xenopus cardiogenesis." Development **121**(2): 515-23.

Nelson, T. J., A. Chiriac, et al. (2009). "Lineage specification of Flk-1+ progenitors is associated with divergent Sox7 expression in cardiopoiesis." Differentiation **77**(3): 248-55.

Ng, E. S., R. P. Davis, et al. (2005). "Forced aggregation of defined numbers of human embryonic stem cells into embryoid bodies fosters robust, reproducible hematopoietic differentiation." Blood **106**(5): 1601-3.

Niebruegge, S., C. L. Bauwens, et al. (2009). "Generation of human embryonic stem cell-derived mesoderm and cardiac cells using size-specified aggregates in an oxygen-controlled bioreactor." Biotechnol Bioeng **102**(2): 493-507.

Niebruegge, S., A. Nehring, et al. (2008). "Cardiomyocyte production in mass suspension culture: embryonic stem cells as a source for great amounts of functional cardiomyocytes." Tissue Eng Part A **14**(10): 1591-601.

Nygren, J. M., S. Jovinge, et al. (2004). "Bone marrow-derived hematopoietic cells generate cardiomyocytes at a low frequency through cell fusion, but not transdifferentiation." Nat Med **10**(5): 494-501.

O'Shea, K. S. (2004). "Self-renewal vs. differentiation of mouse embryonic stem cells." Biol Reprod **71**(6): 1755-65.

Orlic, D., J. Kajstura, et al. (2001). "Bone marrow cells regenerate infarcted myocardium." Nature **410**(6829): 701-5.

Orts Llorca, F. (1963). "[Influence of the endoblast in the morphogenesis and late differentiation of the chick heart.]." Acta Anat (Basel) **52**: 202-14.

Pandur, P., M. Lasche, et al. (2002). "Wnt-11 activation of a non-canonical Wnt signalling pathway is required for cardiogenesis." Nature **418**(6898): 636-41.

Parisi, S., D. D'Andrea, et al. (2003). "Nodal-dependent Cripto signaling promotes cardiomyogenesis and redirects the neural fate of embryonic stem cells." J Cell Biol **163**(2): 303-14.

Parlow, M. H., D. L. Bolender, et al. (1991). "Localization of bFGF-like proteins as punctate inclusions in the preseptation myocardium of the chicken embryo." Dev Biol **146**(1): 139-47.

Passier, R. and C. Mummery (2005). "Cardiomyocyte differentiation from embryonic and adult stem cells." Curr Opin Biotechnol **16**(5): 498-502.

Passier, R., D. W. Oostwaard, et al. (2005). "Increased cardiomyocyte differentiation from human embryonic stem cells in serum-free cultures." Stem Cells **23**(6): 772-80.

Pearce, J. J. and M. J. Evans (1999). "Mml, a mouse Mix-like gene expressed in the primitive streak." Mech Dev **87**(1-2): 189-92.

Peerani, R., B. M. Rao, et al. (2007). "Niche-mediated control of human embryonic stem cell self-renewal and differentiation." Embo J **26**(22): 4744-55.

Pera, M. F., J. Andrade, et al. (2004). "Regulation of human embryonic stem cell differentiation by BMP-2 and its antagonist noggin." J Cell Sci **117**(Pt 7): 1269-80.

Pick, M., L. Azzola, et al. (2007). "Differentiation of human embryonic stem cells in serum-free medium reveals distinct roles for bone morphogenetic protein 4, vascular endothelial growth factor, stem cell factor, and fibroblast growth factor 2 in hematopoiesis." Stem Cells **25**(9): 2206-14.

Povelones, M. and R. Nusse (2002). "Wnt signalling sees spots." Nat Cell Biol **4**(11): E249-50.

Pyle, A. D., L. F. Lock, et al. (2006). "Neurotrophins mediate human embryonic stem cell survival." Nat Biotechnol **24**(3): 344-50.

Qi, X., G. Yang, et al. (2007). "Essential role of Smad4 in maintaining cardiomyocyte proliferation during murine embryonic heart development." Dev Biol **311**(1): 136-46.

Radisic, M., H. Park, et al. (2007). "Biomimetic approach to cardiac tissue engineering." Philos Trans R Soc Lond B Biol Sci **362**(1484): 1357-68.

Raffin, M., L. M. Leong, et al. (2000). "Subdivision of the cardiac Nkx2.5 expression domain into myogenic and nonmyogenic compartments." Dev Biol **218**(2): 326-40.

Ramirez-Bergeron, D. L., A. Runge, et al. (2004). "Hypoxia affects mesoderm and enhances hemangioblast specification during early development." Development **131**(18): 4623-34.

Ramirez-Bergeron, D. L. and M. C. Simon (2001). "Hypoxia-inducible factor and the development of stem cells of the cardiovascular system." Stem Cells **19**(4): 279-86.

Reinecke, H., V. Poppa, et al. (2002). "Skeletal muscle stem cells do not transdifferentiate into cardiomyocytes after cardiac grafting." J Mol Cell Cardiol **34**(2): 241-9.

Reissmann, E., H. Jornvall, et al. (2001). "The orphan receptor ALK7 and the Activin receptor ALK4 mediate signaling by Nodal proteins during vertebrate development." Genes Dev **15**(15): 2010-22.

Reubinoff, B. E., M. F. Pera, et al. (2000). "Embryonic stem cell lines from human blastocysts: somatic differentiation in vitro." Nat Biotechnol **18**(4): 399-404.

Robb, L., L. Hartley, et al. (2000). "Cloning, expression analysis, and chromosomal localization of murine and human homologues of a Xenopus mix gene." Dev Dyn **219**(4): 497-504.

Rosenthal, A., A. Macdonald, et al. (2007). "Cell patterning chip for controlling the stem cell microenvironment." Biomaterials **28**(21): 3208-16.

Rubart, M. and L. J. Field (2006). "Cell-based approaches for cardiac repair." Ann N Y Acad Sci **1080**: 34-48.

Rula, M. E., K. Q. Cai, et al. (2007). "Cell autonomous sorting and surface positioning in the formation of primitive endoderm in embryoid bodies." Genesis **45**(6): 327-38.

Rust, W. L., A. Sadasivam, et al. (2006). "Three-dimensional extracellular matrix stimulates gastrulation-like events in human embryoid bodies." Stem Cells Dev **15**(6): 889-904.

Sachinidis, A., B. K. Fleischmann, et al. (2003). "Cardiac specific differentiation of mouse embryonic stem cells." Cardiovasc Res **58**(2): 278-91.

Satin, J., I. Kehat, et al. (2004). "Mechanism of spontaneous excitability in human embryonic stem cell derived cardiomyocytes." J Physiol **559**(Pt 2): 479-96.

Sauer, H., G. Rahimi, et al. (2000). "Role of reactive oxygen species and phosphatidylinositol 3-kinase in cardiomyocyte differentiation of embryonic stem cells." FEBS Lett **476**(3): 218-23.

Schatten, G., J. Smith, et al. (2005). "Culture of human embryonic stem cells." Nat Methods **2**(6): 455-63.

Schlange, T., B. Andree, et al. (2000). "BMP2 is required for early heart development during a distinct time period." Mech Dev **91**(1-2): 259-70.

Schroeder, M., S. Niebruegge, et al. (2005). "Differentiation and lineage selection of mouse embryonic stem cells in a stirred bench scale bioreactor with automated process control." Biotechnol Bioeng **92**(7): 920-33.

Schuldiner, M., R. Eiges, et al. (2001). "Induced neuronal differentiation of human embryonic stem cells." Brain Res **913**(2): 201-5.

Schultheiss, T. M., J. B. Burch, et al. (1997). "A role for bone morphogenetic proteins in the induction of cardiac myogenesis." Genes Dev **11**(4): 451-62.

Schultheiss, T. M. and A. B. Lassar (1997). "Induction of chick cardiac myogenesis by bone morphogenetic proteins." Cold Spring Harb Symp Quant Biol **62**: 413-9.

Schultheiss, T. M., S. Xydas, et al. (1995). "Induction of avian cardiac myogenesis by anterior endoderm." Development **121**(12): 4203-14.

Segev, H., B. Fishman, et al. (2004). "Differentiation of human embryonic stem cells into insulin-producing clusters." Stem Cells **22**(3): 265-74.

Seguin, C. A., J. S. Draper, et al. (2008). "Establishment of endoderm progenitors by SOX transcription factor expression in human embryonic stem cells." Cell Stem Cell **3**(2): 182-95.

Semoff, S., B. L. Hogan, et al. (1982). "Localization of fibronectin, laminin-entactin, and entactin in Reichert's membrane by immunoelectron microscopy." Embo J **1**(10): 1171-5.

Sharma, S., R. Cabana, et al. (2008). "Cellular volume and marker expression in human peripheral blood apheresis stem cells." Cytometry A **73**(2): 160-7.

Shi, Y., A. Hata, et al. (1997). "A structural basis for mutational inactivation of the tumour suppressor Smad4." Nature **388**(6637): 87-93.

Shimoda, M., M. Kanai-Azuma, et al. (2007). "Sox17 plays a substantial role in late-stage differentiation of the extraembryonic endoderm in vitro." J Cell Sci **120**(Pt 21): 3859-69.

Shrey, K., A. Suchit, et al. (2009). "RNA interference: emerging diagnostics and therapeutics tool." Biochem Biophys Res Commun **386**(2): 273-7.

Song, L., W. Yan, et al. (2007). "Myocardial smad4 is essential for cardiogenesis in mouse embryos." Circ Res **101**(3): 277-85.

St-Jacques, B. and A. P. McMahon (1996). "Early mouse development: lessons from gene targeting." Curr Opin Genet Dev **6**(4): 439-44.

Stary, M., W. Pasteiner, et al. (2005). "Parietal endoderm secreted SPARC promotes early cardiomyogenesis in vitro." Exp Cell Res **310**(2): 331-43.

Stary, M., M. Schneider, et al. (2006). "Parietal endoderm secreted S100A4 promotes early cardiomyogenesis in embryoid bodies." Biochem Biophys Res Commun **343**(2): 555-63.

Sugi, Y. and J. Lough (1994). "Anterior endoderm is a specific effector of terminal cardiac myocyte differentiation of cells from the embryonic heart forming region." Dev Dyn **200**(2): 155-62.

Sugi, Y. and J. Lough (1995). "Activin-A and FGF-2 mimic the inductive effects of anterior endoderm on terminal cardiac myogenesis in vitro." Dev Biol **168**(2): 567-74.

Sugi, Y., J. Sasse, et al. (1993). "Inhibition of precardiac mesoderm cell proliferation by antisense oligodeoxynucleotide complementary to fibroblast growth factor-2 (FGF-2)." Dev Biol **157**(1): 28-37.

Svensson, E. C., R. L. Tufts, et al. (1999). "Molecular cloning of FOG-2: a modulator of transcription factor GATA-4 in cardiomyocytes." Proc Natl Acad Sci U S A **96**(3): 956-61.

Takahashi, K., K. Tanabe, et al. (2007). "Induction of pluripotent stem cells from adult human fibroblasts by defined factors." Cell **131**(5): 861-72.

Takahashi, K. and S. Yamanaka (2006). "Induction of pluripotent stem cells from mouse embryonic and adult fibroblast cultures by defined factors." Cell **126**(4): 663-76.

Takash, W., J. Canizares, et al. (2001). "SOX7 transcription factor: sequence, chromosomal localisation, expression, transactivation and interference with Wnt signalling." Nucleic Acids Res **29**(21): 4274-83.

Takeuchi, J. K. and B. G. Bruneau (2009). "Directed transdifferentiation of mouse mesoderm to heart tissue by defined factors." Nature **459**(7247): 708-11.

Tan, J., Tien, et al. (2002). "Microcontact printing of proteins on mixed self-assembled monolayers." Langmuir(18): 519-523.

Tan, J. L., W. Liu, et al. (2004). "Simple approach to micropattern cells on common culture substrates by tuning substrate wettability." Tissue Eng **10**(5-6): 865-72.

Thomson, J. A., J. Itskovitz-Eldor, et al. (1998). "Embryonic stem cell lines derived from human blastocysts." Science **282**(5391): 1145-7.

Tzahor, E. and A. B. Lassar (2001). "Wnt signals from the neural tube block ectopic cardiogenesis." Genes Dev **15**(3): 255-60.

Ueno, S., G. Weidinger, et al. (2007). "Biphasic role for Wnt/beta-catenin signaling in cardiac specification in zebrafish and embryonic stem cells." Proc Natl Acad Sci U S A **104**(23): 9685-90.

Ungrin, M. D., C. Joshi, et al. (2008). "Reproducible, ultra high-throughput formation of multicellular organization from single cell suspension-derived human embryonic stem cell aggregates." PLoS One **3**(2): e1565.

van der Pol, L. and J. Tramper (1998). "Shear sensitivity of animal cells from a culture-medium perspective." Trends Biotechnol **16**(8): 323-8.

van Laake, L. W., R. Passier, et al. (2007). "Human embryonic stem cell-derived cardiomyocytes survive and mature in the mouse heart and transiently improve function after myocardial infarction." Stem Cell Res **1**(1): 9-24.

Vassalle, M., L. Bocchi, et al. (2007). "A slowly inactivating sodium current (INa2) in the plateau range in canine cardiac Purkinje single cells." Exp Physiol **92**(1): 161-73.

Wakefield, L. M. and A. B. Roberts (2002). "TGF-beta signaling: positive and negative effects on tumorigenesis." Curr Opin Genet Dev **12**(1): 22-9.

Wang, G., H. Zhang, et al. (2005). "Noggin and bFGF cooperate to maintain the pluripotency of human embryonic stem cells in the absence of feeder layers." Biochem Biophys Res Commun **330**(3): 934-42.

Wang, L., L. Li, et al. (2005). "Human embryonic stem cells maintained in the absence of mouse embryonic fibroblasts or conditioned media are capable of hematopoietic development." Blood **105**(12): 4598-603.

Wang, X. and B. Seed (2003). "A PCR primer bank for quantitative gene expression analysis." Nucleic Acids Res **31**(24): e154.

Weber, H., C. E. Symes, et al. (2000). "A role for GATA5 in Xenopus endoderm specification." Development **127**(20): 4345-60.

Weitzer, G. (2006). "Embryonic stem cell-derived embryoid bodies: an in vitro model of eutherian pregastrulation development and early gastrulation." Handb Exp Pharmacol(174): 21-51.

Xu, C., J. Q. He, et al. (2006). "Human embryonic stem cell-derived cardiomyocytes can be maintained in defined medium without serum." Stem Cells Dev **15**(6): 931-41.

Xu, C., M. S. Inokuma, et al. (2001). "Feeder-free growth of undifferentiated human embryonic stem cells." Nat Biotechnol **19**(10): 971-4.

Xu, C., G. Liguori, et al. (1998). "Specific arrest of cardiogenesis in cultured embryonic stem cells lacking Cripto-1." Dev Biol **196**(2): 237-47.

Xu, C., S. Police, et al. (2002). "Characterization and enrichment of cardiomyocytes derived from human embryonic stem cells." Circ Res **91**(6): 501-8.

Xu, R. H., X. Chen, et al. (2002). "BMP4 initiates human embryonic stem cell differentiation to trophoblast." Nat Biotechnol **20**(12): 1261-4.

Xu, R. H., R. M. Peck, et al. (2005). "Basic FGF and suppression of BMP signaling sustain undifferentiated proliferation of human ES cells." Nat Methods **2**(3): 185-90.

Xu, X. Q., R. Graichen, et al. (2008). "Chemically defined medium supporting cardiomyocyte differentiation of human embryonic stem cells." Differentiation **76**(9): 958-70.

Xue, T., H. C. Cho, et al. (2005). "Functional integration of electrically active cardiac derivatives from genetically engineered human embryonic stem cells with quiescent recipient ventricular cardiomyocytes: insights into the development of cell-based pacemakers." Circulation **111**(1): 11-20.

Yamaguchi, T. P. (2001). "Heads or tails: Wnts and anterior-posterior patterning." Curr Biol **11**(17): R713-24.

Yang, L., M. H. Soonpaa, et al. (2008). "Human cardiovascular progenitor cells develop from a KDR+ embryonic-stem-cell-derived population." Nature **453**(7194): 524-8.

Yatskievych, T. A., A. N. Ladd, et al. (1997). "Induction of cardiac myogenesis in avian pregastrula epiblast: the role of the hypoblast and activin." Development **124**(13): 2561-70.

Yeo, C. and M. Whitman (2001). "Nodal signals to Smads through Cripto-dependent and Cripto-independent mechanisms." Mol Cell **7**(5): 949-57.

Younan, W. (1998). "Soft Lithography." Angewandte Chemie International Edition **37**(5): 550-575.

Younan Xia, G. (1998). "Soft Lithography." *Angewandte Chemie International Edition*(37).

Yu, J., M. A. Vodyanik, et al. (2007). "Induced pluripotent stem cell lines derived from human somatic cells." Science **318**(5858): 1917-20.

Yuasa, S., Y. Itabashi, et al. (2005). "Transient inhibition of BMP signaling by Noggin induces cardiomyocyte differentiation of mouse embryonic stem cells." Nat Biotechnol **23**(5): 607-11.

Zandstra, P. W., C. Bauwens, et al. (2003). "Scalable production of embryonic stem cell-derived cardiomyocytes." Tissue Eng **9**(4): 767-78.

Zhang, P., J. Li, et al. (2008). "Short-term BMP-4 treatment initiates mesoderm induction in human embryonic stem cells." Blood **111**(4): 1933-41.

Zhu, W. Z., K. D. Hauch, et al. (2009). "Human embryonic stem cells and cardiac repair." Transplant Rev (Orlando) **23**(1): 53-68.

Zhu, X., J. Sasse, et al. (1999). "Evidence that FGF receptor signaling is necessary for endoderm-regulated development of precardiac mesoderm." Mech Ageing Dev **108**(1): 77-85.

Appendix I

Supplementary Figures for Chapter 2

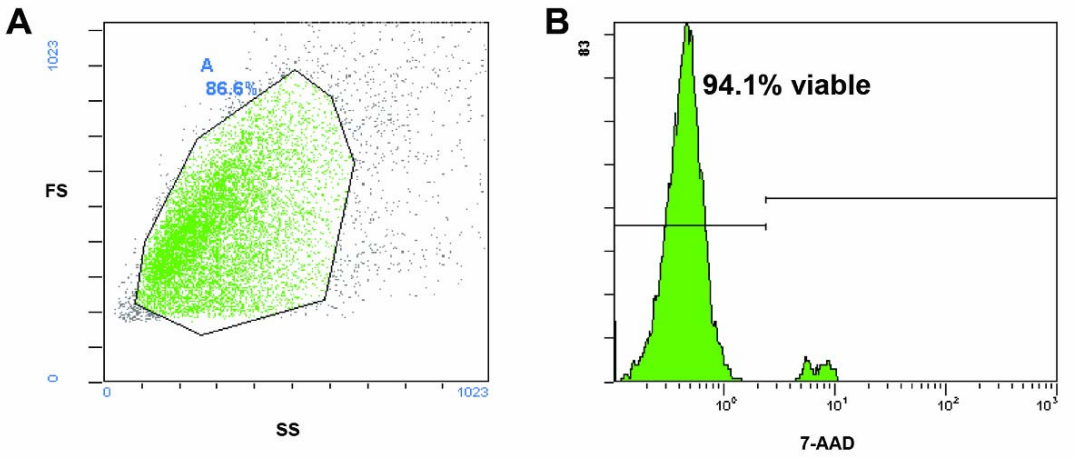

Figure S1-1: Demonstration of cell viability following TripLE enzymatic single cell dissociation of hESCs. A) Flow cytometry-based forward scatter and side scatter analysis of hESCs following enzymatic dissociation. **B)** Flow cytometry-based analysis of 7-AAD viability staining on enzymatically dissociated hESCs.

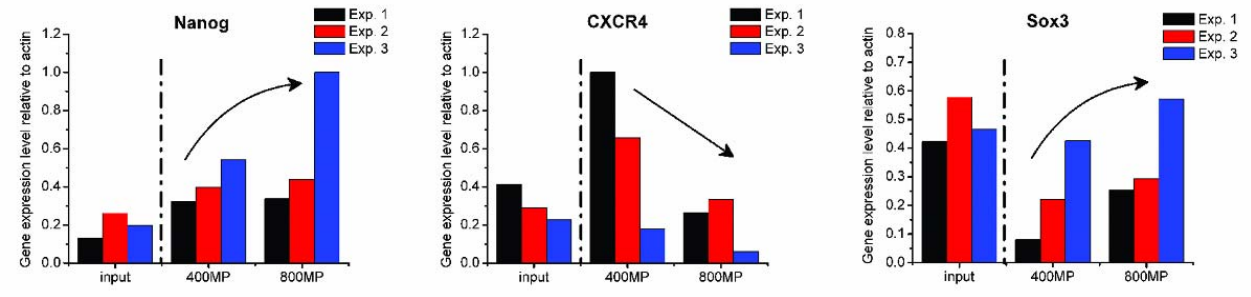

Figure S1-2: Analysis of size controlled MP-hESC colonies reveals the influence of colony size on differentiation trajectory. Representative qRTPCR analysis for 3 out of 7 trials for gene expression of pluripotency marker Nanog, endoderm-associated marker CXCR4, and neural-associated marker Sox3.

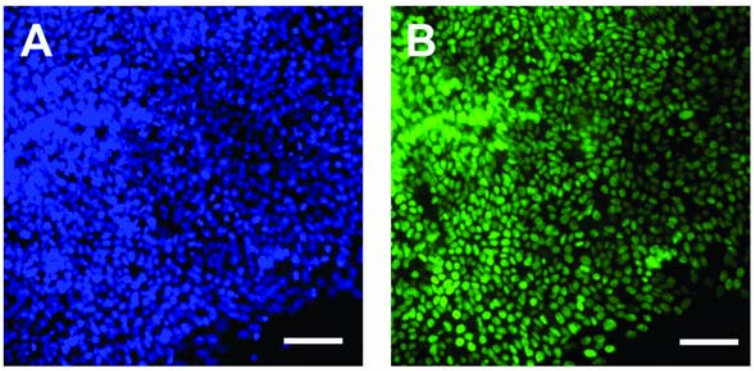

Figure S1-3: Demonstration that Oct4 protein is exclusively expressed in the nucleus in the input hESC population. Immunofluorescence images of hESC colonies stained with anti-Oct4 antibody (right), (left panel Hoechst nuclear stain). Scale bar represents 100 microns.

Appendix II

Supplementary Figures for Chapter 3

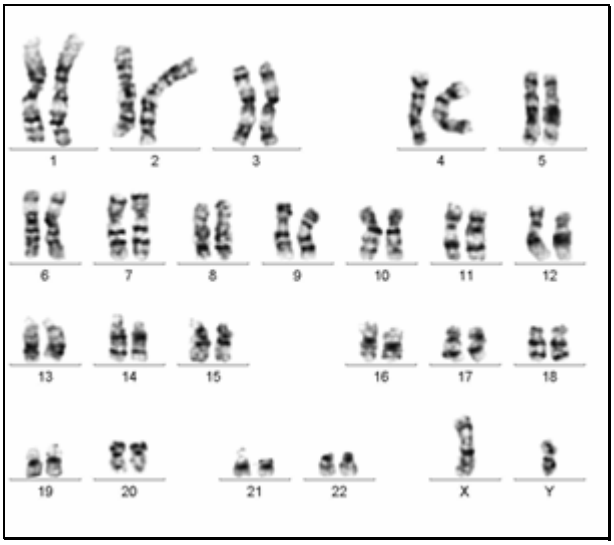

Figure S2-1: Karyotype results of H9 hESCs, Passage 52.

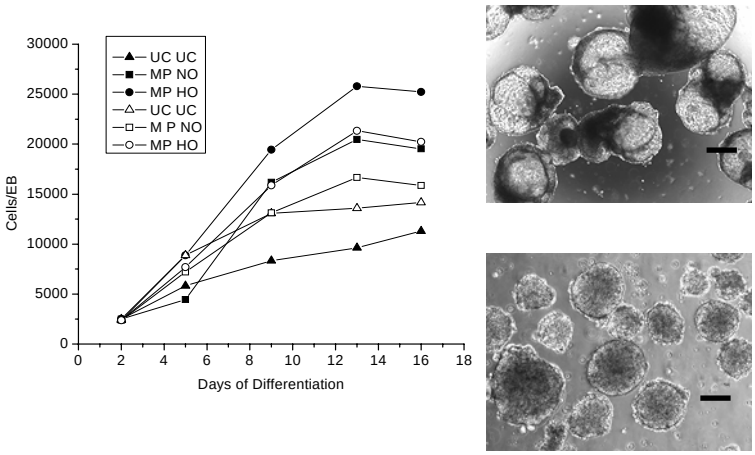

Figure S2-2: EB sizes as cells/EB in spinner culture under uncontrolled (UC) and oxygen-controlled conditions (normoxic (NO); hypoxic (HO)). Each experiment was performed with H9 (black symbols) and HES2 (white symbols) cells **(i)**. H9 EBs were formed by either colony scraping-off (UCEBs; ii) or by micropatterning followed by scraping-off size-controlled EBs (MPEBs, iii). On d16 of differentiation UCEBs exhibit a necrotic morphology, whereas patterned EBs appear compact and more uniform in size.

Appendix III

Supplementary Figures for Chapter 4

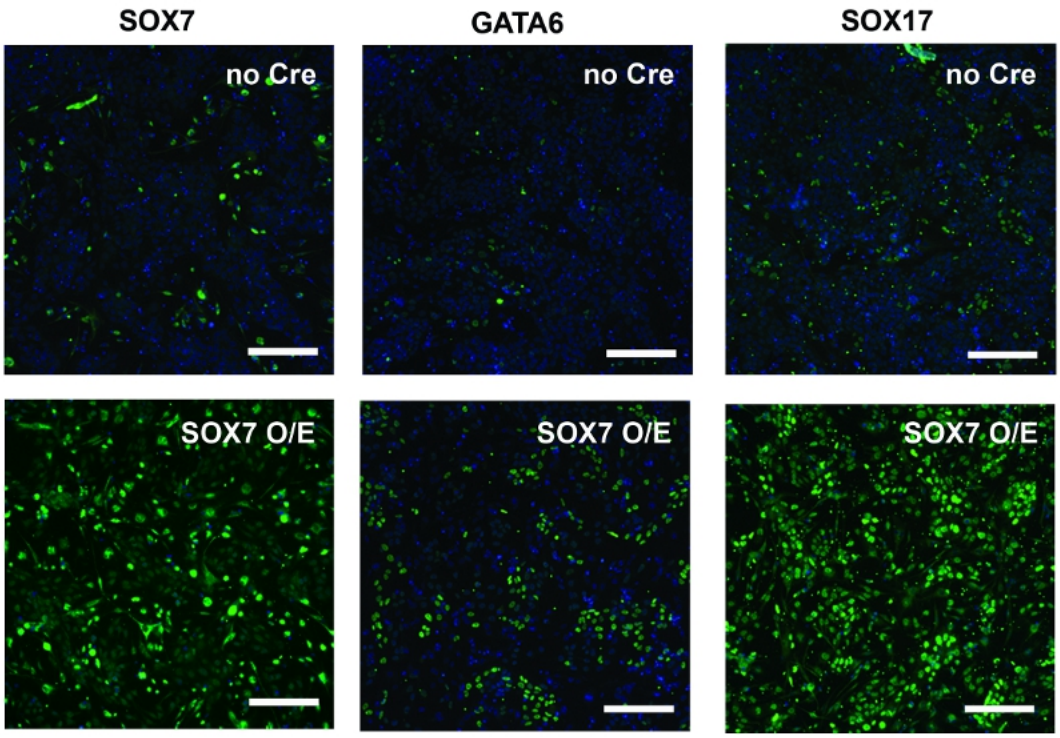

Figure S3-1: Characterization of SOX7-overexpressing (SOX7 O/E) cells. (A) Levels of expression of endoderm-associated proteins Sox7, Gata6 and SOX17 are higher in SOX7 O/E cells than in the non-Cre transfected (no Cre) controls. Scale bar = 250 μm.

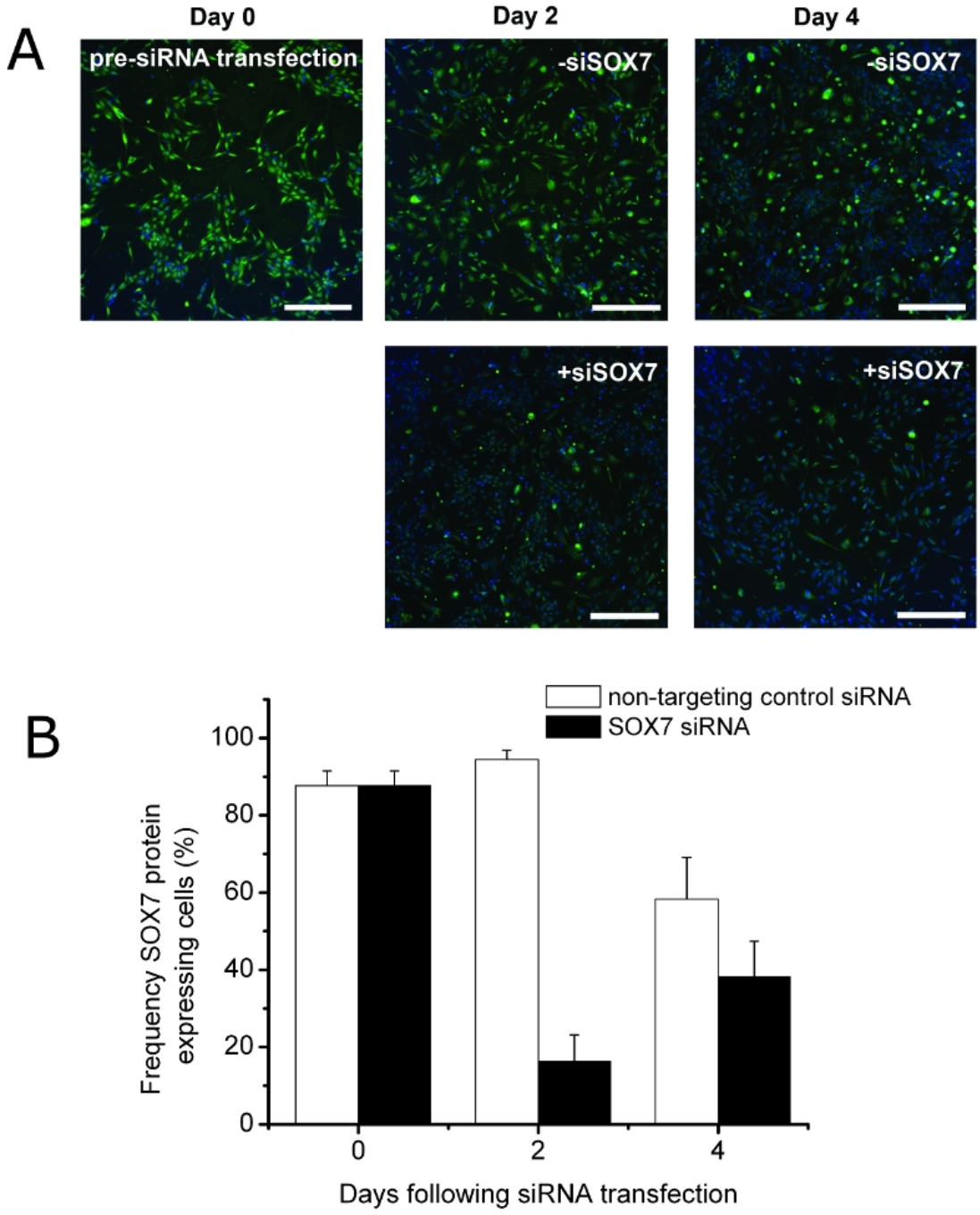

Figure S3-2: Validation of SOX7-specific siRNA. (A) 2 days after transfecting SOX7 O/E cells with siRNA against SOX7, SOX7 protein expression level is lower compared to SOX7 O/E cells transfected with scrambled control siRNA. Scale bar = 250 μm. **(B)** Quantitative analysis of SOX7 protein knockdown in SOX7 O/E cells 2 and 4 days following transfection with siRNA against SOX7.